SICS

CONDENSATION OF VAPOR AS INDUCED BY NUCLEI AND IONS

THIRD REPORT

By CARL BARUS
Hazard Professor of Physics, Brown University

WASHINGTON, D. C.:
Published by the Carnegie Institution of Washington
1908

CONDENSATION OF VAPOR AS INDUCED BY NUCLEI AND IONS

THIRD REPORT

By CARL BARUS
Hazard Professor of Physics, Brown University

WASHINGTON, D. C.:
Published by the Carnegie Institution of Washington
1908

CARNEGIE INSTITUTION OF WASHINGTON

Publication No. 96

BLANCHARD PRESS NEW YORK

PREFACE.

In the following report I have given an account of experiments made with a plug-cock fog chamber during the last year and a half.

The first chapter summarizes the equations frequently needed and adds other important suggestions relating to the efficiency of the apparatus used for condensation of water vapor suspended in air.

I have adduced, in Chapter II, the results of a long series of experiments begun May 9, 1905, to determine whether the colloidal or vapor nucleations of dust-free air show any interpretable variations in the initial regions (ions), which would correspond to variations of a natural radiation entering the chamber from without. The fog-chamber method seems to be too complicated to give trustworthy indications of such changes of ionization as have been since discovered with the aid of the electrical method by Wood and Campbell. An interesting result, however, came out of the experiments in question, as a whole, showing that the vapor nucleation is variable with temperature in the region examined to the extent of about 2 per cent per degree.

The fog chamber used in the present research having undergone varied modifications since the coronas were last standardized (1904), it seemed necessary to repeat the work for the present report. This was particularly necessary because the subsequent investigations were to depend essentially on the values of the nucleation observed. These comparisons are shown in Chapters III and IV. In the former the diffractions are obtained from a single source of light and the angular diameter of the coronas is measured by a goniometer; in the latter the fiducial annuli of two coronas due to identical sources of light are put in contact and the distance apart of the lamps is measured under known conditions. This contact method has many advantages and above all admits of the use of both eyes. In both cases, moreover, the nucleation of dust-free air, in the presence as well as in the absence of penetrating artificial radiation, is redetermined. All results agree among themselves and with the older work, as closely as may be expected in work of the present kind, below the middle green-blue-purple corona (usually corresponding to 10^5 nuclei); but above this there is much divergence, which will probably not be overcome until some means for keeping the air rigorously homogeneous in nucleation throughout a given series of experiments has been devised.

Chapter V contains some remarkable results on the properties of nuclei obtained from the evaporation of fog particles. It will be seen

that such residual water nuclei behave very differently, according as the precipitation takes place on solutional nuclei like those of phosphorus, or upon the vapor nuclei of dust-free wet air, or upon the ions; 80 per cent of the nuclei may vanish in the first evaporation in the latter case, fewer in the second case, and none in the first.

In Chapter VI the endeavor is made to standardize the coronas by aid of the decay constants of the ions as found by the electrical method. The curious result follows that in order to make these data agree with those of Chapters III and IV it is necessary to assume an absorption of nuclei varying as the first power of their number as well as a decay by their mutual coalescence. If a be the number of nuclei (ions) generated per second by the radiation, b the number decaying per second, and c the number absorbed per second, the equation $dn/dt = a + bn^2 + cn$ is suggested.

My thanks are due to Miss L. B. Joslin, who not only assisted me in many of the experiments requiring two observers, but lent me efficient aid in preparing the manuscripts and drawings for the press.

CARL BARUS.

BROWN UNIVERSITY, *July*, 1907.

CONTENTS.

CHAPTER I.

EFFICIENCY OF THE PLUG-COCK FOG CHAMBER.

1. Introduction.—In the last few years I have had occasion to use the fog chamber extensively for the estimation of the number of colloidal* nuclei and of ions in dust-free air under a great variety of conditions. These data were computed from the angular diameter of the coronas of cloudy condensation; and it is therefore necessary to reduce all manipulations to the greatest simplicity and to precipitate the fog in a capacious vessel, at least 18 inches long and 6 inches in diameter. To obtain sufficiently rapid exhaustions it is thus advisable to employ a large vacuum chamber, and the one used was about 5 feet high and 1 foot in diameter. The two vessels were connected by 18 inches of brass piping, the bore of which in successive experiments was increased as far as 4 inches; but 2-inch piping, provided with a 2.5-inch plug stopcock, sufficed to produce all the measurable coronas as far as the large green-blue-purple type, the largest of the useful coronas producible in a fog chamber by any means whatever. Moreover, it is merely necessary to open the stopcock as rapidly as possible by hand, using easily devised annular oil troughs at top and bottom of the plug, both to eliminate all possible ingress of room air and to reduce friction. Fog chambers larger than the one measured were often used, and it is curious to note that the efficiency of such chambers breaks down abruptly, while up to this point different apparatus behaves nearly alike. The vacuum chamber is put in connection with an air-pump, the fog chamber with a well-packed filter by the aid of stopcocks. Water nuclei are precipitated between exhaustions from the partially exhausted fog chamber.

2. The variables.—After reading the initial pressures of the fog and vacuum chambers, it is expedient to open the stopcock quickly and thereafter to close it at once before proceeding to the measurement of the coronas. Eventually, *i. e.*, when the temperature is the same in both the fog and vacuum chambers, they must again be put in communication and the pressures noted, if the details of the experiment are to be computed.

*See Smithsonian Contributions No. 1309, 1901; No. 1373, 1903; No. 1651, 1906; Carnegie Institution of Washington Publications No. 40, 1906; No. 62, 1907. In place of the term "colloidal nuclei," the term "vapor nuclei" will be used in preference in the text below. These vapor nuclei of dust-free wet air are probably aggregates (physical or chemical) of water molecules.

The series of variables given in table 1, where p denotes pressure, ρ density, τ absolute temperature, π vapor pressure, is to be considered. The ratio of volumes of the fog and vacuum chambers was about $v/V = 0.064$.

TABLE 1.—Notation. Drop of pressure $\delta p = p - p_3$, observed; $\delta p = p - p_2$, computed.

State No.	Fog chamber.				Vacuum chamber.				Remarks.
1	p	ρ	τ	π	p'	ρ'	τ	π	Initial states; chambers separated.
2	p_1	ρ_1	τ_1	π_1	p'_1	ρ'_1	τ'_1	π'_1	Adiabatic states, after exhaustion; chambers communicating.
3	$\overline{p}_1$	$\overline{\rho}_1$	$\overline{\tau}_1$	$\overline{\pi}_1$	$\overline{p'}_1$	$\overline{\rho'}_1$	$\overline{\tau'}_1$	$\overline{\pi'}_1$	The same, after condensation of water in fog chamber.
4	p_2	ρ_2	τ	π	p'_2	ρ'_2	τ	π	Chambers separated *before* condensation ensued; original temperature regained.
5	$\overline{p}_2$	$\overline{\rho}_2$	τ	π	$\overline{p'}_2$	$\overline{\rho'}_2$	τ	π	Chambers separated after condensation; original temperature regained.
6	p_3	ρ_3	τ	π	p_3	ρ_3	τ	π	Chambers communicating after exhaustion; original temperature restored.

At the beginning (case 1), the fog chamber is at atmospheric pressure p (nearly), the vacuum chamber at the low pressure p', and both at the absolute temperature τ. On suddenly opening the stopcock the adiabatic pressures, etc., given under No. 2 appear, supposing that no condensation has yet taken place in the fog chamber. If the stopcock could now be suddenly closed and the whole apparatus allowed to regain the original temperature τ, the conditions under No. 4 would obtain. This is virtually the case in Wilson's* piston apparatus, and consequently these variables are comparable with his results (*cf.* sections 3 and 4). In my apparatus, however, condensation takes place within the fog chamber before the stopcock can be closed, and thus an additional quantity of air is discharged from the fog chamber into the vacuum chamber. After condensation and before the stopcock is closed the conditions under No. 3 apply; when the stopcock has been closed and the apparatus allowed to regain the room temperature τ, the conditions are shown in No. 5, and may be observed with crude

*C. T. R. Wilson: Phil. Trans., London, vol. 1992, 1889, pp. 405 *et seq.*

approximation in the isolated chamber. Finally, when the chambers are put in communication, the variables (No. 6) are the same in both.

This account of the phenomena may seem prolix, but it is essential to a just appreciation of the efficiency of the plug-cock fog chamber. Quantities in table 1 referring to a given chamber may be connected at a given time by Boyle's law, as for instance, $(p-\pi)=R\rho\tau$. This gives eleven equations, some of which may be simplified. Corresponding quantities in groups 1 and 2, as, for instance, τ/τ_1, may be connected by the law for adiabatic expansion, giving two equations. In addition to this, an equation stating that a given mass of air is distributed in fog and vacuum chambers (volumes v and V, respectively) is available; or

$$(v\rho+V\rho')=v\rho_1+V\rho'_1=\text{etc.}=(v+V)\rho_3$$

All the quantities π are supposed to be given by the corresponding τ, though at high exhaustions the lower limit of known data, $\pi=f(\tau)$, is often exceeded, at least in case of vapors other than water vapor.

3. Approximate computation of p_1 and p_2.—It will first be necessary to compute p_2, the pressure which would be found in the fog chamber when it has again reached room temperature τ, if there were no further transfer of air from fog chamber to vacuum chamber, due to the condensation of water vapor in the former after adiabatic cooling.

For the purpose of obtaining more nearly symmetric equations it seemed to be expedient to write

$$\tau/\tau_1=\Big((p-\pi)/(p_1-\pi_1)\Big)^{1-c/k} \quad \text{and} \quad \tau/\tau'_1=\Big((p'-\pi)/(p'_1-\pi'_1)\Big)^{1-c/k}$$

at the outset, in correspondence with Boyle's law, and thereafter to correct for the temporary introduction of π into the adiabatic equation. Believing that the completed equations would be much more complicated by contrast than they actually are, I made many of the computations, where a mere guidance as to the conditions involved is aimed at, with these symmetrical equations. The constants for use will be computed by the more rigorous forms of sections 4, 5, 8, and 9. Meanwhile the comparison of both groups of equations will make it easier to pass from the equations with $p-\pi$, wherever they were used in my work, to the correct forms of the next paragraph. It is for this reason that the equations now to be given were retained.

The pressure p_2 is given by the gages of the piston apparatus, since there is but a single chamber, and in this respect the plug-cock apparatus differs from it because the corresponding gage-reading is essentially even less than p_2. (Sections 5 and 9.)

The solution when the air in both chambers is continually saturated leads to transcendental equations for the adiabatic pressures $p_1=p'_1$,

which can therefore only be obtained approximately. If the vapor pressures π_1 and π'_1 correspond to p_1 and p'_1, the results would be

$$(p_1-\pi'_1)^{c/k}=\frac{(p_3-\pi)\ (1+v/V)}{(p'-\pi)^{(k-c)/k}+v/V\cdot\Big(1-(\pi_1-\pi'_1)/(p_1-\pi'_1)\Big)^{c/k}(p-\pi)^{(k-c)/k}}$$

$$(p_1-\pi_1)^{c/k}=\frac{(p_3-\pi)\ (1+v/V)}{\Big(1-(\pi'_1-\pi_1)/(p_1-\pi_1)\Big)^{c/k}(p'-\pi)^{(k-c)/k}+v/V\cdot\ (p-\pi)^{(k-c)/k}}$$

where approximate values must be entered for π_1, π'_1, p_1, in the denominator on the right side of the equation.

Similarly

$$(p_2-\pi)=(p_1-\pi_1)^{c/k}(p-\pi)^{(k-c)/k} \qquad (p'_2-\pi)=(p'_1-\pi'_1)^{c/k}(p'-\pi)^{k-c/k}$$

$$\tau/\tau_1=\Big((p-\pi)/(p_1-\pi_1)\Big)^{(k-c)/k} \qquad \tau/\tau'_1=\Big((p'-\pi)/(p'_1-\pi'_1)\Big)^{(k-c)/k}$$

Making use of the values found incidentally elsewhere, the data of table 2 were computed on a single approximation. They are reproduced in the graph (fig. 1).

TABLE 2.—Successive values of pressure and temperature in the plug-cock fog chamber. Volume ratio of fog and vacuum chambers, $v/V=0.064$; $p=76$; $t=20°$ C.; $\pi=1.7$ cm.; t refers to degrees C., τ to absolute temperature. δp denotes the drop in pressure. $\tau/\tau_1=(p/p_1)^{1-c'/k}$ and $\tau/\tau'_1)=(p/p'_1)^{1-c'/k}$ assumed.

Observed.[1]				Computed.[2]				
p'.	p_3.	$\bar{p}_2$.	$\bar{p}'_2$.	p_1.	p'_1.	p_2.	p'_2.	$\bar{p}_2$.
43.5	45.5	47.9	45.6	46.1	46.1	54.7	44.9	49.9
51.5	52.5	54.3	....	52.5	52.5	59.6	52.0	55.5
59.5	59.7	?62.2	....	59.3	59.3	64.6	59.4	61.5
π_1.	π'_1.	$\bar{\pi}_1$.	t_1.	$\bar{t}_1$.	t'_1.	$\delta p_3=p-p_3$.	$\delta p_2=p-p_2$.	$\delta p_2/\delta p_3$.
0.0	2.2	0.7	−17.8°	+ 5.2°	+24.1°	0.0	0.0	
.2	1.9	.9	− 8.3	9.4	21.3	16.3	11.4	0.70
.5	1.7	1.1	+ .8	12.7	19.8	23.5	16.4	0.69
						30.5	21.3	

[1] These observations merely illustrate the equations. No attempt made at accuracy. See chart.
[2] The values of $\bar{\rho}_1/\rho_1=0.91$, 0.93, 0.95, respectively.

The corrections, (p_2-p_3) varying with $(p-p_3)$, lie on a curve which passes through zero, but with a larger slope than for dry air. In fact, they are much in excess of these cases* and throw the whole phenomenon into a lower region of pressures.

*Am. Journ. Science, XXII, p. 342, 1906.

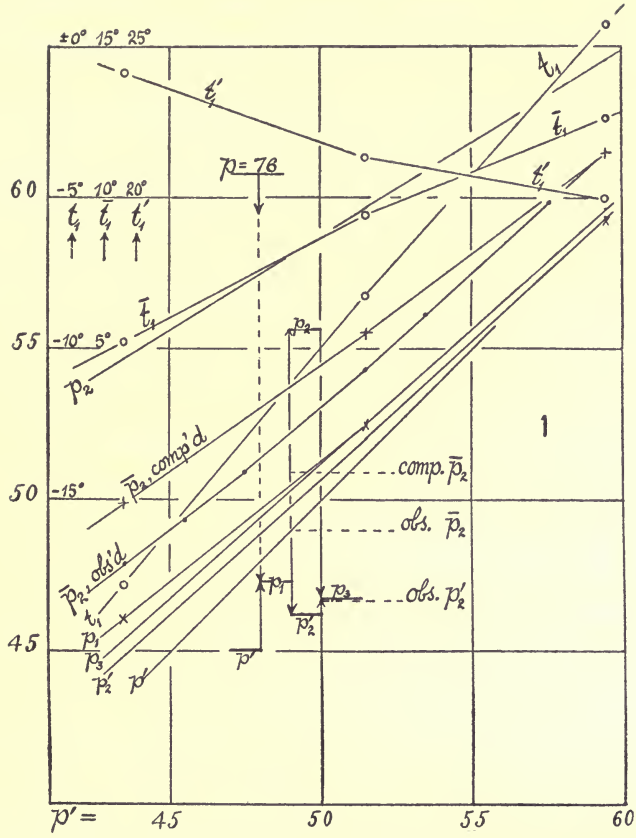

FIG. 1.—Pressures in plug-cock fog and vacuum chambers, for different initial pressures of latter, the former being initially at atmospheric pressure. (See table 1.) The notched curve shows the march of successive pressures for $p'=45$ cm. and $p=67$ cm. in a single exhaustion. The upper curves show corresponding temperatures in the fog and vacuum chambers under like conditions. The adiabatic temperature ratio τ/τ_1 is here an approximation.

A few incidental results deserve brief mention. The first of these is the nearly constant difference of about $\delta p_2 = 2$ cm. between the observed value $\bar{p}_2$ (nominal) and p_3. Since for dry air or not

$$(p'_2 - \pi) + v/V \cdot (p_2 - \pi) = (p_3 - \pi)\ (1 + v/V)$$

is constant for a given exhaustion, $\delta p'_2 = -v/V \cdot \delta p_2$. Hence if $\delta p_2 = 2$ cm., since $v/V = 0.064$, $-\delta p'_2 = 0.064 \times 2 = 0.13$ cm., nearly. This case is illustrated graphically for $p' = 45$ cm. in the notched curves of the figure in a way easily understood. It seems probable that whereas the smaller fog chamber has lost too much air to even approach the isothermal pressures p_2, the large vacuum chamber is only a millimeter short of them when the cock is again closed. The constancy of the observed difference $\bar{p}_2 - p_3$ seemed at first to be referable to the system-

atic method of investigation, though the effect of the precipitated moisture (which has not yet been considered) will largely account for it. (See section 9.)

Anomalous relations in the data for the fog chamber, as in the case of $p'=59.5$ cm., are direct errors of observation. On the other hand, however, since within the ranges of observation $p=a$, $p_2=a_2+b_2p'$, $p_3=a_3+b_3p'$ very nearly, it follows that $(p-p_2)/(p-p_3)$ may approximately be written $A+Bp'$, where a, b, A, B, etc., are constant. Frequently B is negligible, so that $(p_2-p_3)/(p-p_3)$ is constant, in which case the graphs for p_2-p_3 varying with $p-p_3$ pass through the origin.

4. Definite computation of p_1 and p_2.—If the adiabatic equations be written without approximation

$$\frac{\tau}{\tau_1}=\left(\frac{p}{p_1}\right)^{1-c/k} \quad \text{and} \quad \frac{\tau}{\tau'_1}=\left(\frac{p'}{p}\right)^{1-c/k}$$

the equations for p_1 and p_2 become

$$\frac{p_1-\pi'_1}{{p_1}^{1-c/k}}=\frac{(p_3-\pi)\ (1+v/V)}{{p'}^{(1-c/k)}+\frac{v}{V}{p'}^{-c/k}\left(1+\frac{\pi'_1-\pi_1}{p_1-\pi'_1}\right)}$$

and

$$\frac{p_1-\pi_1}{{p_1}^{1-c/k}}=\frac{(p_3-\pi)\ (1+v/V)}{{p'}^{(1-c/k)}\left(1-\frac{\pi'_1-\pi_1}{p_1-\pi_1}\right)+\frac{v}{V}p^{1-c/k}}$$

from which p_1 may be found after putting an approximate form for p_1 (p_3 nearly) into the vapor-pressure term of the second member. A single approximation usually suffices.

From these equations

$$p_2-\pi=\frac{p_1-\pi_1}{{p_1}^{1-c/k}} \quad \text{and} \quad {p'}_2-\pi=\frac{{p'}_1-\pi'_1}{{p'}_1{}^{(1-c/k)}}{p'}^{(1-c/k)}$$

follow at once. Subsidiary equations

$$({p'}_2-\pi)+\frac{v}{V}(p_2-\pi)=(p'-\pi)+\frac{v}{V}(p-\pi)=\left(1+\frac{v}{V}\right)(p_3-\pi)$$

and

$$v/V=\frac{p_3-p'}{p-p_3}=\frac{\delta p'-\delta p_3}{\delta p_3}$$

remain as before in section 3. To compute v/V in this way high exhaustion is essential, otherwise p' and p_3 differ but slightly. Between the present group of equations, which are nearly rigorous, and the preceding group the corrections to be added to the former may be estimated.

5. Computation of v_1/v.—Since $(v_1/v)^{k/c}=p/p_1$, the volume expansion is a cumbersome datum to compute rigorously, and it appears as

$$\frac{v}{v_1}=\frac{p}{p_3-\pi}\,\frac{\left(\frac{p'}{p}\right)^{1-c/k}\left(1-\frac{\pi'_1}{p^{1-c/k}}\right)+\left[\frac{v}{V}\right]\left(1-\frac{\pi_1}{p_1{}^{1-c/k}}\right)}{1+[v/V]}$$

where an approximate value of p_1 (nearly p_3, observed) must be placed

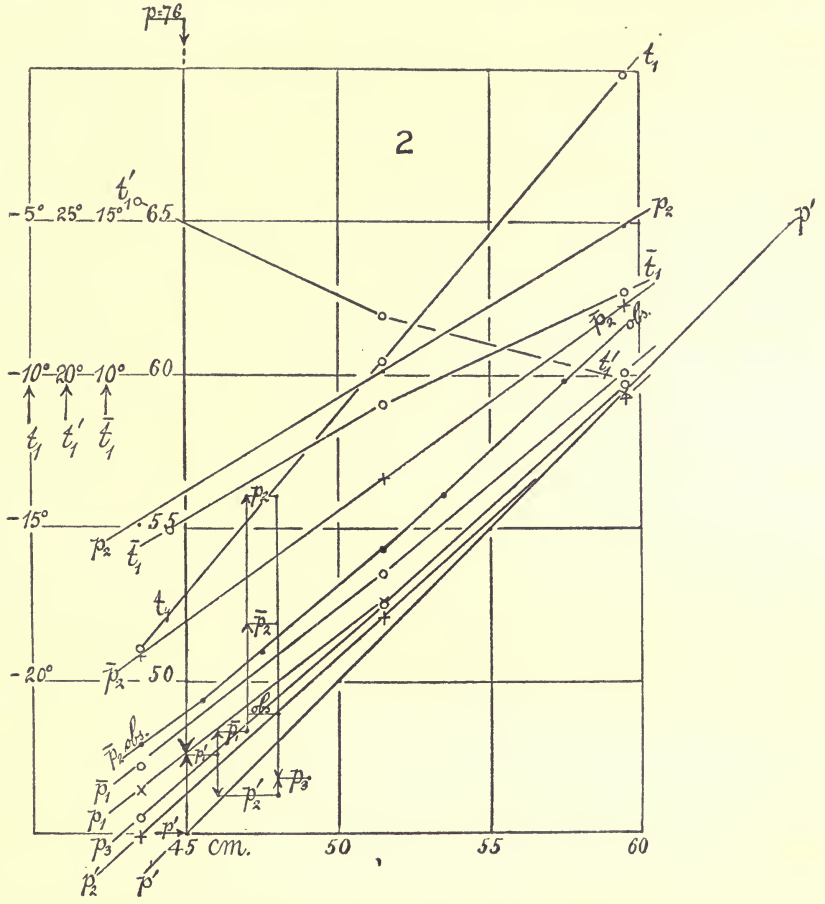

FIG. 2.—Same as fig. 1, if the temperature ratio is corrected and reads $\tau/\tau_1=(p/p_1)^{1-c'/k}$

in the vapor-pressure terms of the second member. For distinction $[v/V]$ here denotes the volume ratio of fog and vacuum chambers. The terms involving vapor pressure may often be neglected, whereupon the equation

$$\frac{v'}{v}=\frac{p'^{(1-c/k)}+v/V\cdot p}{p_3(1+v/V)}=\left(\frac{p}{p_1}\right)^{c/k}$$

reappears, if the equivalent of p_1 be inserted. In these cases p_1 may again be replaced by p_3.

The data for p_1, etc., are given in table 3, and are shown in the graphs of fig. 2, whence their differences from fig. 1 may be ascertained. The respective pressures holding for $p' = 45$ cm. are also shown in a notched curve and will be further elucidated. The ratio $\delta p_2/\delta p_3$ of the isothermal and adiabatic drop is here (table 3) about 0.68, or of the same order as in table 2.

TABLE 3.—Definite computations corresponding to table 2. $p = 76$ cm.; $t = 20°$; $\pi = 1.7$; $\tau/\tau_1 = (p/p_1)^{1-c'/k}$, and $\tau/\tau'_1 = (p/p'_1)^{1-c'/k}$ assumed.

π_1.	π'_1.	$\bar{\pi}_1$.	p'.	p_3.	p_1.	t_1.	t'_1.	p_2.	p'_2.	v_1/v.	$\bar{\rho}_1/\rho$.
						°					
0.1	2.4	0.6	43.5	45.5	46.4	−19.0	25.6	55.1	44.9	1.416	0.920
.2	2.0	.9	51.5	52.5	52.6	− 9.6	21.9	60.1	52.1	1.292	.939
.5	1.7	1.1	59.5	59.7	59.3	− .2	19.8	64.9	59.3	1.181	.958

$\bar{t}_1$.	$\bar{p}_2$.	$\bar{p}_1$.	$10^6 m_1$.	δp_3.	$\delta p_3/p$.	$\frac{\delta p_3-(\pi-\pi_1)}{p-\pi}$	$\delta p_2 = p-p_2$.	$\delta p_3 = p-p_3$.	Ratios $\delta p_2/\delta p_3$.
4.9	50.8	47.2	5.6	30.5	0.401	0.389	0.0	0.0	
9.0	56.6	53.5	4.7	23.5	.309	.297	11.1	16.3	0.677
12.7	62.3	60.1	3.6	16.3	.214	.203	15.9	23.5	.690
							20.9	30.5	

6. Approximate computation of τ_1.—To find the temperature of the fog chamber after the adiabatic temperature τ_1 has been raised by condensation of fog to $\bar{\tau}_1$, it is apparently necessary to compute p_2 first, and then proceed by the method used by Wilson* and Thomson. When the vacuum chamber is large, however, its pressures vary but slightly, and therefore the pressure observed at the vacuum chamber after exhaustion, p_3, when the two chambers are in communication, is very nearly the adiabatic pressure of the fog chamber, p_1. This result makes it easier to compute not only $\bar{\tau}_1$, but incidentally the water, m, precipitated per cubic centimeter (without stopping to compute the other pressures), with a degree of accuracy more than sufficient when the other measurements depend on the size of coronas.

To show this, let d, L, and π refer to the density, latent heat of vaporization, and pressure of water (or other) vapor; let ρ, k, c, τ, denote density, specific heat at constant pressure, specific heat at constant volume, and absolute temperature of the air, the water vapor contained being disregarded apart from the occurrence of condensation. As above let the variables, if primed, belong to the vacuum chamber, otherwise to the fog chamber. Let the subscripts, etc., also be similarly interpreted, so that $\bar{d}$ is the known density of saturated water vapor at $\bar{\tau}°$ absolute.

*C. T. R. Wilson: Phil. Trans., London, vol. 189, p. 298, 1897.

Assuming the law of adiabatic expansion to hold both for gaseous water vapor and for wet air in the absence of condensation, it is convenient in a plug-cock apparatus of fog and vacuum chamber (where p_1 is nearly given by p_3) to reduce to adiabatic conditions; whence

$$\bar{d}=d\left(\frac{p_1-\pi_1}{p-\pi}\right)^{c/k}-\frac{\rho c}{L}\left(\frac{p_1-\pi_1}{p-\pi}\right)^{c/k}(\tau_1-\tau)$$

$$\tau_1=\tau\left(\frac{p_1-\pi_1}{p-\pi}\right)^{(k-c)/k} \qquad m=\frac{\rho c}{L}\left(\frac{p_1-\pi_1}{p-\pi}\right)^{c/k}(\tau_1-\tau)$$

where m is the quantity of water precipitated per cubic centimeter of the exhausted fog chamber. Finally $\bar{d}$, the density of saturated water vapor, must be known as far as $\bar{\tau}$, so that an equation $\bar{d}=f(\bar{\tau})$ is additionally given. Here π_1 the vapor pressure at τ_1, is usually negligible (about 0.5 cm.) as compared with p_1, and p_1 may in practice (where great accuracy is not demanded) be replaced by p_3, which like p is read off, while π holds at τ, which is also read off. In the next section I give a numerical example, taken from table 2, for $p'=43.5$ cm.

If the original equation (isothermal) is taken, $m=5.36\times10^{-6}$ grams per cubic centimeter. If the above equation is taken, $m=5.35\times10^{-6}$. If the same equation is taken and p_1 replaced by p_3, $m=5.30\times10^{-6}$, the error being 1 per cent of the true value, which is near enough in practice or admits of easy correction.

7. Approximate computation of $\bar{p}_2$.—Since the plug stopcock can not be closed before the water condenses in the fog chamber after sudden exhaustion, the pressure observed in the fog chamber when the room temperature reappears is smaller than p_2. An excess of air has passed to the vacuum chamber, so that the pressure within the fog chamber is eventually $\bar{p}_2$, or less. The equation for p_1 and p'_1 remains as in section 3, or better, as in section 4.

The new quantities are

$$\bar{p}_2-\pi=\frac{\bar{\rho}_1}{\rho_1}(p-\pi)^{(k-c)/k}(p_1-\pi_1)^{c/k}$$

$$\bar{p}'_2-\pi=\frac{\bar{\rho}'_1}{\rho_1}(p'-\pi)^{(k-c)/k}(p'_1-\pi'_1)^{c/k}$$

where $\bar{\rho}_1$ is the density of air at $\bar{\tau}_1$. The ratio $\bar{\rho}_1/\rho_1$ may be found when $\bar{\tau}_1$ is known as

$$\frac{\bar{\rho}_1}{\rho_1}=\frac{(\bar{\pi}'_1-\bar{\pi}_1)-(\pi'_1-\pi_1)+(p_1-\pi_1)(1+v/V\cdot\tau'_1/\tau_1)}{(p_1-\pi_1)\ (\tau_1/\tau_1+v/V\cdot\tau'_1/\tau_1)}$$

where $\bar{\tau}'_1$ and τ'_1, $\bar{\pi}'_1$ and π'_1, p_1 and p'_1 are nearly the same. The last equation may usually be written

$$\bar{\rho}_1/\rho_1 = (1 + v/V \cdot \tau'_1/\tau_1)/(\bar{\tau}_1/\tau_1 + v/V \cdot \tau'_1/\tau_1)$$

and the small quantity involving the vapor pressures π treated as a correction. It amounts to about 1 per cent of the large quantity. The values of $\bar{p}_2$ are also given in the table and chart. This shows that $\bar{p}_2$ observed is always smaller than $\bar{p}_2$ computed, even when allowance is made for the condensation of water; *i. e.*, the fog chamber begins to appreciably heat itself above the temperature $\bar{\tau}_1$ before the cock can be closed again, so that when isolated it contains less than its proper quantity of air. Only the initial and the final (both chambers communicating) pressures may therefore be taken at the fog chamber. (*Cf.* section 9.)

8. Rate of reheating of fog chamber.—There is a final question at issue, relating to the rate at which heat flows into the adiabatically cooled fog chamber. Experiments may be made by opening the exhaust cock for stated lengths of time t. The vacuum pressure being $p' = 48.6$, the datum for $t = 0$ second may be computed as $p_2 = 57.8$ cm., or after condensation $\bar{p}_2 = 52.4$ cm. Table 4 contains the results, and they are fully mapped out in chart, fig. 3. The notched curves show the successions of pressure in both chambers. Neither p_2 nor p'_2 may be observed, since the chambers communicate during the opening of the stop-cock for a period certainly longer than 0.1 second. Observable pressures are shown on the vertical line below p_2 and above p'_2. Hence within a quarter of a second the final isothermal pressure ($t = \infty$, chambers communicating) is already regained to more than 60 per cent, and this in spite of the fact that the capacity of the fog chamber is over 6 liters. Hence the attempt to observe $\bar{p}_2$ (isothermal temperature after condensation) at the fog chamber is idle. It practically reaches p_3 if the exhaust cock is open about 10 seconds. The pressure p_2 is never reached, yet $\bar{p}_2$ is exceeded, owing to the counteraction of the vacuum chamber. Finally p_1 may be virtually read off in case of a large vacuum chamber by adding a slight correction for p_3. This is one of the advantages of the method.

TABLE 4.—Rate of heat influx. Barometer, 76.0 cm.

t.	p'.	[1]p'_1.	Observed $\bar{p}_2$.	p'_3.	p_3.
sec.	*cm.*	*cm.*	*cm.*	*cm.*	*cm.*
0.25	48.6	50.2	53.2	50.3	50.6
1	48.6	50.2	52.0	50.2	50.5
2.5	48.6	50.4	51.5	50.4	50.5
5	48.6	50.2	50.9	50.2	50.3
·5	48.6	50.2	52.7	50.2	50.2

From chart $p' = 48.6$; $p_2 = 57.8$; $\bar{p}_2 = 52.4$ cm.
[1]From the chart $p'_1 = 50.2$; $p'_3 = 50.0$.

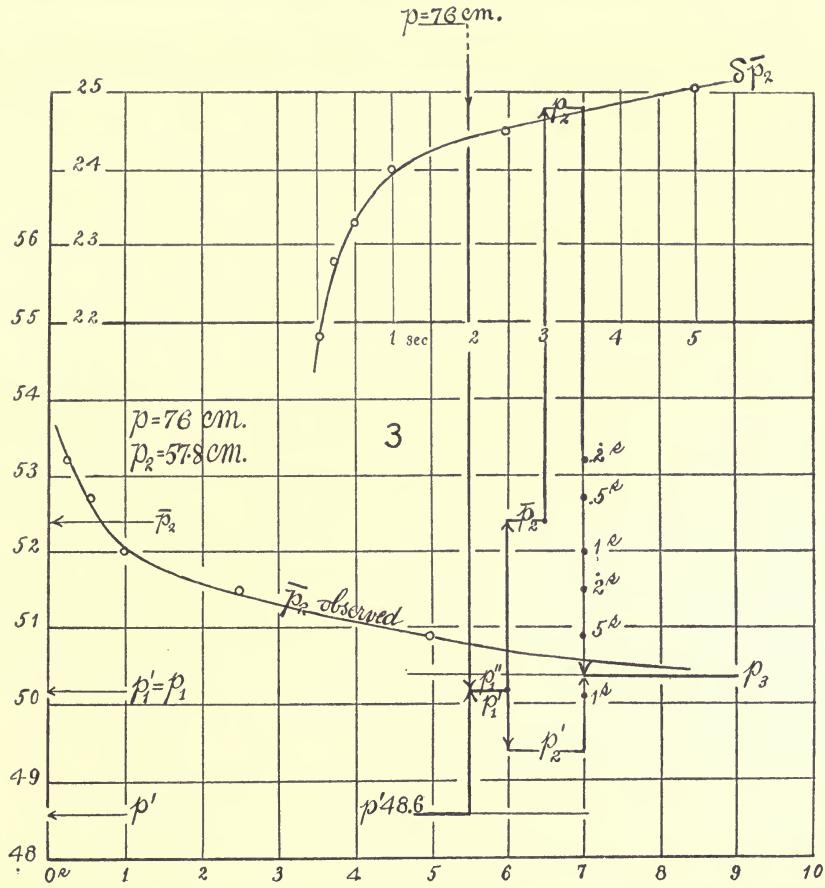

FIG. 3.—Observed value of apparent isothermal pressure $\bar{p}_2$, after lapse of different seconds of time after exhaustion; also corresponding drop of pressure $\delta\bar{p}_2$ from atmospheric pressure.

9. Definite computation of $\bar{\tau}_1$, $\bar{p}_1$, $\bar{\tau}_2$, $\bar{p}_2$, etc.—In view of the equation

$$\frac{\tau}{\tau_1}=\left(\frac{p}{p_1}\right)^{1-c/k}$$

the density of saturated vapor at the temperature $\bar{\tau}$ becomes

$$\bar{d}=d\,\frac{p_1-\pi_1}{p-\pi}\left(\frac{p}{p_1}\right)^{1-c/k}-\rho\,\frac{c}{L}\,\frac{p_1-\pi_1}{p-\pi}\left(\frac{p}{p_1}\right)^{1-c/k}(\bar{\tau}_1-\tau_1)$$

where d is the density of saturated water vapor at τ; ρ, c, L, the density of air, its specific heat at constant volume, and its latent heat. The other quantities have the same meaning as before. Hence the quantity

of water precipitated per cubic centimeter of the exhausted fog chamber is

$$m=\rho\frac{c}{L}\frac{p_1-\pi_1}{p-\pi}\left(\frac{p}{p_1}\right)^{1-c/k}(\bar{\tau}_1-\tau_1)$$

If the coefficient of d in the above equations be written x,

$$\bar{d}=(dx+\frac{\rho cx}{L}\tau_1)-\frac{\rho cx}{L}\bar{\tau}_1=a-b\bar{\tau}_1$$

where a and b are constant, so that $\bar{\tau}$ is the temperature at which the line $\bar{d}$, $\bar{\tau}$, crosses the vapor-pressure curve $\bar{d}=f(\bar{\tau}_1)$, which for water vapor is known as far as —50° C. In place of absolute temperatures τ, degrees centigrade $\bar{t}_1$ and t_1 may be used. Table 5 contains a series of useful data for m, δp (if $p=76$), $\delta p/p$, v_1/v, $\bar{t}_1$, and t_1.

TABLE 5.—Water precipitated at different exhaustions and temperatures. $p=76$ cm.; $\delta p_3=p-p_3$ cm.

$\frac{v_1}{v}$	$\frac{\delta p}{p}$	δp.	At 10° C.			At 20° C.			At 30° C.		
			$m\times10^6$.	t_1.	$\bar{t}_1$.	$m\times10^6$.	t_1.	$\bar{t}_1$.	$m\times10^6$.	t_1.	$\bar{t}_1$.
1.11	0.132	10	1.88	− 1.4	+ 4.6	2.26	+ 8.3	+15.9	2.61	+17.8	26.6
1.24	.263	20	3.41	−14.0	− 1.8	4.18	− 4.8	+10.9	4.91	+ 4.3	22.7
1.43	.395	30	4.48	−28.4	−10.0	5.65	−19.7	+ 4.6	6.75	−11.1	17.8
1.56	.466	40	....	....	....	6.61	−37.1	− 3.3	....	....	....
2.15	.660	50	....	....	....	7.58	−58.3	− 9.5	....	....	....
Incidental data, $\delta p=p-p_1$.											
1.18	0.214	16.3	....	....	....	3.57	−19.0	+12.7	....	....	....
1.29	.309	23.5	....	....	....	4.75	− 9.6	+ 9.0	....	....	....
1.42	.401	30.5	....	....	....	5.58	− .2	+ 4.9	....	....	....

To compute $\bar{p}_2$ and $\bar{p}'_2$ the equations are

$$\bar{p}_2-\pi=\frac{\bar{\rho}_1}{\rho_1}(p_1-\pi_1)\left(\frac{p}{p_1}\right)^{1-c/k} \quad \text{and} \quad p'_2-\pi=\frac{\bar{\rho}'_1}{\rho'_1}(p-\pi'_1)\left(\frac{p^1}{p'_1}\right)^{1-c/k}$$

where $\bar{\rho}_1/\rho_1$, depending upon Boyle's law, will have the same value as before (section 7) and in the approximate form becomes

$$\frac{\tau_1}{\bar{\tau}_1}\frac{1+[v/V](\tau'_1/\tau_1)}{1+[v/V](\tau'_1/\bar{\tau}_1)}$$

Since

$$\frac{\bar{p}_1-\bar{\pi}}{p_1-\pi}=\frac{\bar{\tau}_1}{\tau_1}\frac{\bar{\rho}_1}{\rho_1}$$

with a similar equation for $\bar{p}'_1$, the pressures $\bar{p}_1$ and $\bar{p}'_1$ may be computed, since the values of the second member of the equation are now known.

10. Conclusion.—If the fog chamber is combined with a large vacuum chamber, through a sufficiently wide passageway containing an ordinary plug gas-cock to be opened and closed rapidly by the hand, all the measurable coronas of cloudy condensation, due to the presence of colloidal or vapor nuclei in wet, strictly dust-free air, may be evoked. While such an apparatus admits of capacious fog chambers and extremely simple manipulation, it has not been shown to be inferior in efficiency to any other apparatus whatever.

The conditions of exhaustion must, however, be computed from the initial pressures of the fog and vacuum chambers when separated and their final pressure (after exhaustion) when in communication, in all cases at the same temperature and the volume ratio of the chambers. The chief pressures and temperatures are shown in fig. 2 for different initial pressures of the vacuum chamber, the fog chamber being at atmospheric pressure.

CHAPTER II.

THE CHANGE OF THE VAPOR NUCLEATION OF DUST-FREE WET AIR IN THE LAPSE OF TIME, TOGETHER WITH THE EFFECT OF THE LIMITS OF PRESSURE BETWEEN WHICH A GIVEN DROP TAKES PLACE ON THE EFFICIENCY OF THE FOG CHAMBER.

11. Introduction.—Recently* I published certain results which showed (apparently) that the colloidal nucleation of dust-free air varies periodically in the lapse of time in a way closely following the fluctuations of the barometer. This nucleation (particularly when the larger groups of nuclei lying near the region of ions are taken into consideration) is a maximum when the barometer is a minimum. The development of the investigation was peculiar. At the outset the data appeared like an immediate confirmation of Wood and Campbell's† discovery, which had then just been announced. Maxima of colloidal nucleation appeared where Wood and Campbell had found minima of ionization, and *vice versa*. By supposing that the ions, which are virtually larger than the colloidal nuclei, capture most of the precipitated water, the two sets of results would be mutually corroborative.

Later this cosmical feature of the phenomenon became of secondary importance as compared with an apparent direct effect of fluctuations of the barometer. Nucleation of dust-free air increased when the barometer decreased, and maxima of nucleation were apt to coincide with minima of the barometer. Such a result, whether direct or indirect (removal of radioactive matter from porous earth accompanied by falling barometer), would have been of considerable importance, and great care had to be taken in the endeavor to verify it. Unfortunately the correction to be applied for barometer fluctuation, in its effect upon the aperture of the coronas, was in the same sense and very difficult to estimate; and in fact upon using two fog chambers side by side (one with 2-inch, the other with 4-inch exhaust pipes), adjusted for different sizes of coronas and accentuating the barometric correction, the variations in one vessel might be made to show a tendency to follow the barometer, whereas the other departed from it. Table 6 and fig. 4 give an example of such a case, where δp is the observed fall of pressure $(p-p_3)$, p the pressure of the fog chamber before, p_3 the pressure after

*Carnegie Institution of Washington Publication No. 62, chap. VI, 1907. *Cf.* Science, XXIII, p. 952, 1906; XXIV, p. 180, 1906.

†Wood and Campbell: Nature, LXXIII, p. 583, 1906.

exhaustion with fog and vacuum chamber in communication, all at the same temperature; s is the angular diameter of the corona on a radius of 30 cm., when the source of light and the eye are at 30 cm. and at 250 cm. on opposite sides of the fog chamber. Finally, n shows the number of nuclei per cubic centimeter.

TABLE 6.—Time variation of the larger colloidal nucleation of dust-free air. Conical filter. δp readjusted. App. I, 4-inch pipes; app. II, 2-inch pipes.

Date, etc.		Apparatus I.					Apparatus II.			
		δp_1.	s_1.	p.	s'_1.	$n \times 10^{-3}$.	δp_2.	s_2.	s_2.	$n_2 \times 10^{-3}$.
July 12,	$8^h 50^m$	27.1	3.9	76.2	3.9	19	25.5	2.9	3.3	10
	3 45	27.2	5.1	76.2	4.9	37	25.5	2.6	3.0	7
	5 35	27.1	5.2	76.1	5.1	41	25.7	3.2	3.0	7
July 13,	10 40	27.3	5.2	76.1	4.8	35	25.4	3.1	3.7	16
	3 00	27.1	5.2	76.1	5.1	41	25.4	2.5	3.3	10
	5 30	27.2	5.0	76.0	4.7	33	25.6	2.5	2.4	3.7
July 14,	8 41	27.2	5.6	76.0	5.3	46	25.4	2.6	2.0	2.1
	3 20	27.2	5.0	75.9	4.6	30	25.6	2.4	2.3	3.0
	6 00	27.4	5.7	75.8	5.0	39	25.7	3.0	2.6	5.2
July 15,	8 00	27.3	5.2	75.9	4.7	33	25.6	3.1	3.0	7.4
	3 30	27.2	5.6	75.9	5.2	43	25.2	2.6	3.5	12.7
	5 25	27.2	5.2	75.9	4.8	35	....	....	....	....
July 16,	9 00	27.3	5.5	75.7	4.9	37	25.5	2.9	2.9	6.7
	2 30	27.3	5.4	75.7	4.8	35	25.6	3.1	2.9	6.7
	6 00	27.5	6.3	75.6	5.4	49	25.4	2.8	3.0	7.4
July 17,	9 00	27.3	5.7	75.5	5.0	39	25.7	3.5	2.8	6.2
	4 00	27.3	6.7	75.3	5.8	58	25.6	3.2	2.6	5.2
July 18,	9 51	27.2	5.5	75.8	5.0	39	25.2	2.5	3.4	11.5
	3 55	27.3	5.4	75.8	4.8	35	25.7	2.9	2.4	3.7
	9 15	27.4	5.1	76.3	4.6	30	25.6	2.6	2.4	3.7
	2 30	27.3	5.2	76.2	4.8	35	25.6	2.8	2.7	5.9
	6 10	27.4	6.1	76.2	5.6	54	25.6	2.0	1.9	2.0

While the data for apparatus I still recall the barometer graph, this is not the case for apparatus II, and neither of the graphs I or II are as strikingly suggestive of the variations of atmospheric pressure as was the case in the earlier report. The discrepancy in the new results may be an overcompensation, although all the details of the experiments themselves were gradually more and more fully perfected; or the rise in the region of ions may just balance the decrease of the number of efficient colloidal nuclei due to the increase of the former. In fact the region where ions predominate may rise while the regions where the vapor nuclei are more important may correspondingly decrease, producing a diminished slope of the initial part of the graph such as is often actually observed. It is necessary, therefore, to inquire somewhat more carefully into the errors involved, to investigate some datum or invariant which if kept constant will mean a corona of fixed aperture in the given apparatus, unless there is actual radiation in varying amount entering from without.

I purpose, therefore, in the present paper, to study the same phenomenon for an artificial barometer; in other words, to accentuate the present discrepancies, let the pressure drop from a given upper limit to varying lower limits, as well as from varying upper limits to a given lower limit. The results so obtained are enormously different for the same drop of pressure. Much of this would be anticipated; but the question nevertheless arises whether the colloidal nucleation of the gas is actually dependent in so marked a degree on its initial pressure, or whether this dependence can be explained away.

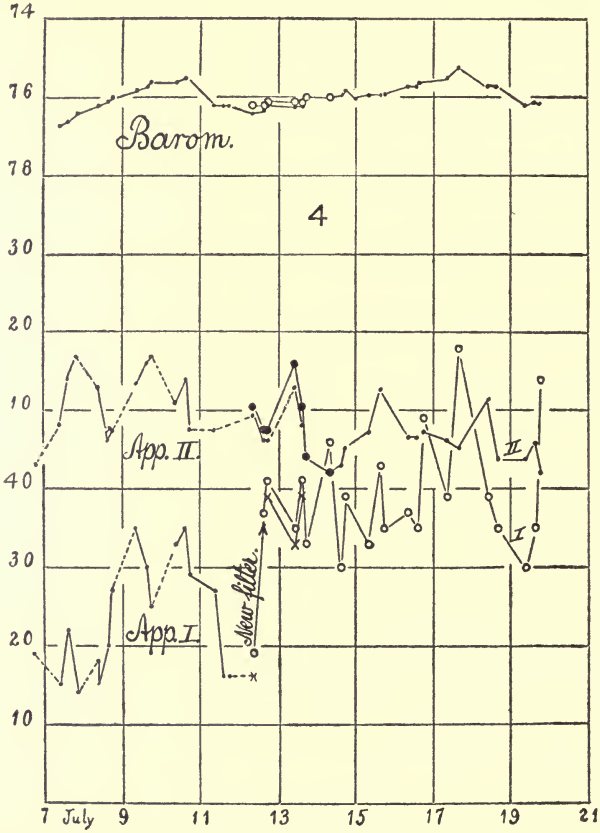

FIG. 4.—Apparent nucleation of dust-free air in lapse of time. Apparatus I with 4-inch exhaust pipes; apparatus II with 2-inch exhaust pipes; otherwise identical. A new and more pervious filter was installed on July 11. The upper curve shows corresponding barometric pressure within the fog chamber.

Later in the course of the work I made additional comparisons with the contemporaneous ionization of the air determined by Miss L. B. Joslin and with the temperature of the fog chamber as distinguished from the temperature of the air. These results as a whole finally showed that a direct dependence of the vapor nucleation of the dust-free air

in the fog chamber on the barometer, on the ionization of the air, on any form of external radiation, or on the temperature of the atmosphere, can not be detected. All the variations may be referred to the temperature of the fog chamber itself, as if it generates increasing numbers of colloidal nuclei as its temperature increases. Since the colloidal nuclei in dust-free moist air are to be associated (from my point of view)* with the saturated vapor, and are only secondarily dependent upon the air itself, the result so obtained is curious, as one would expect a decrease of the colloidal nucleation with rise of temperature. Correction for the increased water precipitated at higher temperatures merely accentuates the difference. If τ_1 is the low (absolute) temperature obtained by sudden expansion adiabatically from τ the ratio τ_1/τ should be wholly dependent upon the corresponding pressures; and yet, for the same ratio, more nuclei are obtained as τ is larger. This difference of behavior is maintained for larger and smaller ratios of τ_1/τ, in like degree.

12. Data.—The results are given in tables 7 and 8, and refer to a fog and vacuum chamber, the volume ratio of which is about $v/V = 0.06$, combined with sufficiently wide piping (2-inch bore) and an interposed (2.5-inch) stopcock. The former communicates with the filter, the latter with the air-pump. At the same temperature the fog and vacuum chambers are initially (before exhaustion) at pressures p and p', finally at pressure p_3, when in isothermal communication after exhaustion; p_2 and p'_2, respectively, would be the pressures at the given temperature if the chambers could be isolated immediately after exhaustion and before the precipitation of fog. P denotes the barometric pressure, and p_m the initial gage-reading within the fog chamber before exhaustion, so that the drop of pressure is (apart from the moisture content, which will be treated in turn below) $\delta p = P - p_m - p_3$, and the drop of pressure takes place from $p = P - p_m$ adiabatically to p_1, isothermally to p_2 if the fog chamber were isolated as specified, or isothermally to p_3 when fog and vacuum chambers are left in communication.

For a given value of P the same drop of pressure δp may thus be obtained in two ways—either by giving a suitable value to p_m, *i. e.*, by starting with a partially exhausted fog chamber and a vacuum chamber at fixed exhaustion p', which implies a nearly fixed p_3; or by keeping p_m constant (small, nearly zero), thus starting with the fog chamber about at atmospheric pressure, and determining p' of the vacuum chamber and therefore p_3.

Briefly, then, the condensational effects of a given difference δp when lying between different pressures p and p_3, are to be tested, and this is best accomplished by constructing separate complete graphs for the aperture $s/30$ of the coronas, first by keeping p' and p_3 nearly constant

*Am. Journ. Sci., XXII, p. 136, 1906.

and varying p_m (lower pressure limit, p, variable) and second by keeping p fixed and varying p' and p_3 (upper pressure limit variable). Tables 7 and 8 show these data, the latter for a wider range of coronas than the

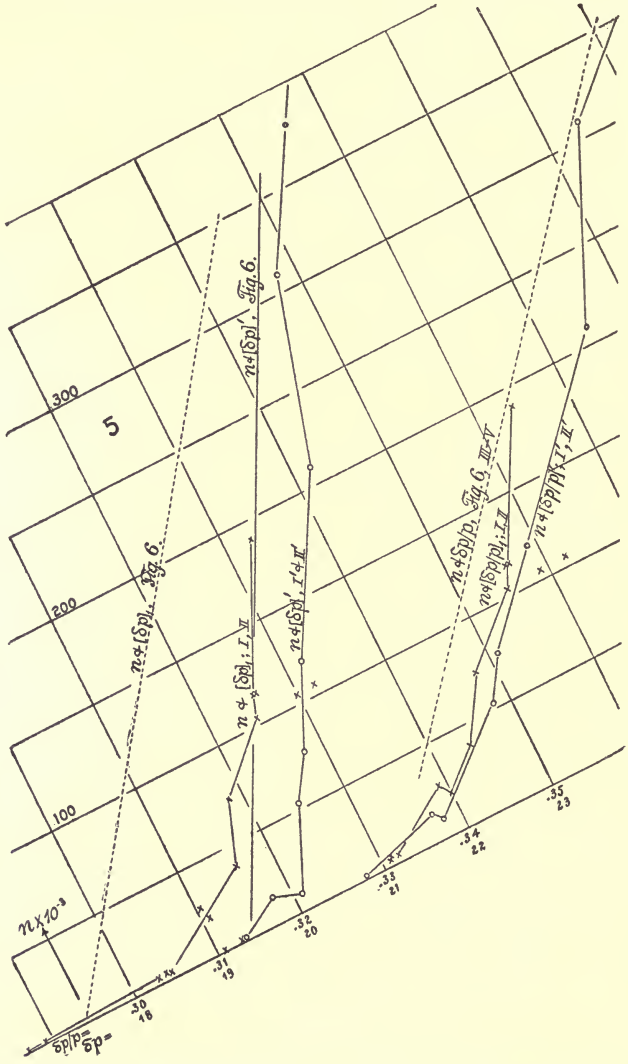

FIG. 5.—Nucleation of dust-free air for different drops of pressure $\delta p = p - p_2$; $[\delta p]'$ denoting that the upper limit, $[\delta p]_1$ that the lower limit of the drop of pressure δp is varied. Also corresponding nucleation referred to the exhaustion $\delta p/p$. Four series. Small ranges of nucleation as compared with fig. 6.

former, while n denotes the number of nuclei per cubic centimeter. From s the number of nuclei, n, per cubic centimeter is computed.

The results, moreover, are graphically given in figs. 5 and 6, the abscissas being the drop $\delta p = p - p_2$, the ordinates $n \times 10^{-3}$. It will be seen at once that the two curves ($[\delta p]_1$ denoting that the lower limit of pressure,

$[\delta p]'$ that the upper limit of pressure is varied) are strikingly distinct in both figures and that the variation of the lower pressure limit $[\delta p]_1$ corresponds, as it should, to a highly increased efficiency of the fog chamber. The coronal fog limits are far apart, being respectively below $[\delta p]_1 = 17.4$ and $[\delta p]' = 19.4$ cm. in fig. 6, where all data (table 8) were obtained in one series of experiments.

TABLE 7.—Effect of varying p in $\delta p = p - p_3 = P - p_m - p_3$. Chamber II. Bar. $= p = P - p_m$. $v/V = 0.064$; $p - p_2 = 0.775\ \delta p$; $\pi = 2.3$; $t = 25°$ C.; $\pi - \pi_1 = 1.8$.

	P.	p_m.	$P-p_3$.	δp.	s.	Cor.	$n \times 10^{-3}$.	$\delta p/p$.	p.
I.....	75.7	[1]0.2	27.3	27.1	6.9	g′ B P	[2]105	0.359	75.5
		.1	.5	.4	6.9	g′ B P	[2]106	.362	75.6
		1.0	.5	26.5	7.0	g′ B P	104	.355	71.7
		2.0	.3	25.3	5.1	.....	39	.344	73.7
		2.0	.6	25.6	6.4	w y	72	.348	73.7
		3.0	.6	24.6	4.5	.....	27	.339	72.7
		3.0	.7	24.7	4.2	.....	21	.340	72.7
		4.0	.8	23.8	2.5	.....	4.3	.332	71.7
		4.0	.7	23.7	2.4	.....	3.5	.331	71.7
		6.0	.6	21.6	1.5	.....	1.4	.311	69.7
II.....	75.7	[3]0.1	27.6	27.5	9.5	w r	190	.364	75.6
		4.0	.7	23.7	2.4	.....	3.9	.331	71.7
		1.0	.6	26.6	7.1	g′ B P	116	.356	74.7
		6.0	.8	21.8	1.8	.....	1.6	.313	69.7
		1.0	.6	26.6	7.5	g′ B P	116	.356	74.7
I′.....	75.5	0.2	24.9	24.7	1.7	.....	1.8	.328	75.3
$t = 21.4°$ C.		....	25.6	25.4	3.6	.....	15	.337	
$\pi = 1.9$.		....	26.4	26.2	5.6	.....	53	.348	
$\pi - \pi_1 = 1.4$.									
II′.....	[4]76.2	.2	25.9	25.7	3.2	cor	9.5	.338	76.0
$t = 23°$ C.			26.9	26.7	6.4	w p	76	.351	
$\pi = 2.1$.			27.4	27.2	6.8	g B P	120	.359	
$\pi - \pi_1 = 1.6$.			28.7	28.5	10.2	w r	210	.375	
			29.4	29.2	12	y r	310	.384	
			30.5	30.3	13?	g B P	380	.399	
			33.5	33.2	13?	Do	410	.437	
[5]I.....	75.5	.2	24.9	24.7	1.7	.....	1.8	.328	75.3
$t = 23°$ C.			25.6	25.4	3.6	.....	15	.337	
$\pi = 2.1$.			26.4	26.2	5.6	.....	53	.348	
$\pi - \pi_1 = 1.6$.									

[1] Water nuclei not precipitated.
[2] Too small. Initial values.
[3] Water nuclei precipitated. Coronas usually blurred.
[4] From Carnegie Institution of Washington Publication No. 62, chapter II, table 26.
[5] *Ibid.*, chapter VI, table X.

In fig. 5 the results of series I′ and II′ are taken from data for the same apparatus in an earlier report to the Carnegie Institution of Washington.* Consequently some reconsideration is needed. In the lapse of time the efficiency of the fog chamber has for some reason increased, for the new results (fig. 6 and dotted line in fig. 5) are distinctly higher in nucleation than those quoted from the report.

*Carnegie Institution of Washington Publication No. 62, chapters II and VI, 1907.

Compared with the graph n and $[\delta p]'$, table 7, where the upper limit only is varied, the graph n and $[\delta p]_1$ lies in the main above it, in the smaller exhaustions, and it should be remembered that the range of variation is here smaller. But it does not lie as much above n and $[\delta p]'$ throughout as would be expected, seeing that only the upper points

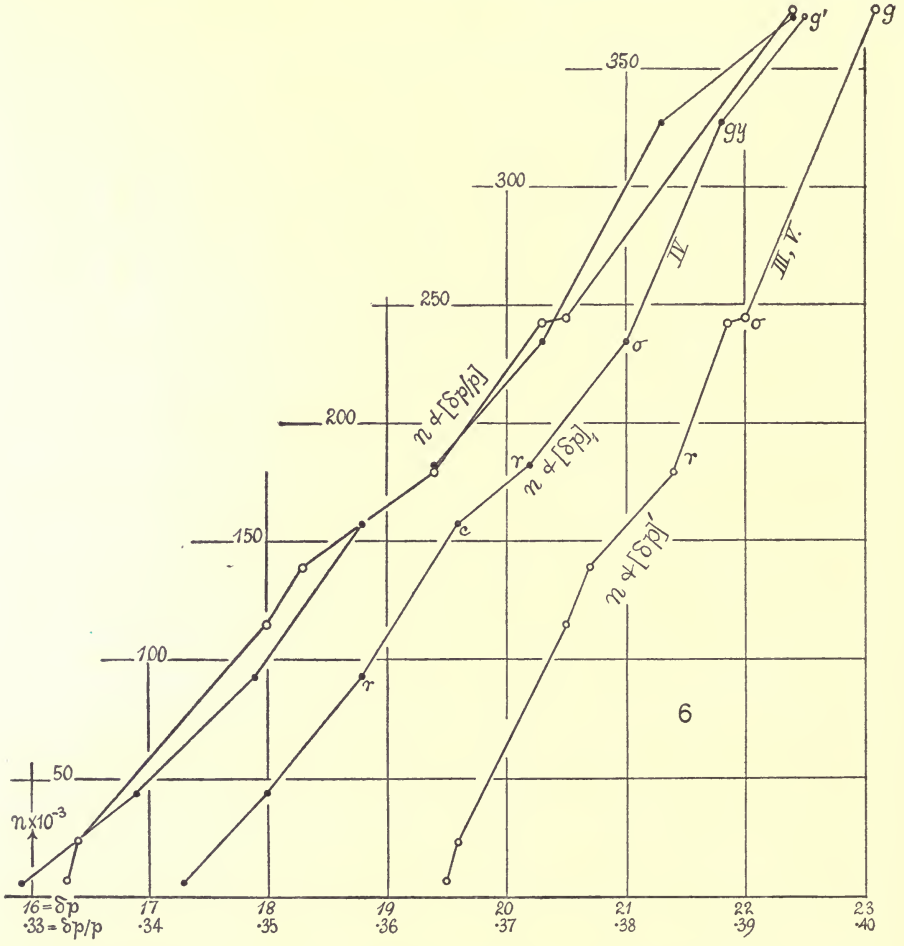

FIG. 6.—Nucleation of dust-free air for different drops of pressure $\delta p = p - p_2$; $[\delta p]'$ denoting that the upper limits, $[\delta p]_1$ that the lower limit of the drop of pressure δp is varied. Also corresponding curve referred to the exhaustion $\delta p/p$. Three series. Larger ranges of nucleation than in fig. 5.

should coincide, intimating that there is some variation as compared with fig. 6 not accounted for. This becomes specially evident when the two graphs for $[\delta p]$ in figs. 5 and 6 are compared, as shown in the former.

TABLE 8.—Data[1] corresponding to table 7 for larger ranges of δp.

	P.	p_m.	$P-p_3$.	$\delta p = p-p_3$.	s.	Cor.	$n \times 10^{-3}$.	p.
III.....	75.8	0.1	27.6	27.5	9.1	w r	179	75.7
$\pi = 2.5$		....	28.5	28.4	11.5	[2]w r o	244	....
$\pi - \pi_1 = 2.0$		....	29.1	29.0	11.8	[2]w r o	332	....
		....	29.9	29.8	....	g	375	....
		....	26.8	26.7	8.0	....	139	....
		....	25.4	25.3	4.3	....	24	....
		....	26.6	26.5	7.3	....	115	....
IV.....	75.8	.1	30.0	29.9	....	g y o	340	75.7
$\pi = 2.5$		1.0	30.1	29.1	....	g′ o	372	74.7
$\pi - \pi_1 = 2.0$		2.0	30.2	28.2	11	g y o	327	73.7
		3.0	30.1	27.1	11	w r o	234	72.7
		4.0	30.1	26.1	9.5	w r	182	71.7
		5.0	30.3	25.3	8.6	w c	157	70.7
		6.0	30.3	24.3	7.0	w r	93	69.7
		7.0	30.3	23.3	5.4	....	44	68.7
		8.0	30.3	22.3	2.8	....	5.7	67.7
V.....	75.8	.1	28.3	28.2	11	y′ r o	242	75.7
$\pi = 2.5$		.1	25.3	25.2	2.9	....	6.6	
$\pi - \pi_1 = 2.0$								

[1] Color distortion. The value of s corresponds to g y at least.
[2] Fog chamber cleaned of water nuclei after each observation.

13. Explanation.—It will next be necessary to endeavor to coordinate the two curves for $[\delta p]_1$ and $[\delta p]'$. If the absolute temperatures of the air within the fog chamber before and after exhaustion are τ and τ_1 (adiabatic pressure p_1) then apart from the condensation of water vapor at the original vapor pressure π at τ, we may write as one *extreme case*,

$$\frac{\tau_1}{\tau} = \left(\frac{p_1 - \pi}{p - \pi}\right)^{(k-c)/k}$$

With a large vacuum chamber the difference between p_1 and p_3 is very small relatively to p_1 and p_3, so that for the present purposes $p - p_3 = p - p_1 = \delta p$ (nearly), whence

$$\frac{\tau_1}{\tau} = \left(1 - \frac{\delta p - (\pi - \pi_1)}{p - \pi}\right)^{(k-c)/k}$$

Similarly we may write as a second *extreme case*,

$$\tau_1/\tau = (1 = \delta p/p)^{(k-c)/k}$$

or the degree of sudden cooling from a fixed temperature τ to the adiabatic temperature τ_1 depends primarily on $\delta p/p$. This would in any case be permissible for comparison in table 6, where a continuous series of experiments is made at the same temperature. The moisture error is thus a constant throughout. Hence the apertures of coronas s, and the nucleation n, will be a function of $\delta p/p$ to the degree specified.

In table 9 I have, therefore, arranged the data for n with reference to the corresponding values of $\delta p/p$, both for the cases of I, II, III, and V, where the upper pressure limit of the drop δp (curve $[\delta p]'$), and cases I′, II′, IV, where the lower pressure limit of the drop δp (curve $[\delta p]_1$), are varied. This result is also given in the chart (figs. 5 and 6) and the mean results of the latter are suggested by the dotted line in the former.

In fig. 5 the curious result is obtained that the data for $[\delta p]'$ are now liable to lie even above those for $[\delta p]_1$ which is the inversion of the former case. As a whole, however, and with due regard to the subtleties involved, the two sets of data practically belong to the same curve, for the departure of either in the long run is seen to be positive as well as negative. The results of fig. 5 (as has been stated) were obtained in a single series of observations, all at the same temperature. If they be compared with fig. 5 (dotted line), containing observations made at other times, they lie distinctly above the graph of the figure, no matter whether $[\delta p/p]'$ or $[\delta p/p]_1$ is in question. Hence it is again probable that something else besides mere variation of the barometer is in question and is not accounted for in the correction. Thus it is next necessary to inquire into the effects of vapor pressure, which in series I and II would differ from series I′ and II′, though in series I, II, III, IV, and V the temperatures are so nearly alike that shifting of graphs due to this disturbance is not appreciable.

TABLE 9.

Summary of table 7.				Summary of table 8.			
$\delta p/p$.	$n\times 10^{-3}$ I′ and II′.	$\delta p/p$.	$n\times 10^{-3}$. I and II.	$\delta p/p$.	$n\times 10^{-3}$. III and V.	$\delta p/p$.	$n\times 10^{-3}$. IV.
0.328	2	0.311	1	0.333	7	0.329	6
.337	15	.313	2	.334	24	.339	44
.337	15	.331	3	.350	115	....	...
.338	10	....	...	.353	139	.349	93
.348	53	.331	4	....	...	.358	157
.348	53	.332	4	.364	179	.364	182
.351	76	.339	27	.373	242	.373	234
.359	120	.340	21	.375	244	....	...
.375	210	.344	39	.383	246	.382	327
.384	310	.348	72	.394	375	.390	372
.399	380	.355	104	.395	340	.395	340
.437	410	.356	116				
		.356	116				
		.359	105				
		.362	106				
		.364	190				

14. The effect of vapor pressure.—The second extreme limit,

$$\tau/\tau_1=\left(1-\left(\delta p-(\pi-\pi_1)\right)/(p-\pi)\right)^{(k-c)/k}$$

may now be used and the data for nucleation, n, expressed in terms of $\delta p-(\pi-\pi_1)/(p-\pi)$ as the variable for comparison. Remembering

that the total variation of pressure to bring out the coronal phenomenon does not much exceed 3 cm., and that the observations below will be made within a single centimeter, the precipitation of moisture may be treated as depending on τ/τ_1, the ratio of the initial and the final temperature of adiabatic cooling if the former is nearly constant and if the same medium is retained, though the case is in reality more complicated. These data are also given in table 9 and have been inserted in fig. 7.

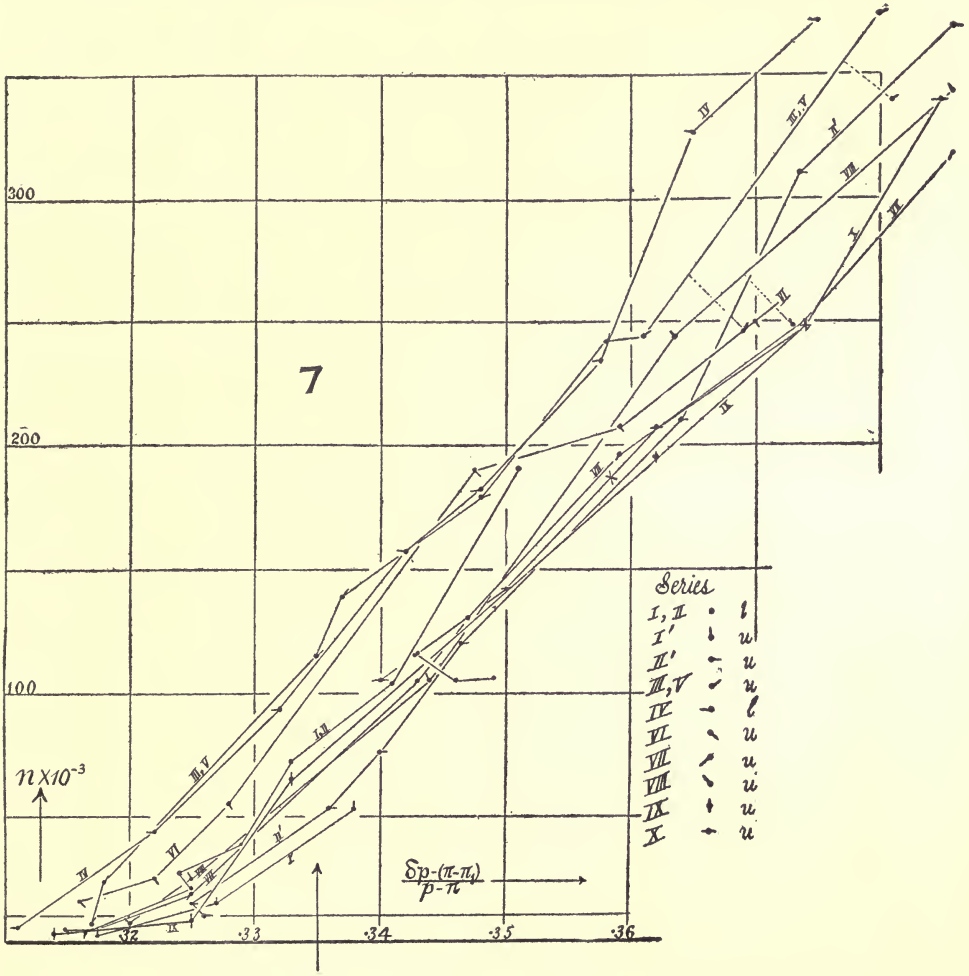

FIG. 7.—Nucleation found at different drops of pressure. Second extreme case.

The graphs III, IV, and V are now even more coincident, whereas I and II, I′ and II′ differ from each other and from III and V in the same sense as above. Hence, apart from barometric pressure, some other cause must have influenced these nucleations.

I conclude, therefore, that by far the greater part of the dependence of the vapor nucleation upon the barometer is the necessary result of the thermodynamics of the case, but that conclusive evidence of the absence of other causes either within or without the fog chamber on the time variation of its nucleation, though extremely difficult to make out, seems as yet to be outstanding.

15. New data for vapor nucleation in the lapse of time.—In table 10 results of the same character as the preceding have been collected. Moreover, by choosing a particular $\delta p-(\pi-\pi_1)/(p-\pi)=0.320$ and reducing all data for n to this value, the result so found ($n_{0.320}\times 10^{-3}$) should be independent of atmospheric pressure, etc., and respond to external radiation if such exists. The data are shown in fig. 8*a*. They are not out of keeping with Wood and Campbell's phenomena as a whole, but they do not follow the barometer. The correction of n is about 1.7 per 0.001 of the pressure ratio, but it is too uncertain in this region, since the graphs are of pronounced curvature.

TABLE 10.—Time variation of the larger colloidal nucleation of wet dust-free air. Conical filter. Apparatus II with 2-inch pipes, cleaned by precipitation before observation. $p_m=0.1$; $p=P-p_m$; $p-p_2=19.9$.

Date, etc.	δp.	s.	P.	$\delta p/p$.	$n\times 10^{-3}$.	$\frac{\delta p-(\pi-\pi_1)}{p-\pi}$	$n_{0.320}\times 10^{-3}$.
Aug. 6, 5^h16^m	25.7	4.2	76.7	0.335	21	0.318	24
5 25	25.7	4.4	76.7	.336	26	.319	28
Aug. 7, 10 00	25.7	4.3	75.0	.339	24	.323	19
10 10	[1]25.7	3.7	75.9	.338	16	.323	11
10 20	25.7	4.1	75.9	.339	20	.323	15
3 5	25.7	4.2	75.7	.340	21	.321	19
3 15	25.7	4.2	75.7	.340	21	.321	19
Aug. 8, 10 40	25.3	3.6	75.7	.335	14	.317	19
10 50	25.5	4.0	75.7	.337	18	.320	18
11 00	26.0	4.9	75.7	.344	36	.327	24
5 40	25.9	4.9	75.7	.342	36	.325	28
	25.6	4.3	75.7	.339	23	.321	21
Aug. 9, 9 30	25.6	3.8	75.8	.338	17	.321	15
9 40	25.8	4.2	75.8	.341	21	.324	14
4 00	25.7	4.5	75.8	.340	27	.319	29
4 10	25.7	[2]3.9	75.8	.340	[2]18	.319	20
4 20	25.7	5.1	75.8	.340	40	.319	42

[1] Not cleaned by precipitation.

Hence in table 11 a larger fiducial value $(\delta p-[\pi-\pi_1])/(p-\pi)=0.335$ was selected in turn, as the graphs in this part of the field (see arrow in fig. 7) are more nearly straight. At the outset complete series of results (August 10, 11, and 12) were investigated; subsequently but three observations in the neighborhood of the abscissa 0.335 fully sufficed. The completed graphs are given in fig. 7 and marked VI to X. Their position is throughout low as compared with III to V, for which there is

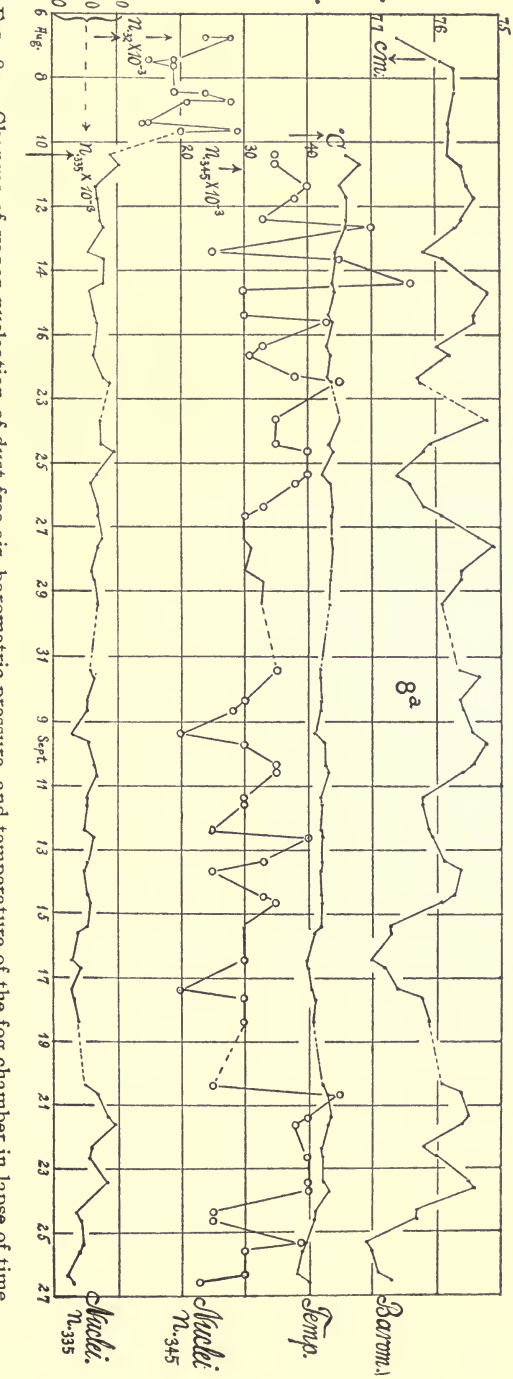

FIG. 8a.—Changes of vapor nucleation of dust-free air, barometric pressure, and temperature of the fog chamber in lapse of time.

now no reason referable to causes within the fog chamber, unless there exists a singularly marked temperature effect, presently to be investigated. Series VI alone is peculiar, showing a strong initial tendency to return to the earlier set, III to V. Water nuclei were precipitated before each observation. The data for $n_{0.335}$ are also inscribed in fig. 8*a* and fig. 8*b*, where they are compared with the barometer and the temperature of the fog chamber in a general way.

Table 11 also contains the corresponding values of $\delta p/p$ and the nucleations n derived from the new investigations in Chapter IV. From these the values $n_{0.340}$ for $\delta p/p = 0.340$ and $n_{0.345}$ for $\delta p/p = 0.345$ are derived to be used in the correlative summary in sec. 20. The nucleations, $n_{0.345}$, which suffice for the purpose, are given with the others in figs. 8*a* and 8*b*.

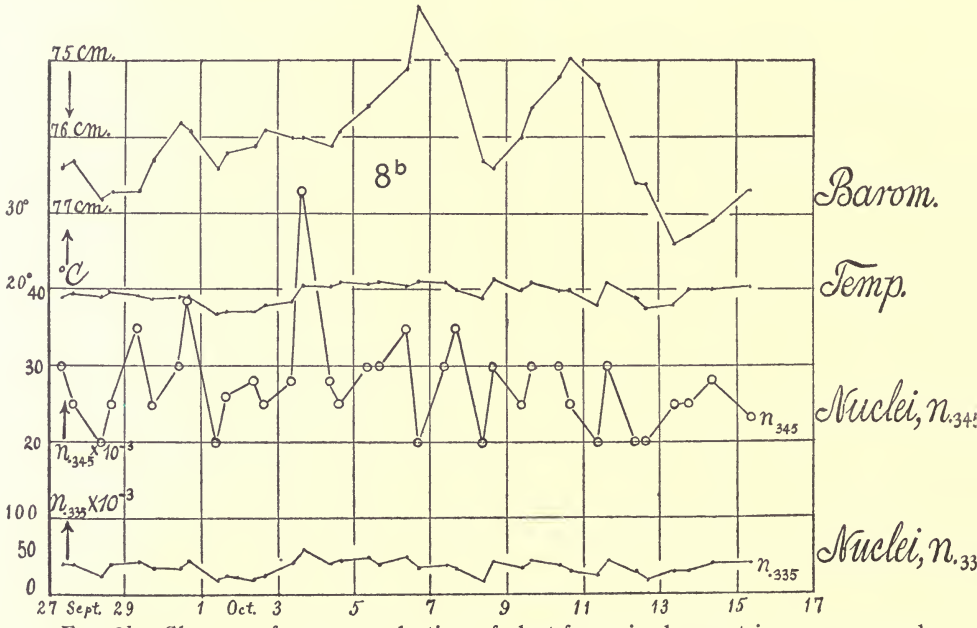

FIG. 8*b*.—Changes of vapor nucleation of dust-free air, barometric pressure, and temperature of the fog chamber in the lapse of time.

The data for $n_{0.335}$ in figs. 8*a* and 8*b* sometimes follow the barometer, sometimes depart widely from it; but coincidence will usually occur only when both accompany the same temperature effect. As a rule there is a rise of nucleation from morning to afternoon, suggesting the phenomenon due to external radiation discovered by Wood and Campbell (section 1), but in these cases temperature is also apt to rise coincidently. The rise in question fails to occur but 4 times out of the 13 observed in August, but 7 times out of the 24 observed in September (2 being neutral), and but 5 times out of the 13 observed in October.

TABLE 11.—Time variation of the larger colloidal nucleation of dust-free wet air. Corresponding to table 10, with allowance for temperature. $\delta p = p - p_3$; $p_m = 0.1$; $p - p_2 = 0.77 \times \delta p$.

Date, etc.	δp.	s.	p.	t.	$\frac{\delta p - (\pi - \pi_1)}{p - \pi}$	$n \times 10^{-3}$.	$n_{033 \cdot 5} \times 10^{-3}$	$\frac{\delta p}{p}$	$n \times 10^{-3}$.	$n_{0 \cdot 340} \times 10^{-3}$ / $n_{0 \cdot 348} \times 10^{-3}$
				°						
Aug. 10, 9h30m	25.7	3.9	75.8	26.0	0.323	18	(90)	0.339	13.3	18.5
4 40	25.7	3.9	....	26.0	.323	18		.339	13.3	35
4 20	25.7	4.4	75.6	28.0	.321	25		.340	18.5	....
4 30	25.7	4.4	....	28.0	.321	25		.340	18.5	....
4 40	25.7	4.4	....	28.2	.322	25	105	.340	18.5	18.5
	25.3	3.7	75.6	28.2	.316	16		.335	11.3	35
	26.2	5.7	....	28.2	.328	55	VI.	.347	39.0	....
	27.6	[1]9.6	....	28.2	.347	190		.365	185	....
	28.4	[2]11.0	....	28.2	.359	207		.376	280	....
	29.2	[3]11.5	....	28.2	.370	250		.386	320	....
Aug. 11, 8 50	27.3	[4]7.8	75.5	25.8	.347	130	70	.362	100	15.2
	25.1	2.3	....	25.8	.317	3	to	.332	2.6	40
	25.7	4.1	....	25.8	.325	19	65	.340	15.2	....
	27.0	[2]7.3	....	26.0	.343	105	VII.	.358	83.5	....
	28.2	[1]10.6	....	26.0	.359	206		.374	253	....
	29.3	[2]11.5	....	26.0	.374	250		.388	320	....
	30.2	g y o	....	26.0	.386	318		.400	....	....
5 00	25.3	3.0	75.4	26.0	.320	7	65	.336	5.5	18.5
	25.7	4.4	....	....	.325	25	to	.340	18.5	38
	27.1	[4]7.3	....	....	.344	105	80	.359	83.5	....
	28.5	[3]11.0	....	....	.363	244		.378	280	....
	29.2	[3]11	75.4	....	.373	248	....	.387	280	....
	30.2	g y	....	....	.386	343	....	.402	....	....
	31.0	g y	....	....	.398	348	....	.411	....	....
Aug. 12, 10 00	25.7	3.1	75.6	26.0	.325	8	75	.340	6.4	6.4
	24.9	2.1	....	....	.314	2.4	....	.330	1.9	33
	26.3	[2]6.1	....	....	.333	65	....	.348	49.0	....
	28.4	[1]10.5	....	....	.362	195	....	.376	245	....
	29.3	[3]12	....	25.2	.374	248	....	.388	360	....
3 30	25.3	2.6	75.7	25.8	.320	5	80	.334	3.7	30
	26.8	7.4	....	....	.340	105	....	.354	86.0	50
	27.5	[4]8.3	....	....	.350	142	....	.363	122	....
	28.4	[2]10.5	....	....	.362	207	....	.375	245	....
	29.3	[3]11.5	....	....	.374	248	....	.387	320	....
	34.3	[6]13	....	....	.443	415	....	.453	460	....
	42.8	[6]13	....	....	.559	450	....	.565	460	....
4 30	30.1	[7]13	76.2	25.5	.385	340	....	.398	460	....
Aug. 13, 10 00	25.9	3.9	....	24.3	.326	18	56	.340	13.3	13.3
	26.6	[1]5.7	....	....	.335	56		.349	39.0	25
	27.3	[5]7.2	....	....	.345	104		.358	80.5	....
3 30	25.8	3.7	75.9	24.3	.326	16	80	.340	11.3	11.3
	26.3	6.5	....	....	.332	78		.347	59.0	45
	26.7	7.0	....	....	.338	96		.352	74.0	....
Aug. 14, 9 30	25.5	3.5	75.4	23.9	.324	14	80	.338	9.5	20
	26.0	6.4	....	....	.331	75		.345	56.5	56.5
	27.0	[8]7.5	....	....	.344	117		.358	89.0	....
3 15	25.7	4.0	....	24.2	.329	19	60	.341	14.2	10
	26.2	5.8	75.2	....	.334	57		.348	41.0	30
	26.7	[5]7.4	....	....	.341	104		.355	86.0	....
Aug. 15, 9 40	25.6	4.1	75.4	23.3	.326	20	65	.339	15.2	18
	26.1	5.3	....	....	.333	45		.346	31.0	30
	26.9	[8]7.5	....	....	.344	116		.357	89.0	....

[1]wc. [2]wro. [3]w'o. [4]wp. [5]gy'o. [6]g. [7]gy. [8]gBP.

TABLE 11.—Time variation of the larger colloidal nucleation of dust-free wet air—Continued.

Date, etc.	δp.	s.	p.	t.	$\frac{\delta p-(\pi-\pi_1)}{p-\pi}$	$n\times 10^{-3}$.	$n_{0.335}\times 10^{-3}$	$\frac{\delta p}{p}$	$n\times 10^{-4}$.	$n_{0.340}\times 10^{-3}$ / $n_{0.348}\times 10^{-3}$
				°						
Aug. 15, 3h00m	25.5	3.9	75.4	23.8	0.324	18	70	0.338	13.3	20
	26.0	5.9	....	....	.331	45		.345	43.0	43
	26.9	[8]7.1	....	....	.343	116		.357	77.5	....
Aug. 16, 9 00	25.7	3.7	76.0	23.0	.325	16	67	.338	11.3	18
	26.1	5.1	....	....	.330	40		.343	27.5	33
	27.1	[8]7.0	....	....	.344	117		.357	74.0	....
3 00	25.8	3.7	75.8	23.5	.327	16	65	.340	11.3	11.3
	26.2	5.3	....	....	.332	45		.345	31.0	31
	27.0	[8]7.3	....	....	.343	117		.356	83.5	....
Aug. 17, 9 00	25.7	3.5	76.3	23.2	.323	12	80	.337	9.5	15
	26.2	4.9	....	....	.330	37		.343	24.6	38
	26.8	[9]7.2	....	....	.338	100		.351	80.5	....
12 00	25.7	3.0	76.2	23.6	.323	7.5	90	.337	5.5	23.5
	25.9	4.8	....	....	.326	34		.340	23.5	45
	26.9	[9]7.2	....	....	.339	116		.353	80.5	....
Aug. 23, 4 00	25.7	4.8	75.2	25.0	.326	34	75	.342	23.5	15
	25.7	4.8	....	....	.326	34		.342	23.5	35
	26.0	5.7	....	....	.331	56		.346	39.0	....
	27.0	[8]6.8	....	....	.344	117		.359	66.5	....
Aug. 24, 9 30	25.7	3.1	76.1	23.1	.324	8.2	75	.338	6.4	15
	26.2	5.4	....	....	.331	48		.344	32.7	35
	27.0	[8]7.0	....	....	.342	117		.355	74.0	....
3 00	25.7	4.0	76.2	24.0	.323	18	95	.337	14.2	20
	26.2	5.3	....	....	.330	46		.344	31.0	40
	26.8	[8]7.4	....	....	.338	116		.352	86.0	....
Aug. 25, 9 00	25.7	3.3	76.6	22.5	.323	10	70	.335	7.7	20
	26.0	4.5	....	....	.327	27		.339	19.5	40
	26.9	[9]6.8	....	....	.339	88		.351	66.5	....
3 00	25.7	3.0	76.4	23.5	.323	7.1	60	.336	5.5	20
	26.0	4.7	....	....	.327	32		.340	22.2	38
	27.0	[9]6.7	....	....	.341	88		.353	64.0	....
Aug. 26, 9 00	25.7	3.3	76.2	23.7	.323	10.5	70	.337	7.7	15
	26.0	4.3	....	....	.327	23		.341	17.5	33
	27.0	[10]6.9	....	....	.341	105		.354	69.5	....
4 00	25.7	4.0	75.9	23.6	.324	18	70	.338	14.2	78
	26.1	5.1	....	....	.330	40		.344	27.5	30
	27.0	[10]6.7	....	....	.342	105		.356	64.0	....
Aug. 27, 9 00	25.9	4.8	75.3	23.7	.330	34	75	.344	23.5	18
	26.4	[9]6.8	....	....	.336	89		.350	66.5	30
	26.8	[8]7.6	....	....	.342	116		.356	94.0	....
3 00	25.9	[11]5.3	75.1	23.8	.331	44	70	.345	31	20
	26.0	[9]6.2	....	....	.332	67		.346	52	31
	27.0	[8]7.6	....	....	.346	117		.360	94	....
Aug. 28, 9 00	25.9	4.1	75.6	23.5	.329	21	60	.342	15.2	10
	26.4	[9]6.1	....	....	.336	66		.349	49	30
	27.0	[8]7.3	....	....	.344	117		.357	83.5	....
3 00	25.7	4.5	75.6	23.4	.327	27	65	.340	19.5	19.5
	26.3	5.8	....	....	.335	58		.348	41.0	33
	27.2	[12]7.6	....	....	.347	117		.360	94.0	....
Aug. 29, 9 30	25.9	4.3	75.9	23.3	.328	24	70	.341	17.5	13
	26.2	5.4	....	....	.332	48		.345	32.7	32.7
	26.8	[11]7.2	....	....	.340	104		.353	80.5	....
Sept. 7, 10 00	25.7	3.8	75.6	22.0	.328	17	60	.340	12.3	12.3
	26.0	5.3	....	....	.332	44		.344	31	35
	26.8	[11]7.1	....	....	.342	101		.354	77.5	....

[8]g BP. [9]w e. [10]g y o. [11]w y. [12]w Br BP.

TABLE 11.—Time variation of the larger colloidal nucleation of dust-free wet air—Continued.

Date, etc.	δp.	s.	p.	t.	$\frac{\delta p-(\pi-\pi_1)}{p-\pi}$	$n\times 10^{-3}$.	$n_{0.335}\times 10^{-3}$	$\frac{\delta p}{p}$	$n\times 10^{-3}$.	$n_{0.340}\times 10^{-3}$ / $n_{0.348}\times 10^{-3}$
				°						
Sept. 7, 3^h45^m	25.6	4.1	75.3	22.0	0.327	20	70	0.340	15.2	15.2
	26.3	[13]6.6	....	....	.337	90		.349	61.5	40
	27.0	[8]7.6	....	....	.347	117		.359	94.0	....
Sept. 8, 9 00	25.7	4.1	75.6	22.0	.327	20	55	.340	15.2	15.2
	26.3	5.9	....	....	.336	62		.348	43.0	30
	27.0	[8]7.2	....	....	.345	105		.357	80.5	....
4 00	25.7	4.1	75.5	22.0	.328	19	55	.340	15.2	15.2
	26.3	5.7	....	....	.336	55		.348	39	28
	26.7	[11]7.6	....	....	.342	104		.354	94	....
Sept. 9, 9 30	25.8	3.8	75.4	21.0	.332	17	30	.342	12.3	8
	26.3	5.4	....	....	.338	48		.349	32.7	20
	26.7	[8]7.4	....	....	.344	116		.354	86	....
3 00	25.7	4.4	75.2	22.6	.328	25	55	.342	18.5	13
	26.3	6.0	....	....	.337	64		.350	46	30
	27.2	[8]7.4	....	....	.349	117		.362	86	....
Sept. 10, 9 00	25.8	4.5	75.4	22.8	.329	27	65	.342	19.5	10
	26.5	6.8	....	....	.338	87		.351	66.5	35
	27.0	[8]7.4	....	....	.345	117		.358	86	....
2 30	25.9	4.8	75.5	23.2	.330	35	70	.343	23.5	10
	26.3	[9]6.6	....	....	.335	82		.348	61.5	35
	27.0	[8]7.8	....	....	.345	117		.358	100	....
Sept. 11, 9 00	25.7	3.0	76.2	22.0	.325	7	55	.337	5.5	15
	26.3	5.2	....	....	.333	42		.345	29	30
	27.1	[8]7.0	....	....	.344	105		.356	74	....
2 30	25.8	3.5	76.2	22.2	.326	12	55	.339	9.5	13
	26.5	5.8	....	....	.335	59		.348	41	30
	27.1	[11]7.4	....	....	.344	105		.356	86	....
Sept. 12, 9 15	25.7	3.8	76.1	22.0	.325	17	50	.338	12.3	15
	26.3	4.9	....	....	.333	37		.346	24.6	25
	27.0	[8]7.3	....	....	.343	117		.355	83.5	....
2 30	25.7	3.6	76.0	22.2	.326	14	65	.338	10.5	18
	26.3	6.0	....	....	.334	64		.346	46.0	40
	27.0	[8]7.2	....	....	.343	105		.355	80.5	....
Sept. 13, 9 00	25.8	3.6	75.8	22.2	.328	14	55	.340	10.5	10.5
	26.1	5.2	....	....	.332	42		.344	29	33
	27.0	[8]7.1	....	....	.344	105		.356	77.5	....
3 40	25.7	3.7	75.6	22.0	.327	16	50	.340	11.3	11.3
	26.3	5.6	....	....	.336	53		.348	36.7	25
	27.0	[7]7.2	....	....	.345	105		.357	80.5	....
Sept. 14, 10 00	25.7	4.0	75.7	22.2	.327	18	55	.339	14.2	17
	26.3	5.8	....	....	.335	57		.347	41	33
	27.0	[8]7.1	....	....	.345	105		.357	77.5	....
3 30	25.7	4.0	75.9	22.2	.326	18	60	.339	14.2	18
	26.3	5.8	....	....	.334	57		.346	41	35
	27.0	[8]7.1	....	....	.344	105		.356	77.5	....
Sept. 15, 9 30	25.8	2.7	76.7	22.0	.323	6	55	.336	4.1	13
	26.3	4.4	....	....	.331	25		.343	18.5	30
	27.0	[13]6.7	....	....	.340	93		.352	64	....
2 30	25.8	2.9	76.7	21.0	.326	7	40	.336	5.1	13
	26.3	4.4	....	....	.333	25		.343	18.5	30
	27.2	[11]7.4	....	....	.345	105		.355	86	....
Sept. 16, 10 45	25.9	2.9	77.0	19.8	.327	7	30	.336	5.1	13
	26.5	4.7	....	....	.335	32		.344	22.2	30
	26.9	[9]6.4	....	....	.340	89		.349	56.5	....

[7]gy. [8]gBP. [9]we. [11]wy. [13]wo.

TABLE 11.—Time variation of the larger colloidal nucleation of dust-free wet air—Continued.

Date, etc.	δp.	s.	p.	t.	$\frac{\delta p-(\pi-\pi_1)}{p-\pi}$	$n\times 10^{-3}$.	$n_{0.335}\times 10^{-3}$	$\frac{\delta p}{p}$	$n\times 10^{-3}$.	$\frac{n_{0.340}\times 10^{-3}}{n_{0.318}\times 10^{-3}}$
				°						
Sept. 17, 4h45m	25.8	3.0	76.8	20.0	0.326	7	45	0.336	5.5	12
	26.2	4.0	....	....	.332	18		.341	14.2	35
	26.9	[9]6.8	....	....	.341	95		.350	66.5	....
9 00	25.7	2.8	76.6	20.5	.325	6	30	.335	4.6	8
	26.2	3.4	....	....	.332	12		.342	8.7	20
	27.0	[9]7.2	....	....	.342	103		.352	80.5	....
	26.6	5.2	....	....	.337	43		.347	29	....
4 00	26.0	3.4	76.2	21.0	.331	11	37	.341	8.7	3
	27.3	[8]7.4	....	....	.348	117		.358	86	30
	26.8	[9]7.0	....	....	.342	96		.352	74	....
Sept. 18, 9 00	25.5	3.0	76.1	21.0	.324	7	40	.335	5.5	18
	26.4	5.5	....	....	.337	51		.347	35	30
	27.1	[10]7.3	....	....	.346	105		.356	83.5	....
Sept. 20, 9 00	25.6	3.8	75.9	22.2	.325	17	50	.337	12.3	15
	26.7	[9]5.5	....	....	.340	51		.352	35	25
	27.0	([7])	....	....	.344	105		.356	....	....
4 00	25.7	4.1	75.6	23.0	.327	19	70	.340	15.2	15
	26.6	[11]7.4	....	....	.339	98		.352	86.0	45
	27.0	[14]7.9	....	....	.344	140		.357	100	....
Sept. 21, 9 00	25.8	4.5	75.5	23.5	.328	27	85	.342	19.5	3
	26.3	[13]6.8	....	....	.335	87		.348	66.5	40
	26.8	[14]7.9	....	....	.342	140		.356	103	....
2 45	26.0	4.8	75.6	23.0	.331	34	98	.344	23.5	10
	26.3	[13]7.4	....	....	.335	98		.348	86	38
	27.2	[8]7.7	....	....	.347	117		.360	97	....
Sept. 22, 8 45	25.9	3.5	76.2	22.0	.327	12	60	.340	9.5	9.5
	26.1	5.2	....	....	.330	42		.343	29	(?)
	27.0	([11])	....	....	.342	94		.354	....	....
3 15	25.9	3.5	76.0	22.2	.328	13	55	.340	9.5	10
	26.1	5.1	....	....	.331	40		.343	27.5	40
	27.0	[11]7.7	....	....	.343	99		.355	97.0	....
Sept. 23, 10 30	25.9	4.8	75.5	22.3	.331	34	85	.343	23.5	10
	26.3	[13]6.8	....	....	.336	98		.348	66.5	40
	27.0	[8]7.5	....	....	.346	117		.358	89.0	....
5 00	25.7	4.6	75.4	23	.327	29	70	.340	20.7	25
	26.2	6.1	....	....	.334	66		.347	49	40
	26.8	[8]6.9	....	....	.343	104		.355	69.5	....
Sept. 24, 9 00	25.8	2.8	76.3	21	.327	6	35	.338	4.6	10
	26.4	5.1	....	....	.336	40		.346	27.5	25
	27.1	[8]6.8	....	....	.345	105		.355	66.5	....
3 00	25.8	3.5	76.3	20.8	.327	12	43	.338	9.5	13
	26.3	4.9	....	....	.334	37		.345	24.6	24.6
	27.0	[11]7.0	....	....	.344	99		.354	74	....
Sept. 25, 9 00	25.9	2.4	77.1	19.6	.326	3	45	.336	3.0	15
	26.3	4.2	....	....	.332	22		.341	16.3	40
	27.0	[9]6.8	....	....	.341	89		.350	66.5	....
2 45	25.7	2.7	77.0	19	.325	6	40	.334	4.1	15
	26.3	4.4	....	....	.333	25		.342	18.5	30
	27.0	[9]6.5	....	....	.342	82		.351	59.0	....
Sept. 26, 8 40	25.9	2.5	76.9	18.2	.329	4	20	.337	3.3	10
	26.3	3.9	....	....	.334	17		.342	13.3	30
	27.0	[9]6.7	....	....	.343	85		.351	64.0	....
2 50	25.7	2.3	76.7	20.0	.325	3	30	.335	2.6	12
	26.3	4.2	....	....	.333	22		.343	16.3	23
	27.3	[9]6.4	....	....	.347	75		.356	56.5	....

[7] g y. [8] g BP. [9] w e. [10] g y o. [11] w y. [13] w o. [14] w Br cor.

TABLE 11.—Time variation of the larger colloidal nucleation of dust-free wet air—Continued.

Date, etc.	δp.	s.	p.	t.	$\frac{\delta p-(\pi-\pi_1)}{p-\pi}$	$n\times 10^{-3}$.	$n_{0.335}\times 10^{-3}$	$\frac{\delta p}{p}$	$n\times 10^{-3}$.	$n_{0.340}\times 10^{-3}$ / $n_{0.348}\times 10^{-3}$
				°						
Sept. 27, 8h45m	25.9	3.4	76.4	19.0	0.330	11	40	0.339	8.7	10
	26.3	5.0	....	....	.335	38		.344	26.0	30
	27.1	[13]7.1	....	....	.346	99		.355	77.5	....
3 15	25.6	3.0	76.3	19.5	.325	7	40	.335	5.5	15
	26.4	5.2	....	....	.336	42		.346	29.0	25
	26.8	7.3	....	....	.342	116		.351	83.5	....
Sept. 28, 9 00	25.8	2.6	76.8	19.0	.327	5	25	.336	3.7	10
	26.7	5.0	....	....	.339	38		.348	26.0	20
	27.1	[9]6.6	....	....	.344	83		.353	61.5	....
3 15	25.7	3.0	76.7	19.5	.325	7	40	.335	5.5	15
	26.6	5.3	....	....	.337	45		.347	31.0	25
	27.0	[9]6.6	....	....	.343	82		.352	61.5	....
Sept. 29, 8 45	25.7	2.7	76.7	19.2	.326	6	45	.335	4.1	15
	26.2	4.8	....	....	.333	34		.342	23.5	35
	27.0	[13]7.1	....	....	.343	99		.352	77.5	....
5 00	25.7	3.2	76.3	18.8	.328	9	35	.337	6.8	15
	26.6	5.5	....	....	.340	51		.349	35.0	25
	27.0	[11]7.1	....	....	.345	99		.354	77.5	....
Sept. 30, 10 10	26.0	4.6	75.8	19.0	.334	30	35	.343	20.7	10
	26.6	[9]6.6	....	....	.342	81		.351	61.5	30
	27.0	[8]7.5	....	....	.348	117		.356	89.0	....
4 00	25.7	3.6	75.9	19.2	.330	14	45	.339	10.5	15
	26.6	[13]6.8	....	....	.342	99		.351	66.5	40
	27.0	[7]7.4	....	....	.347	105		.356	86.0	....
Oct. 1, 9 45	25.7	3.1	76.4	16.8	.329	8	20	.336	6.4	10
	26.5	4.6	....	....	.340	30		.347	20.7	20
	27.0	[11]7.4	....	....	.347	99		.354	86.0	....
3 00	25.8	3.0	76.2	17.2	.331	7	25	.339	5.5	10
	26.3	5.0	....	....	.338	37		.345	26.0	26
	27.2	[8]7.0	....	....	.350	103		.357	74.0	....
Oct. 2, 9 00	25.7	2.3	76.1	17.0	.331	3	20	.338	2.6	6.4
	25.9	3.1	....	....	.333	8		.340	6.4	28
	26.7	[9]6.3	....	....	.344	71		.351	54.5	....
3 00	26.0	4.4	75.9	18.0	.335	25	25	.343	18.5	10
	26.5	5.7	....	....	.341	55		.349	39.0	25
	27.1	[7]7.4	....	....	.350	105		.357	86.0	....
Oct. 3, 8 45	25.7	3.3	76.0	18.5	.329	10	40	.338	7.7	13
	26.3	5.3	....	....	.337	45		.346	31.0	28
	27.0	[13]7.1	....	....	.346	100		.355	77.5	....
3 00	25.7	3.7	76.0	20.5	.327	16	60	.338	11.3	20
	26.4	[9]6.8	....	....	.337	87		.347	66.5	53
	27.0	[7]7.8	....	....	.345	105		.355	100.0	....
Oct. 4,* 9 15	25.7	3.8	76.1	20.5	.327	17	40	.338	12.3	15
	26.5	5.5	....	....	.338	51		.348	35.0	28
	26.9	[13]7.3	....	....	.343	101		.353	83.5	....
3 00	25.9	3.7	75.9	21.0	.330	16	45	.341	11.3	10
	26.3	5.4	....	....	.336	48		.347	32.7	25
	27.3	[15]8.0	....	....	.349	140		.360	108.	....
Oct. 5, 9 00	25.7	3.5	20.8	75.6	.329	12	50	.340	9.5	9.5
	26.6	[11]6.8	....	....	.341	93		.352	66.5	30
	27.1	[1]7.8	....	....	.348	140		.359	100	....
3 20	25.7	4.2	75.4	21.0	.330	21	40	.341	16.3	10
	26.2	5.8	....	....	.337	59		.348	41.0	30
	27.0	[8]7.3	....	....	.348	117		.358	83.5	....

[1] w c. [7] g y. [8] g BP. [9] w e. [11] w y. [13] w o. [15] w P cor. *Room heated hereafter.

TABLE 11.—Time variation of the larger colloidal nucleation of dust-free wet air—Continued.

Date, etc.	δp.	s.	p.	t.	$\frac{\delta p-(\pi-\pi_1)}{p-\pi}$	$n\times 10^{-3}$.	$n_{0.335}\times 10^{-3}$	$\frac{\delta p}{p}$	$n\times 10^{-3}$.	$n_{0.340}\times 10^{-3}$ / $n_{0.348}\times 10^{-3}$
				°						
Oct. 6, 9h00m	25.7	4.6	75.1	20.5	0.331	29	50	0.342	20.7	10
	26.4	[13]6.7	....	....	.341	92		.352	64.0	35
	26.8	[11]7.7	....	....	.347	104		.357	97.0	....
4 30	25.7	4.9	74.3	21.0	.335	36	35	.346	24.6	(?)
	26.3	[13]7.0	....	....	.343	97		.354	74.0	20
	27.0	[1]9.0	....	....	.353	175		.363	152	....
Oct. 7, 9 30	25.8	4.9	74.9	21.0	.334	36	40	.344	24.6	(?)
	26.1	[13]6.6	....	....	.338	88		.348	61.5	30
	27.0	[8]7.4	....	....	.350	117		.360	86.0	....
4 00	25.9	4.9	75.1	20.0	.335	36	35	.345	24.6	(?)
	26.3	[13]6.8	....	....	.341	87		.350	66.5	25
	27.0	[8]7.2	....	....	.350	111		.360	80.5	....
Oct. 8, 9 00	25.9	3.0	76.3	18.8	.331	7	20	.339	5.5	9
	26.3	4.4	....	....	.336	25		.345	18.5	20
	26.9	[9]6.1	....	....	.344	65		.353	49.0	....
3 00	26.0	3.5	76.4	21.5	.329	12	45	.340	9.5	9.5
	26.7	6.1	....	....	.338	66		.349	49.0	30
	27.3	[11]7.5	....	....	.346	112		.357	89.0	....
Oct. 9, 8 45	25.8	3.8	76.0	20.0	.330	17	35	.339	12.3	13
	26.3	5.1	....	....	.337	40		.346	27.5	25
	26.9	6.8	....	....	.345	89		.354	66.5	....
3 00	25.7	3.6	75.6	21.0	.329	14	45	.340	10.5	10
	26.3	[9]5.9	....	....	.337	62		.348	43.0	30
	27.0	[7]6.9	....	....	.347	94		.357	69.5	....
Oct. 10, 9 00	25.9	4.9	75.2	19.8	.335	39	40	.344	24.6	(?)
	26.6	[11]7.5	....	....	.344	103		.354	89.0	30
	26.2	[9]6.3	....	....	.339	71		.348	54.5	....
	27.0	[8]7.2	....	....	.350	117		.359	80.5	....
3 30	25.9	4.9	75.0	20.0	.336	36	30	.345	24.6	(?)
	26.3	[9]6.6	....	....	.342	82		.351	61.5	25
	27.0	[16]8.2	....	....	.351	140		.360	117	....
Oct. 11, 9 15	25.7	3.7	75.3	18.0	.333	16	25	.341	11.3	7
	26.4	5.8	....	....	.343	59		.351	41.0	20
	27.0	[11]6.9	....	....	.351	102		.359	69.5	....
3 30	25.9	4.9	75.3	21.0	.330	36	45	.344	24.6	(?)
	26.3	[9]6.4	....	....	.339	74		.349	56.5	30
	27.0	[8]6.9	....	....	.348	95		.359	69.5	....
Oct. 12, 8 45	26.0	3.6	76.6	19.0	.331	15	30	.339	10.5	10
	26.9	5.2	....	....	.343	43		.351	29.0	20
	27.4	[8]7.3	....	....	.349	118		.358	83.5	....
3 00	26.1	3.8	76.6	17.6	.334	17	20	.341	12.3	8
	26.6	5.1	....	....	.340	40		.347	27.5	20
	27.0	5.8	....	....	.346	60		.353	41.0	....
Oct. 13, 9 00	26.0	2.3	77.4	18.0	.328	3	30	.336	2.6	15
	26.4	4.6	....	....	.333	30		.341	20.7	25
	27.0	5.3	....	....	.341	46		.349	31.0	....
6 30	25.8	2.8	77.3	20.0	.324	6	30	.334	4.6	13
	26.6	4.5	....	....	.335	28		.344	19.5	25
	27.1	6.7	....	....	.341	85		.351	64.0	....
Oct. 14, 9 15	25.7	3.0	77.1	20.0	.324	7	40	.333	5.5	15
	26.4	4.7	....	....	.333	32		.342	22.2	28
	27.2	6.2	....	....	.344	69		.353	52.0	....
Oct. 15, 9 00	25.9	3.0	76.7	20.4	.327	7	40	.338	5.5	10
	26.5	5.0	....	....	.335	38		.346	26.0	23
	27.2	6.7	....	....	.345	85		.355	64.0	....

[1]wc. [7]gy. [8]gBP. [9]we. [11]wy. [13]wo. [16]wP.

16. Effect of the barometer.—If we look more specifically at the new data beginning with August 10, coincidences of minima and maxima of the nucleation with maxima and minima of the barometric pressure occur only on August 13, 25, and 27, and these are not pronounced. In September there is no detailed similarity until September 16, but both curves have dropped somewhat toward the marked minimum. After September 20, however, the apparent agreement of curves is conspicuous up to September 24 and would be decisive if the run of temperature were not similar. During the remainder of the month there is no agreement—rather an opposition—and the two curves are remarkably at variance during the unusually low barometer in the early part of October. The peak of the barometric curves from October 4 to 8 has nothing to suggest it in the nucleation curve. We may conclude, therefore, that a direct barometric effect is absent, that such coincidences as seem to occur are referable to other causes, and that the method used for the elimination of barometer discrepancies is to the same degree vouched for.

17. Effect of temperature.—Throughout all of the observations the tendency of temperature of the fog chamber to rise from morning to afternoon is most probably to be regarded as the cause of a similar tendency in the nucleation. There are exceptions, most of which, however, may be explained away. The curves show a similar general march from August 10 to 23 and from here to August 29. From September 7 to 18 there is much detailed agreement, as, for instance, on September 8 to 10 and 15 to 16. The same is true after September 20, where markedly coincident variation occurs.

So in October the agreement of curves is apt to be very close, as, for instance, the effect from September 30 to October 3, the general fall thereafter, and the effect from October 7 to October 9. All of this will appear more strikingly when the observations are averaged for several consecutive days, and most of the lack of synchronism is doubtless due to the difficulty of finding the true value of nucleation.

18. Effect of ionization.—To find whether there is any relation of the change of nucleation in the fog chamber in the lapse of time with a state of ionization of the atmosphere, measurements were made of the latter quantity by Miss L. B. Joslin, using Ebert's aspirator apparatus. The data are given in table 12, where V denotes the fall of potential during the fiducial time of aspiration (about 10 minutes), Q the charge per cubic centimeter, and n the corresponding number of ions per cubic centimeter. These data are constructed in the lower curves of fig. 9, together with the cotemporaneous nucleations and temperatures of the fog chamber, on a somewhat larger scale than heretofore. It would be difficult to

TABLE 12.—Ionization of the atmosphere in the lapse of time—Ebert's apparatus.

Date.	Time.	V.	Q.	$n \times 10^{-3}$.	Date.	Time.	V.	Q.	$n \times 10^{-3}$.
Sept. 14	11.3^h	9.3	+0.53	1.56	Sept. 29	10.0^h	6.7	+0.38	1.12
		8.2	− .47	1.38			9.2	− .52	1.53
	3.5	10.8	+ .61	1.76	Oct. 1	10.0	7.5	+ .43	1.26
		12.6	− .71	2.01			8.9	− .51	1.50
Sept. 15	10.4	8.3	+ .47	1.40		3.5	6.2	+ .35	1.05
		10.1	− .58	1.71			4.8	− .27	.79
	3.5	9.9	+5.6	1.65	Oct. 2	10.0	6.5	+ .37	1.09
		7.1	− .40	1.18			9.6	− .55	1.62
Sept. 17	11.0	9.6	+ .55	1.62		3.5	1.1	+ .06	.19
		9.4	− .54	1.59			7.2	− .41	1.20
	3.7	6.8	+ .39	1.14	Oct. 3	10.5	8.3	+ .47	1.40
		7.7	− .44	1.29			2.3	− .13	.38
Sept. 18	10.5	3.6	+ .20	.60		3.0	7.7	+ .44	1.29
		3.9	− .22	.65			7.1	− .40	1.18
	3.5	4.5	+ .25	.76	Oct. 4	3.5	7.3	+ .42	1.21
		3.1	− .18	.52			2.8	− .16	.47
Sept. 19	10.0	7.5	+ .43	1.26	Oct. 5	10.3	6.7	+ .38	1.12
		7.7	− .44	1.29			7.8	− .45	1.32
	4.0	7.3	+ .42	1.21	Oct. 6	10.5	4.5	+ .26	.76
		2.4	− .14	.41			2.8	− .16	.47
Sept. 20	10.3	5.6	+ .32	.94	Oct. 8	10.0	14.0	+ .80	2.35
		3.7	− .21	.63			10.6	− .60	1.78
	3.5	7.1	+ .40	1.18		3.5	7.6	+ .43	1.25
		5.1	− .29	.85			5.3	− .30	.88
Sept. 21	10.0	6.0	+ .34	1.00	Oct. 9	10.0	3.7	+ .21	.63
		6.9	− .39	1.14			4.2	− .24	.70
	3.0	5.6	+ .32	.94		3.0	4.0	+ .22	.66
		8.6	− .49	1.44			1.8	− .10	.31
Sept. 22	10.0	5.0	+ .29	.85	Oct. 10	10.0	7.8	+ .44	1.30
		14.9	− .85	2.50			3.3	− .19	.56
	3.0	6.5	+ .37	1.09		3.5	7.5	+ .43	1.26
		6.9	− .39	1.14			4.8	− .27	.79
Sept. 25	12.5	7.8	+ .45	1.32	Oct. 11	10.3	7.8	+ .45	1.32
		5.8	− .33	.97			4.7	− .27	.79
	3.5	3.9	+ .22	.65		3.5	7.1	+ .40	1.18
		1.8	− .10	.31			2.5	− .14	.41
Sept. 26	10.0	8.9	+ .51	1.50	Oct. 12	3.5	5.9	+ .34	1.00
		7.1	− .40	1.18			7.0	− .40	1.17
	4.0	3.6	+ .20	.60	Oct. 13	11.5	6.7	+ .38	1.12
		6.0	− .34	1.00			11.3	− .65	1.91
Sept. 27	10.0	5.9	+ .34	1.00		3.5	4.6	+ .26	.76
	....	....	....	....			3.6	− .20	.60
	3.5	5.6	+ .32	.94	Oct. 15	10.2	8.3	+ .47	1.40
		2.8	− .16	.47			2.3	− .13	.38
Sept. 28	3.5	3.9	+ .22	.65		3.5	10.4	+ .59	1.74
		5.6	− .32	.94			2.4	− .14	.41

detect any detailed similarity in the two sets of results. Thus the maximum of nucleation on September 20 to 24 is in no way suggested by the ionization. Both curves tend to descend toward the end of the month, but this may be due to causes to which both are tributary. As such an effect will appear again in the average results, it may be dismissed here.

Fig. 9 also contains the nucleations $n_{0.345}$ for $\delta p/p = 0.345$ for comparison. Remarks may be made with reference to them similar to those just stated. The enlarged scale admits of an easier comparison of $n_{0.335}$ and $n_{0.345}$, which hold for different hypotheses.

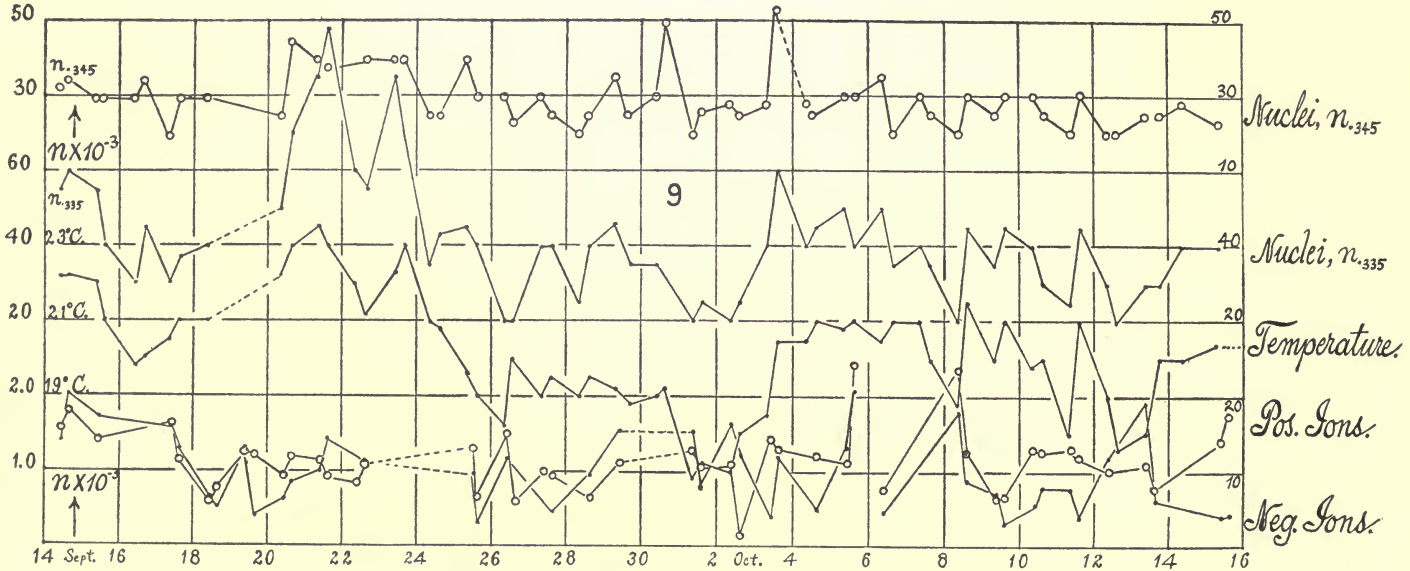

FIG. 9.—Vapor nucleation of dust-free air, temperature of the fog chamber, and positive and negative ionization, all compared in the lapse of time.

19. Mean results.—The most satisfactory criterion of the variation of nucleation in the lapse of time would perhaps have been the slope of the n lines as given by the three observations in terms of the abscissa, $x=(\delta p-[\pi-\pi_1])/(p-\pi)$; but as these points lie on a graph whose curvature is often marked, the curvature would in general be hard to estimate and the ordinate $n_{0.335}$ for $x=0.335$ has therefore been preferred and is summarized in table 13.

TABLE 13.—Summary of table 9. Observations a. m. and p. m. $\delta p-(\pi-\pi_1)/(p-\pi)=0.335$.

Date.	Temperature.	$n_{0.335}\times 10^{-3}$.	Date.	Temperature.	$n_{0.335}\times 10^{-3}$.	Date.	Temperature.	$n_{0.335}\times 10^{-3}$.
	°			°			°	
Aug. 10	26	90	Aug. 25	22	70	Sept. 12	22	50
	28	105		23	60		22	65
11	26	70	26	24	70	13	22	55
	26	70		24	70		22	50
12	26	75	27	24	75	14	22	55
	26	80		24	70		22	60
13	24	56	28	24	60	15	22	55
	24	80		24	65		21	40
14	24	80	29	23	70	16	20	30
	24	60	Sept. 7	22	60		20	45
15	23	65		22	70	17	21	30
	24	70	8	22	55		21	37
16	23	67		22	55	18	21	40
	24	65	9	21	30	20	22	50
17	23	80		23	55		23	70
	24	90	10	23	65	21	23	85
23	25	75		23	70		23	98
24	23	75	11	22	55			
	24	95		22	55			

The endeavor may be made to test the value of $n_{0.335}$ for longer intervals of time. As the series is often interrupted, 2-day to 4-day intervals for the present suggest themselves. Consequently, if the data of table 13 (which is a summary of table 11) be so compared, the values given in table 14 appear.

If the results of table 13 be further corrected for dependence of the precipitation on the changes of temperature of the fog chamber, data given in an earlier report* and elsewhere are available.

At $\delta p=22$ cm. the amount of water precipitated per cubic centimeter is at

$t=$	10°	20°	30°
$m\times 10^6=$	4.2	5.5	6.7

Hence on the average the correction may be taken as $\frac{6.7-4.2}{5.5\times 20}=2.3$ per cent of the values of m at 20° C.

*Smithsonian Contributions No. 1651, p. 135, 1905.

Since $n = 6m\,s^3/\pi a^3$ approximately (where a is the optical constant of coronas and s their angular diameter on a radius of 30 cm.) for a given s, n varies as m. Therefore n must be increased to 2.3 per cent of its value per degree of temperature of the fog chamber above 20° C. In this way the corrected data of table 14 were found.

TABLE 14.—Nucleations (averaged in groups of 2 to 4 days) in the lapse of time. $n \times 10^{-3}$ at $\delta p/p = 0.345$,[1] and at $\delta p - (\pi - \pi_1)/(p - \pi) = 0.335$.

Date.	Temperature.	Barometer.	$n_{0.335}$.	Corrected $n_{0.335}$.	$n_{0.345}$.	Corrected $n_{0.345}$.	Ionization.	
							$+n$.	$-n$.
	°C.	cm.						
Aug. 10–13	25.8	75.71	77,000	87,000	37,600	43,000	....	....
14–17	23.8	75.71	72,000	78,000	38,000	41,900	....	....
23–26	23.6	76.07	73,000	79,000	35,900	39,100	....	....
27–29	23.8	75.50	68,000	74,000	31,400	34,400	....	....
Sept. 7–10	22.3	75.44	57,000	60,000	31,600	33,400	....	....
11–13	22.0	75.98	56,000	59,000	30,500	32,000	....	....
14–16	21.2	76.47	47,000	49,000	32,200	33,200	1600	1570
17–20	21.6	76.08	45,000	47,000	30,000	31,200	1090	900
21–23	22.5	75.72	75,000	79,000	40,000	42,500	970	1550
24–27	19.6	76.63	37,000	37,000	28,500	28,200	1000	790
28–30	19.0	76.37	37,000	37,000	29,200	28,500	885	1230
Oct. 1– 3	18.0	76.10	32,000	30,000	25,400	24,100	1040	1110
4– 5	20.8	75.75	44,000	45,000	28,300	28,900	1167	395
6– 7	20.6	74.85	40,000	41,000	27,500	27,900	760	470
8– 9	20.3	76.08	36,000	36,000	26,300	26,500	1220	920
10–11	19.7	75.17	35,000	35,000	26,300	25,100	1260	640
12–13	18.7	76.97	27,000	27,000	22,500	21,800	960	1220
14–15	20.2	76.90	40,000	40,000	25,500	25,600	1570	400

[1] These will be considered in section 20.

Table 14 also contains the data for the corresponding averages of temperature, barometric pressure, and ionization, and all data have been further given in the graphs fig. 10, with the times (abscissas) laid off on a smaller scale to bring out the relative variations. It is again apparent that no relation of the nucleation curve to the barometer curve or to the ionization curve can be made out. On the other hand, the vapor nucleations of the dust-free wet air in the fog chamber agree very fully with the cotemporaneous variations of the temperature of the fog chamber (not of the temperature of the atmospheric air without, of which they are also independent). It is even possible to make out the rate at which nuclei are produced when the temperature of the fog chamber increases. Taking the mean trend of both curves (nuclei and temperature), it appears that nearly 8000 colloidal nuclei are generated (apparently) in dust-free wet air, by a rise of temperature of 1° C.

20. Nucleations depending upon $\delta p/p$.—In the above experiments the nucleations were compared at a fixed value, 0.335, of the variable $(\delta p - [\pi - \pi_1])/(p - \pi)$. If, however, the corresponding value of the

relative drop $\delta p/p$ (which assumes that all the water vapor is expanded adiabatically without condensation) be computed, the latter will vary with temperature in a way correlative with the vapor pressures contained in the former. The nucleations computed for this particular series of values of $\delta p/p$ will also vary, and the rate was found to be about 6000 nuclei per degree. This is so near the temperature effect given in section 19 that there must be a common cause underlying both.

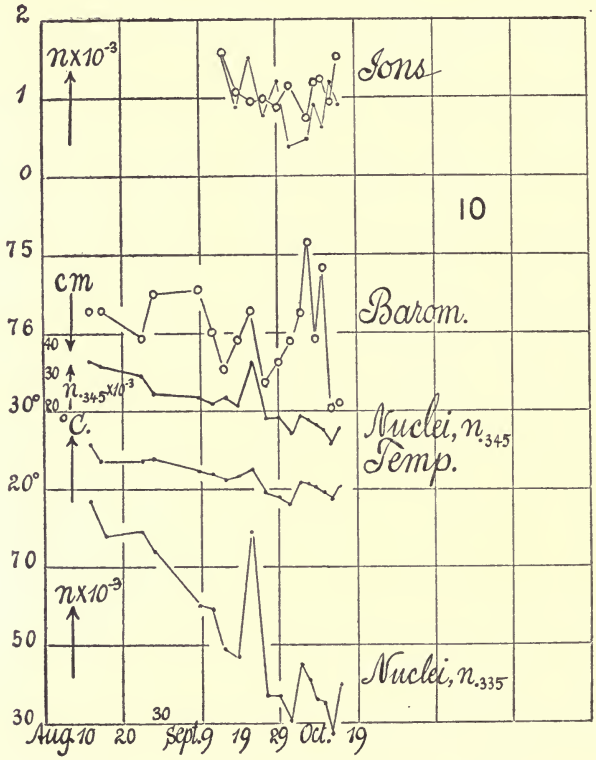

FIG. 10.—Vapor nucleation of dust-free air, temperature of fog chamber, barometric pressure, and positive and negative ionization (the former with small circles) in lapse of time, averaged for period two to four days.

Hence in table 11, n was also computed in its dependence on $\delta p/p$, and advantage was additionally taken of the new values of n given in Chapter III for the higher coronas. Two fiducial values of the variable $\delta p/p$ were tested; the former, $\delta p/p = 0.340$, being, as a rule, too small, the latter, $\delta p/p = 0.345$, was selected. The tables contain both of the corresponding values of nucleation, $n_{0.340}$ and $n_{0.345}$; but the last only has been given on the charts (figs. 8, 9, and 10). The other does not differ essentially from it. All values are summarized in succession in table 15.

Fig. 8 contains an extended comparison of the old curve for $n_{0.335}$ and the new curve for $n_{0.345}$, under the conditions which are given. In their narrower variations the two curves are similar and the details already specified for $n_{0.335}$ need not therefore be repeated for $n_{0.345}$. Pronounced maxima and minima will in particular be found coincident.

The same will be observed in the case of fig. 9, where a larger scale is introduced for $n_{0.335}$. The question of greatest interest is now the comparison of mean data such as are given in table 14 in the lapse of time.

The data for $n_{0.345}$ have been corrected for the effect of temperature t, on the amount of water precipitated, by taking from the recent results referred to the temperature coefficients $\delta n/n\delta t$, example of the values for different relative drops being

$\delta p/p=$	0.1	0.2	0.3	0.4	0.5
$10^3\delta n/n\delta t=$	14	18	23	27	30

These data would not, however, seriously modify the trend of the curves.

The graph (fig. 10), which also contains these nucleations, shows that the effect of temperature in the lapse of time has not been eliminated by replacing the extreme variable $(\delta p-[\pi-\pi_1])/(p-\pi)$ by the other extreme variable $\delta p/p$. In other words, if the nucleation corresponding to a fixed exhaustion $\delta p/p=0.345$ is studied in the lapse of time, the successive nucleations* show a dependence on the temperature of the fog chamber which can no longer be explained away. Both the details and the general character of the graphs for $n_{0.345}$ follow the fluctuations of temperature to an extent which may be estimated from the figure as an increment of about 2000 nuclei per rise of temperature of 1° C. at about 20° C. and for $\delta p/p=0.345$. Finally, there is no adequate reason why the effect of cooling below a higher surrounding temperature should be more efficient than the corresponding effect below a slightly lower temperature; for the rate of reheating would depend on the difference of temperatures.

21. Possible suggestions as to the temperature effect.—To obtain a suggestion as to the reason of the apparent increase of the size of colloidal nuclei with rise of temperature (*cæt. par.*) effectively, therefore, of their apparent increase in number at a given supersaturation, it is expedient to recall the form of Helmholtz's modification of Kelvin's vapor-pressure equation. If the ratio r of pressures at a convex surface r and at a plane surface be p_r/p_∞, R the gas constant of water vapor, ϑ its absolute temperature, s the density, and T the surface tension of the liquid,

$$p_r/p_\infty=\epsilon^{2T/Rs\vartheta r}$$

*American Journal, XXIII, 1907, 10, p. 209.

TABLE 15.—Corresponding to table 11, but containing nucleations for $\delta p/p = 0.340$ and $\delta p/p = 0.345$.

Date.	Temperature.	$n_{0.340} \times 10^{-3}$.	$n_{0.345} \times 10^{-3}$.
Aug. 10	26	18.5	35
	28	18.5	35
11	25.8	15.2	40
	26	18.5	38
12	26	6.4	33
	25.8	30	50
13	24.3	13.3	25
	24.3	11.3	45
14	23.9	20	56
	24.2	10	30
15	23.3	18	30
	23.8	20	43
16	23.0	18	33
	23.5	11.3	31
17	23.2	15	38
	23.6	23.5	45
23	25.0	15	35
24	23.1	15	35
	24.0	20	40
25	22.5	20	40
	23.5	20	38
26	23.7	15	33
	23.6	18	30
27	23.7	18	30
	23.8	20	31
28	23.5	10?	30
	23.4	19.5	33
29	23.3	13	33
Sept. 7	22.0	12.3	35
	22.0	15.2	40
8	22.0	15.2	30
	22.0	15.2	28
9	21.0	8	20
	22.6	13	30
10	22.8	10	35
	23.2	10	35
11	22.0	15	30
	22.2	13	30
12	22.0	15	25
	22.2	18	40
13	22.2	10.5	33
	22.0	11.3	25
14	22.2	17	33
	22.2	18	35
15	22.0	13	30
	21.0	13	30
16	19.8	13	30
	20.0	12	35
17	20.5	8	20
	21.0	3	30
18	21.0	18	30
Sept. 20	22.2	15	25
	23.0	15	45
21	23.5	3 (?)	40
	23.0	10	38
22	22.0	9.5	....
	22.2	10	40
23	22.3	10?	40
	23.0	25	40
24	21	10	25
	20.8	13	25
25	19.6	15	40
	19.0	15	30
26	18.2	10	30
	20.0	12	23
27	19.0	10	30
	19.5	15	25
28	19.0	10	20
	19.5	15	25
29	19.2	15	35
	18.8	15	25
30	19.0	10	30
	19.2	15	40
Oct. 1	16.8	10	20
	17.2	10	26
2	17.0	6.4	28
	18.0	10	25
3	18.5	13	28
	20.5	20	53
4	20.5	15	28
	21.0	10	25
5	20.8	9.5	30
	21.0	10	30
6	20.5	10	35
	21.0	....	20
7	21.0	....	30
	20.0	....	25
8	18.8	8	20
	21.5	9.5	30
9	20.0	13	25
	21.0	10	30
10	19.8	....	30
	20.0	....	25
11	18.0	7	20
	21.0	....	30
12	19.0	10	20
	17.6	8	20
13	18.0	15	25
	20.0	13	25
14	20.0	15	28
15	20.4	10	23

whence it appears that the increment of ϑ and R may replace each other.

A small radius at a high temperature is as effective as a larger radius at a low temperature ϑ, and that is substantially what the above data have brought out. Naturally the equation has been pushed beyond its limits, for the meaning of T for particles not large as compared with molecular dimensions is obscure; but it appears in other cases and is probably true here that the suggestions of the equation are trustworthy in a general way. Computing

$$p_r/p_\infty = \Big((p-\delta p)/p\Big)^r \frac{\pi}{\pi_1}$$

by the aid of the adiabatic equation we may write $10^6 r = 19.5/\vartheta_1 \log_{10}$ (p_r/p_∞) where $\log_{10} p_r/p_\infty = 0.8$, and $\vartheta_1 r = 2/10^5$, nearly. But $\vartheta_1 = 262°$ if the gas is originally at temperature $t = 20°$, whence $r = 75/10^9$. Since $dr/r = -d\vartheta_1/\vartheta_1$, an increment of the radius of but 0.038 under the given conditions is equivalent to a rise of temperature of 1° C. of the air within the fog chamber or to 2000 more available nuclei, according to the above figure.

22. Another suggestion.—The increment of about 2000 nuclei per degree of temperature under the conditions given may also be looked on as a parallel to what occurs in case of a radiant field like that produced by the X-rays. One may regard ionization as a state of dissociation sufficiently advanced to set free electrons and from this point of view equivalent to a very high degree of temperature. One may thus expect a passage of the vapor nuclei of wet dust-free air into the ions through a continuous gradation of nuclei, and may note that vapor nuclei and ions always occur together. True, the latter have been associated with the radiation penetrating the atmosphere, with good reason, but the possibility of a collateral cause of the ionization within the fog chamber may nevertheless be entertained.

23. Conclusion.—It is shown by direct observation that the number of nuclei caught in dust-free wet air at low barometer pressure is greatly in excess of the number caught (*cæt. par.*) at high barometer. This result may be accounted for as a necessary consequence of the thermo-dynamics of the experiment, however large and unexpected the variations appear.

The comparison of the nucleation of dust-free air with the cotemporaneous changes of atmospheric ionization shows no correspondence whatever. This is curious, because the ions, though much fewer in number, are larger in size than even the larger colloidal nuclei, and therefore capture much of the moisture at low exhaustion. One must conclude that the variations of the ionization are not sufficient to be detected in the presence of the other nucleation.

For the same reason would it be unwarrantable to look for effects due to variations of any external radiations. In other words, it is improbable that Wood and Campbell's phenomena can be detected by the fog chamber, and the results which seemed at first in accord with it are due to a rise of temperature. The results show that $\delta p/p$ is a suitable variable for the comparisons of nucleations in a plug-cock fog chamber like the above.

Finally the temperature conditions within the fog chamber produce a very definite effect, amounting to an increase (*cæteris paribus*) of about 2000 available vapor nuclei per degree centigrade near 20° and the given exhaustion $\delta p/p = 0.345$ or $v_1/v = 1.35$. Estimating the average number of efficient nuclei present at 25,000, this amounts to an increment of about 8 per cent per degree. Anomalous as it may seem that rise of temperature should increase the number of efficient nuclei (*cæt. par.*), probably by increasing their size throughout, nothing has been suggested to explain this result away. Virtually the same thing is done by radiation, though in much more marked degree than by temperature, so that one might regard ionization as a state of dissociation sufficiently advanced to set free corpuscles, or equivalent to a high degree of temperature. One might therefore expect a passage of the vapor nuclei of wet dust-free air into the ions, through a continuous gradation of nuclei; and in fact (granting that other valid explanations for the occurrence of ions have been given), they always occur together.

The present and a variety of other results made it necessary to re-standardize the coronas in terms of the number of nuclei represented, and the work will be given in the next chapter. Some of these data have already been utilized in the above.

CHAPTER III.

THE NUCLEATION CONSTANTS OF CORONAS.

RESULTS WITH A SINGLE SOURCE OF LIGHT.

24. Introduction.—At this point it seemed essential to restandardize the coronas in terms of the numbers of nuclei represented by a given angular aperture and type of corona at a given exhaustion and temperature. The measurements* carried out for this purpose in my earlier memoirs were made under very different conditions; and though reductions to the present results are feasible in a measure, it will obviously be preferable to repeat the work anew. This is particularly the case because the corrections referred to are liable to be large and because the results in the following chapters will essentially depend on the number of fog particles per cubic centimeter. This datum will here as elsewhere be called the nucleation, and in dust-free wet air the types of nuclei present will be the ions and the vapor nuclei only. These will, as a rule, be inefficient in the presence of phosphorus nuclei.

25. Apparatus and methods.—The apparatus used is the same as heretofore described in the Carnegie Institution of Washington Publication No. 62, p. 74, and is shown in fig. 11. It consists of a large vacuum chamber V connected with the relatively small fog chamber F, the volume ratio being about $v/V=0.06$. The latter was cylindrical in form, with its long axis horizontal, so as to admit of the measurement of coronas of large aperture. This angle may exceed 60° in the extreme cases and there must be some depth (exceeding 5 inches) if the coronas are to be sufficiently intense. The need of large fog chambers is therefore apparent and the plug-cock fog chamber seems to be the only apparatus adapted to the present purposes.

The connecting pipe was about 18 inches long, 2 inches in diameter, and the stopcock 2 inches in bore. Phosphorus nuclei were used. To guard against subsidence and undersaturation, the cloth lining of the fog chamber was fitted close to the walls and but two opposite narrow horizontal strips were left open for the observation of coronas.

The method used was the one previously employed. The highly nucleated medium (5×10^6 phosphorus nuclei per cubic centimeter) was successively expanded by a fixed amount, and the nucleated air removed from the fog chamber was replaced by filtered air. The residual nuclea-

*Smithsonian Contributions, No. 1373, vol. 29, pp. 1 to 173, 1903; *ibid.*, No. 1651, vol. 34, pp. 1 to 226, 1905.

tion therefore varies in geometric progression with the number of exhaustions, apart from necessary corrections. The observations were made in time series by two observers, Miss L. B. Joslin assisting me with

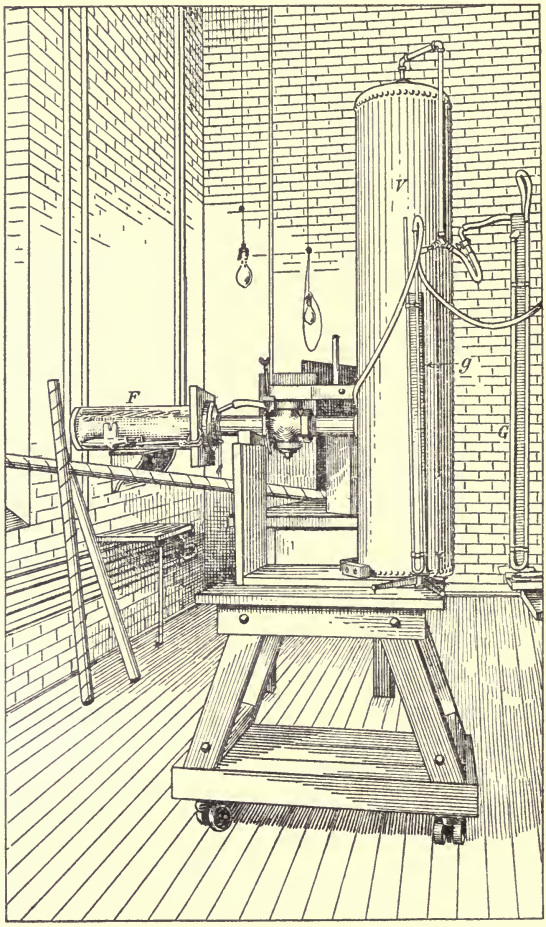

FIG. 11.—Fog chamber F, and vacuum chamber V.

the work. Details will be given in connection with the data. The initial isothermal (τ) pressures p and p' of the fog and vacuum chambers and the final isothermal (τ) pressure p_3, when in communication after exhaustion, were carefully determined previous to the experiment with coronas. These were needed for the computation of the amount of water precipitated per cubic centimeter in each of the series of exhaustions. In addition to this the pressure $[p_2]$ for finding the ratio of the geometric sequence was necessary and found as follows: In each exhaustion the stopcock was opened suddenly at the beginning of each

minute and kept open for 5 seconds; it was then closed until the end of the minute. Hence $[p_2]$ is the isothermal pressure observed in the fog chamber under the given conditions, determining the density of air and the nucleation left after each exhaustion. The ratio is therefore

$$y=\frac{p-\pi-[\delta p_2]}{p-\pi} \tag{1}$$

where π is the vapor pressure at the given isothermal temperature τ of observation.

As soon as the exhaust cock was closed the filter cock of the fog chamber was opened, in order to evaporate the fog particles with the least amount of subsidence or other loss. Observation of aperture was made during the 5 seconds in question.

The relative number of nuclei for a series of coronas of decreasing aperture is obtained in this way. It is furthermore necessary to standardize one of the coronas absolutely. This was done as described in the earlier work (Smithsonian Contributions, No. 1651), and, if d denotes the diameter of the fog particles and s the chord of the angular diameters ϕ of the corona observed with a goniometer with a radius of 30 cm.,

$$2 \sin \phi/2 = s/30 \tag{2}$$

$$ds = 0.0032 \tag{3}$$

was accepted when the eye and the source of light were at distances $D=30$ and 250 cm., respectively, on opposite sides of the fog chamber.

With a constant a selected we may then compute the nucleation n' for the smaller white-centered or normal coronas as

$$n'=\frac{6m}{\pi a^3}s^3 \tag{4}$$

where m is the amount of water precipitated per cubic centimeter in the exhausted vessel and n' the number of nuclei per cubic centimeter so computed. The theory of diffraction would give a collateral approximation

$$n'=\frac{6m}{\pi(73.2\,\lambda)^3}=\frac{m}{0.205(10^4\,\lambda)^3}$$

26. Equations and corrections.—In the present experiment no correction was made for the time loss of nuclei, for convection losses during influx and efflux (vortices washing against the walls of the vessel), nor for evaporation loss (loss of water nuclei on evaporation such as occurs with ions but not with solutional nuclei like those here produced by phosphorus, etc.). The justification of this was tested by making series of measurements with widely different exhaustions, $[\delta p_2]$, both as to the amount of the latter and number of exhaustions in the series, as will be shown.

TABLE 16.—Coronas standardized. Phosphorus nuclei. Bar. 77.7 cm.; temp. 20°. Cock open 5 seconds; time between observations 60 seconds; $\delta p' = 18.2$; $\delta p_3 = 17.0$; $[\delta p_2] = 16.2$ at 5 seconds, 16.8 at 60 seconds; $y = 0.779$; $S = 7.2$; $a = 0.0032$; $D = 30$ cm. and 250 cm.

No.	Corona.	s.	$10^{-3}n' = 0.190s^3$.	$n_0 \times 10^{-3}$ ratio.	$n \times 10^{-3}$.	$d = 0.0183 \times n^{-1/3}$.	$s' = a/d$.
1	Fog	....	....	4010	4010	0.000115	27.8
2	r' fog	30	....	....	3230	124	25.8
3	r' fog	....	....	....	2420	135	23.7
4	r' fog	....	....	....	1840	149	21.5
5	w c	....	....	....	1390	164	19.5
6	w v	....	....	....	1050	180	17.8
7	dk b	....	....	....	791	196	16.3
8	G b p	14	....	....	594	220	14.5
9	g' b p	13	....	....	446	241	13.3
10	g y o	13	....	....	333	264	12.1
11	y o	11	....	....	248	291	11.0
12	w c	10	....	....	183	321	10.0
13	w p	8.1	....	....	132	359	8.9
14	g b p	7.5	....	....	91.8	406	7.9
15	w o	7.0	65	4090	62.2	462	6.9
16	cor	6.1	43	4170	41.3	529	6.0
17	....	5.4	30	4630	25.9	618	5.2
18	....	4.3	15	3960	15.2	738	4.3
19	....	3.2	6.2	3440	7.2	948	3.4
20	....	2.0	1.5	3680	1.6	.001564	2.0
21	....	1.0	.2	2170	.4	2473	1.3

TABLE 17.—Coronas standardized. Phosphorus nuclei. Barometer 77.7 cm.; temperature 20°. Cock open 5 seconds; 60 seconds between observations; $\delta p' = 18.2$; $\delta p_3 = 17.0$; $[\delta p_2] = 16.2$ after 5 seconds; 16.8 after 60 seconds. Distance 30 cm. and 250 cm.; goniometer radius 30 cm.; $y = 0.779$; $S = 6.8$;[1] $ds = 0.0032$.

No.	Corona.	s.	$10^3 n' = 0.190s^3$.	$n_0 \times 10^{-3}$ ratio.	$n \times 10^{-3}$.	$d = 0.0183 \times n^{-1/3}$.	$s' = a/d$.
1	R' fog	....	....	5100	5100	0.000106	30.0
2	R' fog	30	....	....	3950	116	27.6
3	R' fog	....	....	....	3050	126	25.4
4	w R'	....	....	....	2350	138	23.2
5	w r	....	....	....	1790	151	21.2
6	w v	....	....	....	1360	165	19.4
7	st. b	....	....	....	1020	181	17.7
8	B. P.	....	....	....	769	202	15.8
9	g b p	....	....	....	579	220	14.5
10	g y o	13	....	....	435	241	13.3
11	w o	11.7	....	....	32.7	265	12.1
12	w r o	10.5	....	....	241	295	10.9
13	w P	9.0	....	....	176	327	9.8
14	g' B P	7.8	....	....	125	366	8.8
15	w o	7.5	80	4710	87	416	7.7
16	w b r	6.8	60	5160	59	470	6.8
17	....	5.9	39	5060	39	540	5.9
18	(late)	4.9	22	4660	24.7	630	5.1
19	(early)	4.2	14	5200	13.7	766	4.1
20	....	3.4	7.4	5760	6.5	980	3.2
21	....	2.4	2.7	6530	2.1	.001430	2.2
22	....	1.8	1.1	8260	.7	.002030	1.6

[1]Use mean $S = 7.2$ as in table 16.

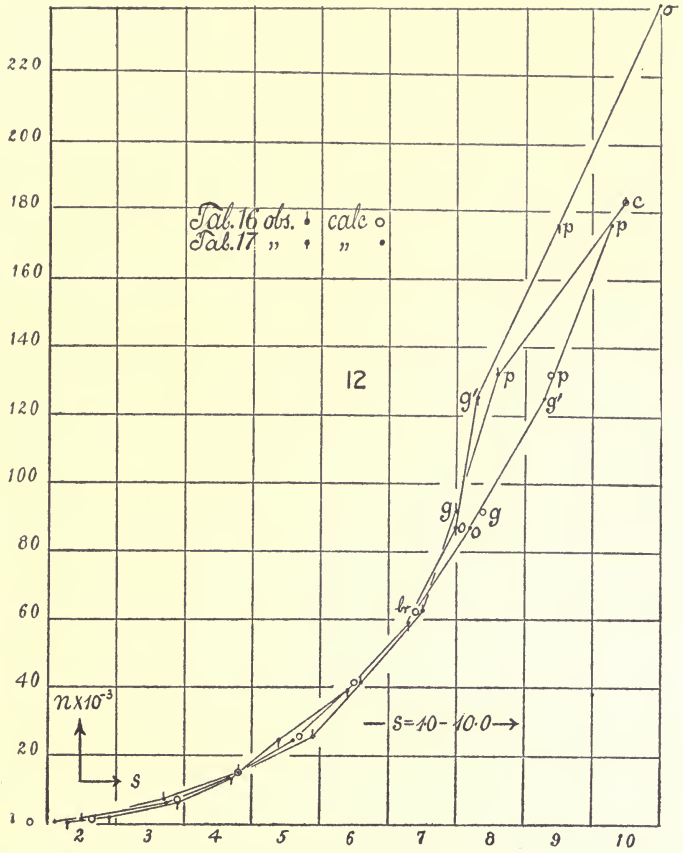

FIG. 12.—Nucleation *n*, in terms of the apertures of coronas. Small nucleation, moderate exhaustion.

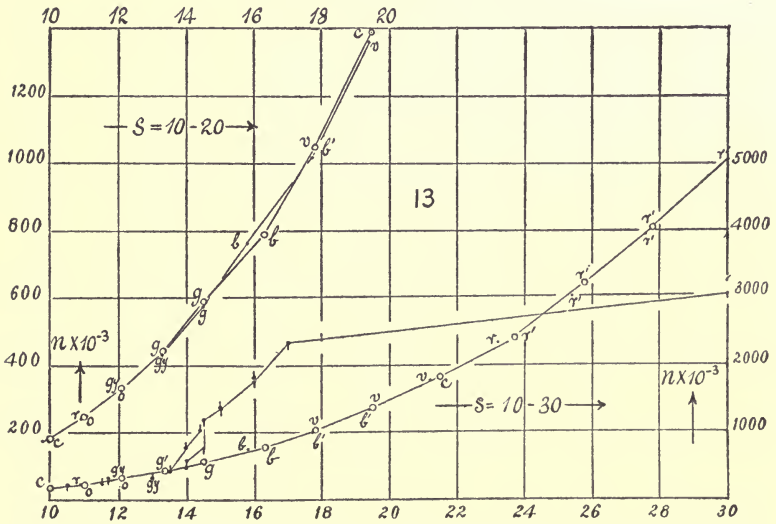

FIG. 13.—Nucleation *n*, in terms of the apertures of coronas. Large nucleations, moderate exhaustions.

The chief corrections are for subsidence of fog particles and for the change of m with a drop of pressure and temperature. For a rectangular vessel of height h, subsidence loss during a time t may be written vt/h, where v is the rate of subsidence in centimeters per second. Since $d^2 = 324 \times 10^{-8} v$ and $ds = a$, it may also be written for the fixed time t

$$\frac{vt}{h} = \frac{Sd^2}{a^2} = \frac{S}{s^2} \tag{5}$$

where S is the subsidence constant for the loss during the fixed time t. Hence for a rectangular vessel

$$S = \frac{t}{h}\left(\frac{10^4 a}{18}\right)^2 \tag{6}$$

and for a cylindrical vessel of radius r and horizontal axis

$$S = \frac{2t}{\pi r}\left(\frac{10^4 a}{18}\right)^2 \tag{7}$$

equations which will be useful below.

In the present case we may therefore write the nucleation obtained in successive identical exhaustions beginning with n_0

$$n_0 = n_0 y^0 \qquad n_1 = n_0 y\left(1 - \frac{S}{s_0^2}\right) \qquad n_2 = n_0 y^2\left(1 - \frac{S}{s_0^2}\right)\left(1 - \frac{S}{s_1^2}\right)$$

$$\cdots\cdots\cdots\cdots\cdots\cdots \tag{8}$$

$$n_z = n_0 y^z\left(1 - \frac{S}{s_0^2}\right) \cdots \left(1 - \frac{S}{s^2_{z-1}}\right) = n_0 y^z \prod\left(1 - \frac{S}{s^2}\right)$$

as further explained in the earlier volume. Again, since for normal coronas n_z is supposed to be given by $n = 6ms^3/\pi a^3$, S may be computed by two successive exhaustions as

$$S = s^2_z\left(1 - \frac{s^3_{z+1}}{y s^3_z}\right) \tag{9}$$

Hence the terms of the series

$$n_z/n_0 = y^z \prod_{s=0}^{s=z-1}\left(1 - \frac{S}{s^2}\right)$$

may also be computed, and since $n_z = \frac{6m}{\pi a^3} s^3_z$, the equation

$$n_0 = \frac{6ms^3_z}{\pi a^3} \cdot \frac{1}{y^z \prod\left(1 - \frac{S}{s^2}\right)} \tag{10}$$

is available for computing the initial nucleation n_0, and hence all subsequent nucleations, absolutely. Naturally a number of observations n_z and s_z will be used for computing n_0 and S. The equation shows very well how the constants n_0, S, a, m, are involved.

From n_z the diameter d_z of the zth fog particle may then be computed

$$d_z = n^{-1/3}_z \sqrt[3]{6m/\pi} \tag{11}$$

and similarly the zth aperture s_z will be, since $ds = a$

$$s_z = \frac{a}{\sqrt[3]{6m/\pi}} n^{1/3}_z \tag{12}$$

to be compared with the observed value of s_z. It is clear that d and s will be independent of m, while n varies directly with it. Examples of all these relations will be found in the following section.

27. Data for moderate exhaustions.—These data are given in tables 16 and 17. The drop of pressure is 17 cm. and the barometer unusually high at 77.7 cm. Consequently the relative drop is $\delta p_3/p = 0.219$ and $v_1/v = 1.19$, temperature 20° C. The symbols denote $\delta p' = p - p'$, $\delta p_3 = p - p_3$, $[\delta p_2] = p - [p_2]$, as explained in sections 25 and 26, where the meaning of y, a, S, D, etc., will also be found.

The first column shows the number z of the exhaustion, the second and third the selected annuli of the coronas and their apertures s, measured to the outer edge of red or the first annuli. In the fourth column $n' = 6ms^3/\pi a^3$, while the fifth shows successive values of n_0 and their mean. The sixth column gives the computed absolute nucleation, the seventh the corresponding diameter of the fog particle, and the eighth the computed aperture s. The data have been left as originally computed, for their relations are chiefly of interest; but the value of $m = 3.2 \times 10^{-6}$ here used is too small and will be corrected in section 34.

These data are shown graphically in figs. 12 and 13, the computed values of s being taken as abscissas, the computed n as ordinates. To admit the enormous range of the nucleation n the ordinates are appropriately changed in the scale of 10. The observed data are given in the same diagram, but with a different designation for the points.

28. Remarks on the tables and charts.—One may observe at the outset that the initial nucleation n is about the same in both cases, being $n = 5{,}100{,}000$ and $4{,}010{,}000$ smaller in the second. The same order of values will be found for the nucleations n in very different orders of exhaustions in the succeeding tables.

The following values of S were computed as shown in equation 9 from the data of tables 16 and 17:

$s=$	7.0	6.1	5.4	4.3	3.2	2.0	1.0
$S=$		7.4	3.9	10.4	8.7	6.9	3.3
$s=$	7.5	6.8	5.9	4.9	4.2	3.4	2.4	1.8
$S=$		2.0	7.6	9.1	4.8	5.8	5.8	2.9

Leaving out the smallest coronas and those which are no longer normal, the data $S=7.2$ and $S=6.8$ were taken as fair averages in the two cases. The data for n_0 show that the first table (16) is somewhat overcompensated, while the second (17) is undercompensated by the values of S entered. The high value of $[\delta p_2]=16.8$ was accepted with misgivings, but there is no evidence against it. It is interesting to compare with the above values of S those which may be computed from subsidence data in the way given in equation 7. From this it appears that $S=1.7$ for $t=5$ seconds of subsidence of fog. Now, the time needed for complete evaporation was about 15 or 20 seconds, whence it follows that S must be of the order of 5 to 7, agreeing therefore very well with the datum computed from coronas. For the very small coronas subsidence is too rapid to enter into any correction of this kind.

The selection of a constant $a=ds=0.0032$ is the weakest part of the above deduction. It is based on the earlier memoir and obtained from the subsidence of observed coronas. Since the theory of diffraction for an angular radius ϕ of the coronas gives

$$\sin\phi = s/60 = 1.22\,\lambda/d \tag{13}$$

for the first minimum annulus of wave-length λ, and $ds=a$,

$$a = 73.2\,\lambda \tag{14}$$

whence $a=0.0032$ would correspond to blue violet. With an eye at but 30 cm. from the fog chamber, the equation for $\sin\phi$ is certainly not quite true and a must be variable with λ, except perhaps for the smaller normal coronas, which are so closely packed that a mean value of λ is suggested.

If m be taken as 3.2×10^{-6}, equation 4 shows $n'=190\,s^3$. Equation 14 incorporated in equation 4 would imply for $10^6\ m=3.2$

$$n^1 = \frac{6m\,s^3}{\pi(73.2\,\lambda)^3} = \frac{15.6s^3}{(10^4\,\lambda)^3}$$

$10^4\,\lambda_r=7.6$	$10^4\lambda_o=6.0$	$10^4\,\lambda_v=4.0$
$n'=0.036\,s^3$	$n^1=0.072\,s^3$	$n^1=0.240\,s^3$

according as the first red, orange, or violet minimum were used, data which merely imply an order of values, as equation 13 is not fully applicable.

Tables 16 and 17 and figs. 12 and 13 show a satisfactory order of agreement between the observed and computed values of s and the corresponding data computed for n as far as $s=7$ to 10 cm., where the middle green coronas enter. The agreement thereafter improves again until the higher green coronas are passed, when further divergence is marked. I will not enter into this here, as the subject has been discussed

in the earlier memoir. It is necessary, moreover, to investigate some other method of obtaining s for the very large coronas, such as is given in Chapter IV. In the present memoir the discrepancy is accentuated by the short periods of 1 minute between the observations. This is not sufficient for the complete mixture of the inflowing air and the nucleated air within the fog chamber. As a result there are apt to be color distortions and bands of color before the real corona appears, while the latter is not quite sharp. It was thought that longer intervals of waiting between the exhaustions would have introduced other discrepancies or losses of nuclei. Experiments made under these conditions did not, however, much improve the irregularities, as may be seen in section 36. Furthermore, in the larger coronas it is difficult to determine the actual limits of the diffused annuli by the present single-source method. The same difficulty will appear in the next section. Finally the d and s values computed from equations 11 and 12 show

$$d = 0.0183\ n^{-1/3} \qquad s = 0.175\ n^{1/3}$$

For the lower coronas these s values agree with the observed data quite within the errors of observation, remembering that the coronas were not perfectly sharp. For the higher coronas they are probably close to the truth, provided the green and blue coronas be measured to the purple rings. Both d and s will be discussed below and another reduction will be attempted.

29. Data for low exhaustions.—Inasmuch as the only correction added was for subsidence, it is necessary to test in how far convection losses of nuclei upon evacuation, losses on evaporation, and losses in the lapse of time (decay) are relatively small. This may be done by comparing the data for very low exhaustions with the data for relatively high exhaustions. In the former case many exhaustions must be made and a longer time will elapse between the first and last of the equal intervals than in the second case, where there will be relatively few exhaustions and a relatively small lapse of time. If the errors in question are negligible, the same initial nucleation and the same diameter of fog particles for the same coronas will be obtained. The subsidence constant S appears as follows:

$s=$	6.9	5.8	5.4	4.8	4.1	3.3	2.7	2.0	1.0
$S=$	15.4	2.6	5.5	6.7	6.8	3.9	3.9	——	

$s=$	6.7	6.2	6.0	5.3	4.5	4.0	3.3	2.5	1.7
$S=$	4.1	——	7.6	8.4	3.8	5.8	5.5	4.1	

The mean values are $S_1 = 6{\cdot}8$, $S_2 = 4{\cdot}9$. Hence $S = 5{\cdot}9$ was taken. Experiments showed $[\delta p_2]$ for 5 seconds of opening of the exhaust cock to be equivalent to $y = 0{\cdot}873$. The computed diameter

$$d = (6m/\pi n)^{1/3} = 0.0161 n^{-1/3}$$

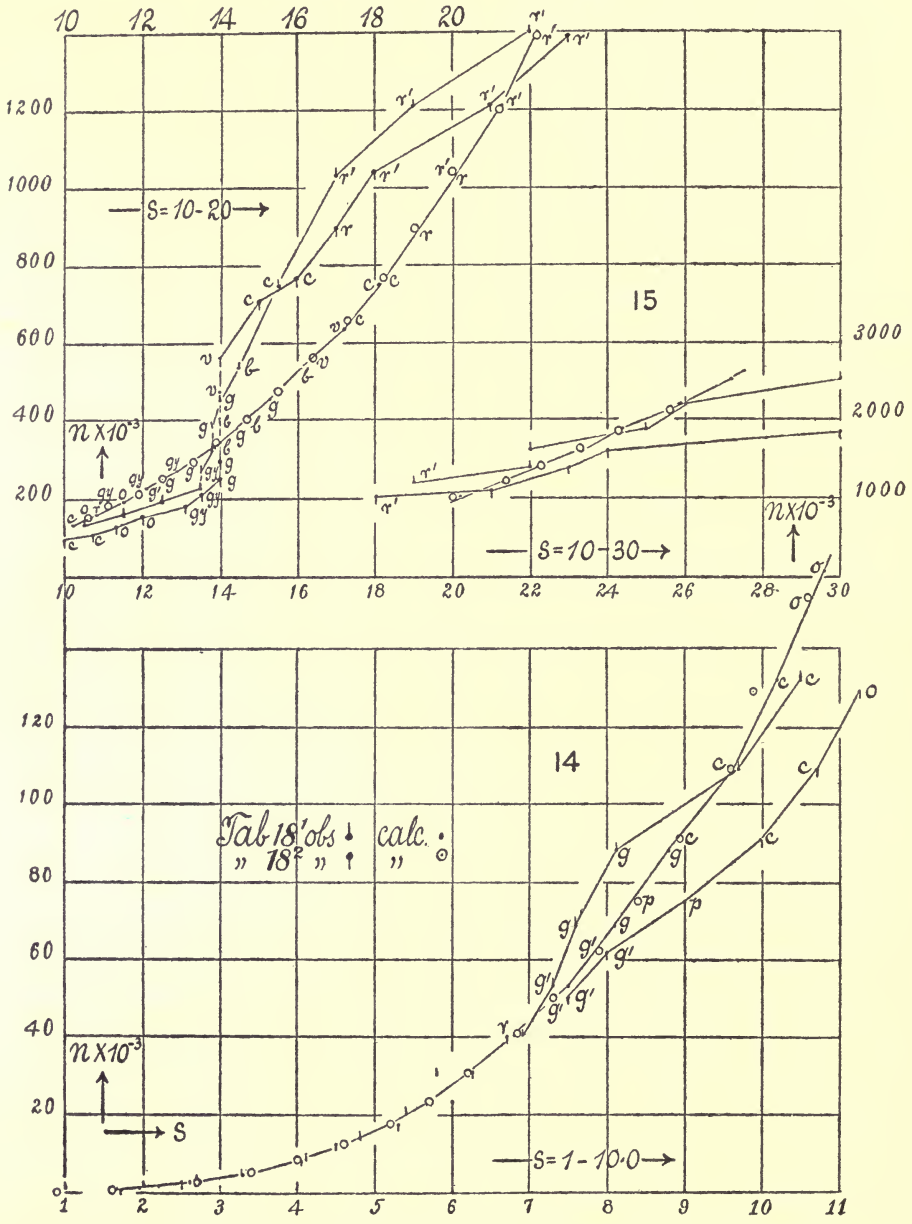

FIG. 14.—Nucleation n, in terms of the apertures of coronas. Low nucleations; low exhaustions.

FIG. 15.—Nucleation n, in terms of the apertures of coronas. High nucleation; low exhaustion.

TABLE 18.—Coronas standardized. Phosphorus nuclei. Bar. 75.1 cm.; temp. 26°; 60 seconds between observations; cock open 5 seconds. $\delta p' = 10.7$; $\delta p_3 = 10.0$; $[\delta p_2] = 9.2$; $\gamma = 0.873$; $S = 6.8$; $a = 0.0032$.

No.	Corona.	s.	$10^3 n' = 0.128 s^3$.	$n_0 \times 10^{-3}$ (ratio).	$n \times 10^{-3}$.	$d = 0.0161 \times n^{-1/3}$.	$s' = a/d$.
1	R fog	30	....	2540	2540	0.000118	27
2	R fog	26	....	....	2200	124	25.9
3	R fog	25	....	....	1880	131	24.4
4	R fog	22	....	....	1630	137	23.3
5	R fog	22	....	....	1400	144	22.2
6	w R′	19	....	....	1210	150	21.3
7	! w R	17	....	....	1030	159	20.1
8	! w c	16.5	....	....	....	163	19.6
9	[1]w c	15.5	....	....	748	177	18.1
10	[1]v	....	....	....	635	186	17.2
11	Blue	14.5	....	....	537	199	16.1
12	g B P	14	....	....	454	209	15.3
13	g B P	13.8	....	....	383	222	14.4
14	g B P	13.8	....	....	322	233	13.7
15	g y o	13.5	....	....	271	247	12.9
16	[1]g y o	13.5	....	....	228	264	12.1
17	y o	12.5	....	....	191	278	11.5
18	y r	11.5	....	....	160	298	10.8
19	w c	10.5	....	....	132	316	10.2
20	w P cor	9.7	....	....	108	335	9.6
21	g BP	8.1	....	....	88	362	8.8
22	g BP	7.6	....	....	68.7	393	8.1
23	....	7.3	....	....	53.0	428	7.5
24	....	6.9	42.0	2650	40.3	470	6.8
25	....	5.8	25.0	2100	30.2	518	6.2
26	....	5.4	20.1	2430	21.1	584	5.5
27	....	4.8	14.2	2560	14.1	665	4.8
28	....	4.1	8.8	2590	8.6	785	4.1
29	....	3.3	4.6	2580	4.5	976	3.3
30	....	2.7	2.6	2880	2.3	.001220	2.6
31	....	2.0	1.0	1810	1.4	1438	2.2
32	....	1.0	.1	2970	.9	1660	1.9
33	....	.0	.0	4850	.5	2038	1.6
II. Same. Bar. 75.4 cm.; temp. 24° C.; $S = 4.9$.							
1	Fog	....	....	....	2120	0.000125	25.6
2	Fog	30	....	....	1850	131	24.3
3	Fog	24	....	....	1610	138	23.2
4	R fog	23	....	....	1390	144	22.2
5	R fog	21	....	....	1210	150	21.3
6	R fog	18	....	....	1040	160	20.0
7	R fog	17	....	....	893	168	19.0
8	C fog	16	....	....	767	176	18.2
9	C fog	15	....	....	658	185	17.3
10	v-c	14	....	....	561	195	16.4
11	Violet	14	....	....	477	207	15.5
12	B	14	....	....	406	218	14.7
13	g-b	14	....	....	346	230	13.9
14	g b p	14	....	....	294	241	13.3
15	g′ b p	14	....	....	251	256	12.5
16	g y o	13	....	....	213	268	11.9
17	g y o	13	....	....	181	288	11.1

[1] Mixed colors.

TABLE 18—Continued.

No.	Corona.	s.	$10^3 n' = 0.128 s^3$.	$n_0 \times 10^{-3}$ (ratio).	$n \times 10^{-3}$.	$d = 0.0161 \times n^{-1/3}$.	$s' = a/d$.
18	w o	12.0	....	....	153	0.000301	10.6
19	w o	11.3	....	....	129?	322	9.9?
20	w c	10.7	....	....	109	335	9.6
21	w c	10.0	....	....	91	358	8.9
22	w P	9.0	....	....	75	382	8.4
23	g' b p	8.0	....	....	62	407	7.9
24	g' b p	7.5	....	....	50	438	7.3
25	w r	6.7	38.5	2060	40	471	6.8
26	w e	6.2	30.5	2090	30.9	513	6.2
27	cor	6.0	27.6	2490	23.5	563	5.7
28	cor	5.3	19.1	2290	17.7	617	5.2
29	cor	4.5	11.6	1930	12.8	688	4.6
30	cor	4.0	8.2	2070	8.4	793	4.0
31	cor	3.3	4.6	1910	5.1	936	3.4
32	cor	2.5	2.0	1720	2.5	.001180	2.7
33	cor	1.7	.6	2690	.5	2040	1.6
34	cor	.0	.0		.1	3500	.9

The data of table 18 are arranged as above for table 16. The adiabatic drop of pressure is 10 cm. from 75.1 cm. and the relative drop therefore $\delta p_3/p = 0.133$ and the volume expansion about $v_1/v = 1.107$. The water precipitated per cubic centimeter is about $m = 2.2$ grams per cubic centimeter, in both series at 26° and 24°. Hence $n = 0.128 s^3$. A more recent value of m will be inserted for definite purposes in section 34.

These data are given in the charts (figs. 14 and 15) with a usual distinction between observed and computed values of the coronal apertures s. The divergence again begins in the region of green coronas, but is here on opposed sides of the line computed for the two series. The reason of this is the lack of homogeneity of the wet nucleated air, when the interval between observations is but 1 minute. The colors of coronas are mixed and the individual observations to this extent uncertain. With these differences the periods occur in the usual way.

An interesting result of this series is the occurrence of *crimson* and *red* coronas of the *first order*, above the violet. In other words the initial fogs soon dissolve into true coronas. But their size is difficult to estimate in case of the single-source method, because of their filmy character.

One may note that the initial nucleations $n_0 = 2{,}320{,}000$ and 2,470,000 correspond to the values of the table 19.

30. Data for high exhaustions.—The corresponding results for an adiabatic drop of pressure of 27.1 cm. from 75 cm. are found in table 19. There are three series. The relative drop of pressure is $\delta p_3/p = 0.273$, the volume expansion $v_1/v = 1.254$. Hence, in the absence of phosphorus nuclei, precipitation will take place, in the given apparatus, on

the nuclei of dust-free air, which are within reach of the exhaustion to the extent of about $n=57{,}000$. Coronas can not be brought to vanish, but up to the final limit the water nuclei are alone active. The amount of water precipitated per cubic centimeter at 25° was taken as $m=4.1\times10^{-6}$. Hence $n'=0.242\ s^3$. The subsidence constants appear as

$s=$	7.4	5.8	4.9	‖	7.2	6.3	5.3	4.6	‖	7.3	5.6	5.0
$S=$	14.6	2.7		‖	−1.1	3.6	2		‖	16.4	−2.0	

an irregular series of values, due to the increasing efficiency of the vapor nuclei of dust-free air. The values of S found in tables 16 and 17 are therefore taken in preference. The observed drop $[\delta p_2]$ corresponds to $y=0.656$. The diameter of particles is $d=0.0199n^{-1/3}$. The value of m taken will be replaced by a more recent value in section 34.

TABLE 19.—Coronas standardized. Phosphorus nuclei. Bar. 75.0 cm.; temp. 25°; 60 seconds between observations; cock open 5 seconds. $\delta p'=27.1$; $\delta p_3=20.5$; $[\delta p_2]=25.0$; $y=0.656$; S=6.5 assumed; $a=0.0032$.

	No.	Corona.	s.	$n'10^{-3}=0.242s^3$.	$n_0\times10^{-3}$.	$n\times10^{-3}$.	$d=n^{-1/3}\times0.0199$.	$s'=a/d$.
I.	1	R fog	20	....	2320	2320	0.000150	21.3
	2	w c	15	....	....	1500	173	18.5
	3	violet	15.5	....	....	955	202	15.8
	4	G b p	15	....	....	608	235	13.6
	5	g y o	14	....	....	387	273	11.7
	6	w r	10.5	....	....	246	317	10.1
	7	P cor	8.6	....	....	152	373	8.6
	8	w o	7.4	98	2510	90.8	442	7.2
	9	cor	5.8	42.2	2080	52.5	532	6.0
	10	[1]cor	4.9	28.5	2370	27.9	657	4.9
	11	cor	4.8	26.6	(4610)	13.4	840	3.8
II.	1	Fog	....	....	2470	2470	0.000148	21.6
	2	R′ fog	23	....	....	1610	170	18.8
	3	Fog	....	....	....	1040	197	16.3
	4	g b p	16	....	....	673	227	14.1
	5	g′ o	....	....	....	430	264	12.1
	6	y o	11.8	....	....	272	307	10.4
	7	w P cor	9.3	....	....	170	359	8.9
	8	w y	7.2	90.3	2160	103	424	7.5
	9	cor	6.3	60.5	2520	593	510	6.3
	10	cor	5.3	36.1	2730	32.6	624	5.1
	11	[1]cor	4.6	23.5	(3530)	16.4	783	4.1
	12	D. F. air	6.1	54.9	....	....	....	....
III.	1	Fog	23	....	2270	2270	0.000152	21.0
	2	R fog	....	....	....	1470	175	18.3
	3	violet	17	....	....	951	202	15.8
	4	g b p	15	....	....	610	235	13.6
	5	g y o	13.6	....	....	388	273	11.8
	6	w r	10.6	....	....	246	317	10.1
	7	w P cor?	8.0	....	....	152	373	8.6
	8	w o	7.3	94.1	2390	89.5	445	7.2
	9	cor	5.6	42.6	1880	51.4	535	6.0
	10	cor	[2]5.0	29.7	2530	26.7	666	4.8

[1] Nuclei of dust-free air and water nuclei remain constant.
[2] Nuclei of dust-free air in presence of water nuclei.

The preceding data are shown in fig. 16, with a distinction between the observed and computed values of s. The usual difficulties due to impure colors are apparent. In view of the high exhaustions many typical coronas do not appear and the small coronas are lost by the efficiency of vapor nuclei as stated.

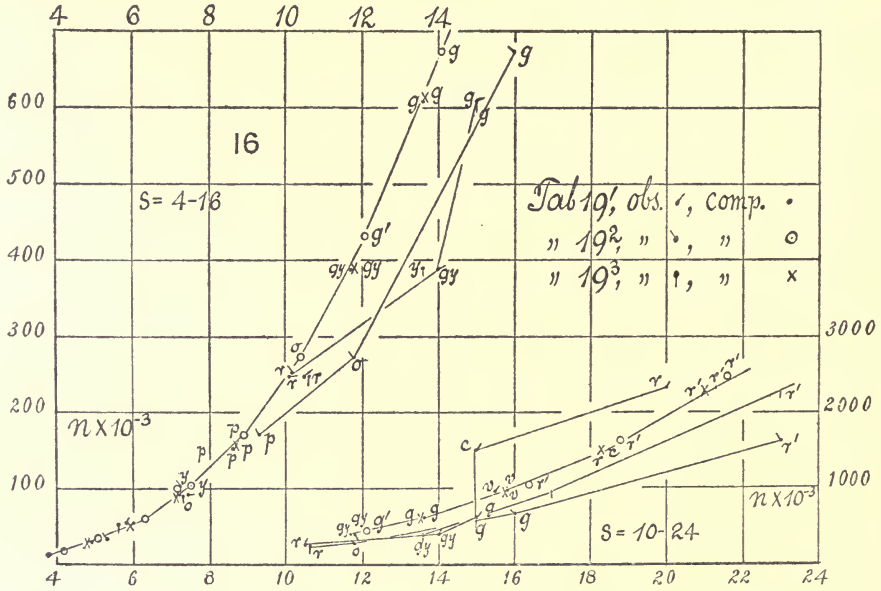

FIG. 16.—Nucleation n, in terms of the apertures of coronas. High exhaustion.

31. Standardization with ions.—The endeavor to standardize the coronas by precipitating the fog particles upon ions lead to peculiar results, which makes it necessary to discuss the subject independently in Chapter V. In fact, about one-half of the water nuclei which should be present after the first evaporation of fog particles vanishes independently. Half the ions are thus not represented by fog particles, except in the first precipitation. The remainder in the subsequent exhaustions behave more normally.

32. Further data.—Results obtained in case of the intermediate exhaustions $\delta p_3 = 17$ cm. are liable to be most serviceable for the construction of a practical table, and two further series were therefore investigated under atmospheric conditions different from the above. These results are given in table 20 and in figs. 17 and 18. In both series the agreement between the observed and computed values of s within $s = 10$ is surprisingly close. The attempt was, moreover, to compute tables 16 and 17 under modified suppositions, putting $[\delta p_2] = 16.3$ as in table 20 and then reducing all data to 24°. The results are of no marked advantage over the earlier data and are therefore omitted.

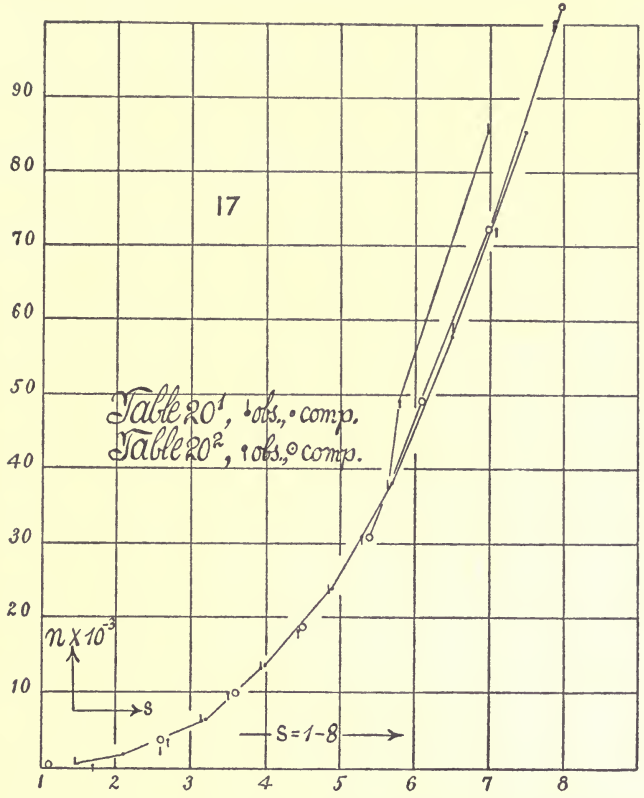

FIG. 17.—Nucleation n, in terms of the apertures of coronas. Low nucleation, moderate exhaustion.

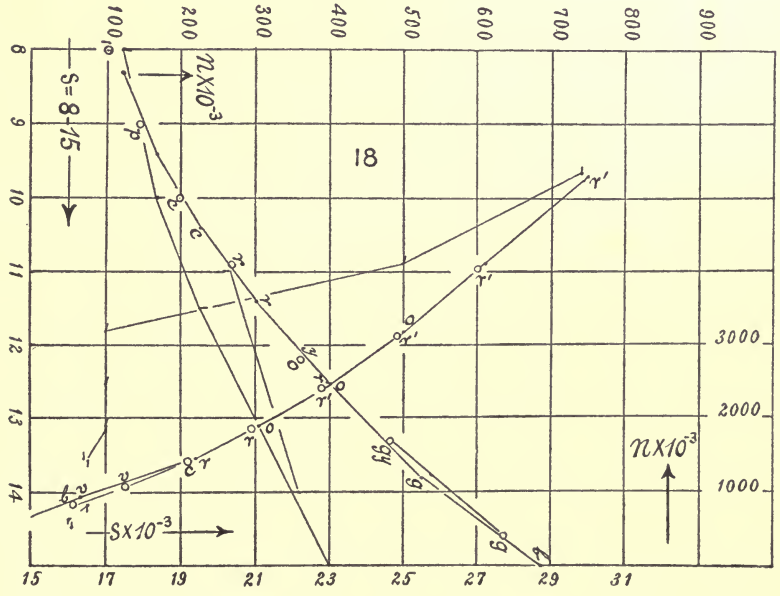

FIG. 18.—Nucleation n, in terms of the apertures of coronas. High nucleation, moderate exhaustion.

TABLE 20.—Coronas standardized with phosphorus nuclei. Bar. 76.2 cm.; temp. 24° C.; cock open 5 seconds; 60 seconds between observations. $\delta p' = 18.1$ cm.; $\delta p_3 = 17.1$; $[\delta p_2] = 16.3$ after 60 seconds; distances 40 cm. and 250 cm.; goniometer arms 30 cm.; $y = 0.78$; $S = 6.5$; $ds = 32$.

	No.	Corona.	s.	$10^3 n' = 0.210 s^3$.	$n_0 \times 10^{-3}$ (ratio).	$n \times 10^{-3}$.	$d = n^{-1/3} \times 0.019$.	$s' = a/d$.
I.	1	Fog	(30)	....	5302	5302	0.000108	30.0
	2	Fog	25	....	....	4110	119	27.2
	3	w o	17	....	....	3180	129	25.0
	4	w o	17	....	....	2470	141	23.0
	5	w o	17	....	....	1900	153	21.1
	6	w r o	16	....	....	1470	167	19.4
	7	v	....	....	....	895	198	16.3
	8	b	16	....	....	686	216	15.0
	9	b g	16	....	....	524	235	13.8
	10	w y o	15	....	....	397	258	12.5
	11	w r o	13	....	....	301	284	11.4
	12	w c	11.5	....	....	226	312	10.4
	13	w P	10	....	....	167	345	9.4
	14	cor	8	....	....	122	383	8.3
	15	....	7	72.0	4470	85.5	431	7.5
	16	....	6.5	57.7	5300	57.8	491	6.5
	17	....	5.7	38.8	5410	38.1	564	5.7
	18	....	4.9	24.8	5530	23.8	660	4.9
	19	....	4.0	13.4	5260	13.5	800	4.0
	20	....	3.2	6.9	5840	6.3	0.001027	3.2
	21	....	2.6	3.7	11070	1.8	1560	2.1
	22	....	1.5	.7	5970	.6	3170	1.5

	No.	Corona.	s.	$10^3 n' = 0.210 s^3$.	$n_0 = 10^{-3}$.	$n \times 10^{-3}$.	$d = n^{-1/3} \times 0.019$.	$s' = a/d$.
II.	1	Fog	....	....	4040	4040	0.000120	27.0
	2	w r′	(18)	....	....	3130	130	24.8
	3	w e	....	....	....	2410	138	22.8
	4	! w r	17.0	....	....	1860	154	20.9
	5	w c	16.5	....	....	1430	168	19.2
	6	v	....	....	....	1090	184	17.5
	7	b g	16.5	....	....	836	202	16.1
	8	g	16.0	....	....	635	221	14.6
	9	g y	....	....	....	481	242	13.0
	10	w o	14.0	....	....	361	267	12.2
	11	w r	11.0	....	....	268	295	10.9
	12	w c	10.0	....	....	198	326	10.0
	13	cor	9.0	....	....	144	363	9.0
	14	....	7.9	....	....	104	404	8.0
	15	....	7.1	75.2	4200	72.4	456	7.0
	16	....	5.8	41.0	3370	49.1	520	6.1
	17	....	5.3	31.3	4090	30.9	605	5.4
	18	....	4.5	19.1	4160	18.5	717	4.5
	19	....	3.5	9.0	3710	9.8	888	3.6
	20	....	2.7	4.2	4710	3.6	0.001240	2.6
	21	....	1.7	1.0	....	.3	2840	1.1
	22	....	r	....	....	.03	6130	.5
	23	....	o	....	....	.0	....	.0

33. The violet and green coronas.—The object of the series of experiments made at very low exhaustions ($\delta p = 10$) and compared with a series for high exhaustions ($\delta p = 20.5$) was an estimation of the importance of the time effect and of the convective effect in causing loss of nuclei. If the latter series be reduced to the former by modifying the constants in terms of pressure and temperature the coincidence of the graphs is complete, as shown in fig. 19. This indicates that the method of reduction is reliable.

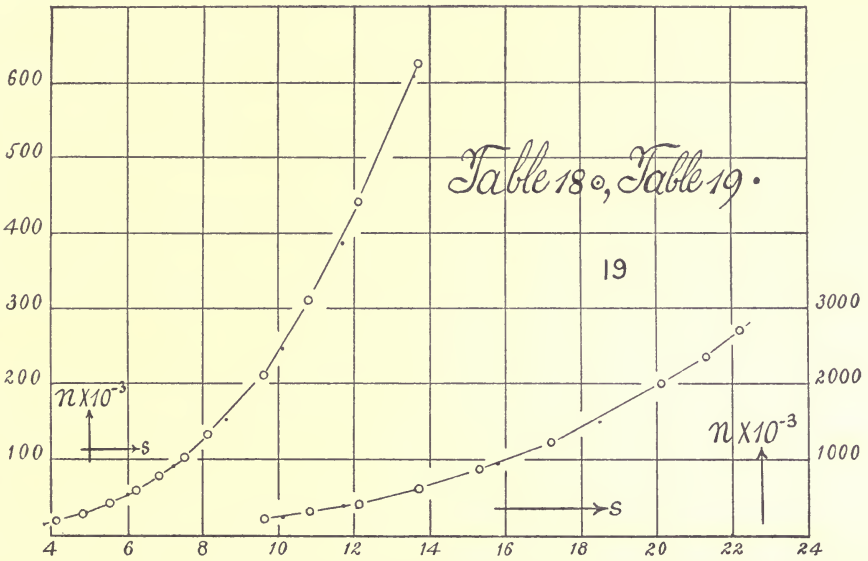

FIG. 19.—Nucleation n, in terms of the apertures of coronas. Results in tables 18 and 19 compared.

TABLE 21.—Violet and green coronas, d and s values.

Color.	Tables 16 and 17.[1]		Table 18.		Table 19.		Table 20.		Mean $d \times 10^6$ and s.
	$\delta p_3 = 17$.		$\delta p_3 = 10$.		$\delta p_3 = 20.5$.		$\delta p_3 = 17$.		
	$d \times 10^6$.	s.	$d \times 10^6$.	s.	$d \times 10^6$.	s.	$d \times 10^6$.	s.	
Violet (2) . . .	190	17.0	190	17.2	200	15.8	200	16.3	191
	170	18.5	200	16.0	....	....	180	17.5	16.8
	....	....	....	....	200	15.8	....	....	....
Green (2) . . .	220	14.4	220	14.4	230	13.6	230	13.8	228
	230	14.4	240	13.3	230	14.1	220	14.6	14.0
	....	....	....	....	230	13.6	....	....	....
Green (3) . . .	410	7.8	390	8.1	410	7.9	380	8.3	398
	370	8.6	420	7.6	390	8.2	400	8.0	8.1
	....	....	....	....	410	7.9	....	....	....
Green (4) . . .	....	....	....	....	....	....	....	....	....

[1] Computed with $n' = 0.199s^3$ and $y = 0.786$, the latter being more in keeping with table 20.

To find, however, in how far the results themselves are trustworthy, it will be necessary to find the computed values in the different series of the diameter of the particles producing a given corona. For this purpose the violet and green coronas are suitable. There are three of the latter, the two upper being very brilliant. In the former report the diameters of particles were estimated as $d=0.000460$ cm. for the middle green corona. Ratios of 4, 3, and 2 were usually apparent, the data being multiples of a diameter something larger than $d=0.00015$, the corona for which is not producible. In the present experiments the values of d and s for the green coronas are given in table 21.

While there is considerable fluctuation, the data approach very closely to a common mean, remembering that the color itself necessarily has a certain latitude and wide differences of exhaustion are involved. The ratio 2, 3, 4 of diameters of fog particles is not as well suggested in the present result as in the former, while the absolute sizes themselves are throughout smaller. It is nevertheless convenient to retain the ratio for the division of coronas into successive series. If these may be considered as beginning with deep red and ending with violet the following group may be postulated:

TABLE 22.—Showing cycles.

v_1,	($d=0.00011$ cm.)	v_2,	$d=0.00019$ cm.	v_3,	$d=0.00033$ cm.	v_4,	$d=0.00044$ cm.
g_1,	(13 cm.)	g_2,	23 cm.	g_3,	40 cm.	g_4,	52 cm.
r_1,	16 cm.	r_2,	32 cm.	r_3,	48 cm.	r_4,	64 cm.

Only the red and crimson of the first series are certainly observable with the above apparatus. Their aperture is about 60°, their rings diffuse, and their disk filmy, so that in a small apparatus they would be mistaken for clear air. The second series is producible and vivid throughout, and the same is even more true of the third. The fourth is already closely packed, while the fifth and subsequent series merge into each other too rapidly for separation.

Series 3 and 4 were obtained in great number in my work with atmospheric nucleation. Selecting some twenty or more cases the mean ratio $1/s_3 : 1/s_4 = 0.146 : 0.206 = d_3 : d_4$. Hence the ratio of 3 : 4 is very well sustained. The goniometer distance from the fog chamber was nearly a meter in this case. In the present experiments, however, the short goniometer distance ($D=30$ cm.), though adapted for the best seeing, is not so suitable for measuring diameters. Apart from this, the former experiments were made with plate-glass apparatus. In cylindrical apparatus, as in the present case, there must have been appreciable refraction due to differences of thickness. Hence it is probable that the series 1 is actually the first occurring, although the smallest active particles (violet) must exceed 0.0001 cm. in diameter. The same terminal conditions are suggested by the axial colors of the

steam jet. It seems curious that the diffraction phenomenon should begin with particles of the order of three times the wave-length of light.

Using the method of contact of coronas from two sources described below, the ratio of diameters of the first four series is much more nearly as 1, 2, 3, 4, for the green coronas for instance, than in the present experiments.

34. Insertion of new values for m.—The values of m used in the above tables were throughout obtained from the earlier experiments. As the relations of n are not affected and as m does not influence d and s (see equations, section 26) the latter will be left in this form. The nucleation n varies as m. Since that time, however, new data for m were investigated compatibly with Chapter II. Inserting these in tables 16 and 17 and agreeing that n shall hold for $\delta p/p = 0.219$ and 20°, $10^6\, m = 3.2$ must be replaced by $10^6\, m = 3.6$. In table 20, similarly, for $\delta p/p = 0.224$ and 20° C., $10^6\, m = 3.6$ must be replaced by $10^6\, m = 3.7$. These results have been compiled in table 23, which is adapted for practical purposes. The results are nearly coincident. These data will be used in preference for the computation of nucleation.

TABLE 23.—Values of s and n referred to new values of m.

	Table 16.		Table 17.		Table 20, I.		Table 20, II.	
	s.	$n \times 10^{-3}$.	s.	$n \times 10^{-3}$.	s.	$n \times 10^{-3}$.	s.	$n \times 10^{-3}$.
	r′ 27.8	4490	r′ 30.2	5710	r′ 30.0	5460	r′ 27.0	4163
	r′ 25.8	3620	r′ 27.6	4400	r′ 27.2	4233	r′ 24.8	3223
	r′ 23.7	2708	r′ 25.4	3420	o 25.0	3276	r′ 22.8	2482
	r′ 21.5	2064	r′ 23.2	2630	o 23.0	2545	r 20.9	1916
	c 19.5	1558	r 21.2	2010	o 21.1	1957	c 19.2	1473
	v 17.8	1176	v 19.4	1520	r o 19.4	1514	v 17.5	1123
	b 16.3	886	b′ 17.7	1140	v 16.3	922	b g 16.1	861
	g 14.5	665	B 15.8	861	b 15.0	707	g 14.6	654
	g′ 13.3	500	g 14.5	649	b g 13.8	540	g y 13.3	495
	g y 12.1	373	g y 13.3	487	y o 12.5	409	o 12.2	372
	y o 11.0	278	o 12.1	366	r o 11.4	310	r 10.9	276
	c 10.0	205	r o 10.9	270	c 10.4	233	c 10.0	204
	p 8.9	148	p 9.8	197	p 9.4	172	9.0	148
	g 7.9	103	g′ 8.8	140	8.3	126	8.0	107
	o 6.9	69.6	o 7.7	97	7.5	88.	7.0	76.6
	6.0	46.3	b r 6.8	66	6.5	59.5	6.1	50.6
	5.2	29.0	5.9	43	5.7	39.2	5.4	31.8
	4.3	17.0	5.1	27.6	4.9	24.5	4.5	19.0
	3.4	8.1	4.1	15.3	4.0	13.9	3.6	10.1
	2.0	1.6	3.2	7.3	3.2	6.5	2.6	3.7
	1.3	.4	2.2	2.3	2.1	1.9	1.1	.3
	....	....	1.6	.8	1.5	.6	.5	.03
$10^6 m =$	3.6	....	3.6	....	3.7	....	3.7	....
$\delta p/p =$	.219	....	.219	....	.224	....	.224	....
$d =$	$.0190 n^{-1/3}$	....	$.0190 n^{-1/3}$	....	$.0192 n^{-1/3}$	....	$.0192 n^{-1/3}$	....
$s =$	$.168 n^{1/3}$	....	$.168 n^{1/3}$	....	$.167 n^{1/3}$	....	$.167 n^{1/3}$	....

To reduce the other tables to the same standards (remembering that n varies as m, while d and s are independent of it), is not necessary for the present comparisons. In table 18, however, $10\ m^6 = 2.1$ should be replaced by $10^6\ m = 2.3$, where $\delta p/p = 0.133$. In table 19, $\delta p/p = 0.273$, $10^6\ m = 4.1$ is to be replaced by $10^6\ m = 4.3$. In all cases the initial nucleations are thus increased. The new values for m are referred to 20° C. and the temperature coefficient is about 2 per cent per degree.

35. Wilson's* data and conclusions.—The following table (24) contains Wilson's exhaustions (v_1/v) at 18° to 19° C. and the corresponding disk colors as I interpret them. It also contains the equivalent relative drop of pressure $\delta p/p$ used above. From these and the colors, the diameters of fog particles (d) may be estimated, provided the series in which these colors lie is known; hence $d_{3,2}$ refers to the probable case of the occurrence of the third and second series, $d_{2,1}$ to the very improbable case of the occurrence of the second and first series. Hence if the values m be found for the corresponding temperature and expansions ($\delta p/p$) the nucleations $n_{3,2}$ and $n_{2,1}$ respectively follow. Wilson gives but a single series between green coronas. There are two such series and three definite green coronas producible, and I shall assume that the very vivid upper one is meant. The first series is not producible by any means known to me, except in the lower red coronas. Hence I ignore $n_{2,1}$ and take $n_{3,2}$, in which case the data are distributed similarly to my own, so far as the slope of the curves is concerned.

TABLE 24.—Estimation of the nucleation and size of nuclei corresponding to Wilson's colors for wet dust-free air. Temp. 18° to 19° C.

v_1/v.	$10^3 \times \delta p/p$.	Disk color.	$d_{3,2} \times 10^5$.	$d_{2,1} \times 10^5$.	From d.		From color.	
					$n_{3,2} \times 10^{-3}$.	$n_{2,1} \times 10^{-3}$.	$n_{3,2} \times 10^{-3}$.	$n_{2,1} \times 10^{-3}$.
1.410	384	g	40	23	160	870	190	870
1.410	384	g	....	....	....	....	....	....
1.413	386	g	....	....	....	....	....	....
1.416	388	bg	....	....	....	....	....	....
1.418	389	b	....	....	....	....	....	....
1.419	390	v	33	19	290	1460	265	1500
1.420	390	v	....	....	....	....	....	....
1.420	390	r p	....	....	....	....	....	....
1.426	394	r	32	16	325	2650	320	2150
1.429	396	r g	....	....	....	....	....	....
1.436	400	y w	....	....	....	....	....	....
1.448	401	w	....	....	....	....	....	....
1.469	418	g w	23	12	910	6500	910	7000
1.373	360	Fog limit.						
1.31	317	+ions, condensation limit.						
1.25	270	−ions, condensation limit.						

*Phil. Trans. Roy. Soc., vol. 189, p. 265, 1897. *Cf.* p. 285.

There is another way in which the estimate in question may be made. Let the nucleations corresponding to the colors be taken and reduction made for the different drops of pressure in question. This is merely a corroboration of the method of computation. The coincidence is as close as may be expected, as the methods of approach are widely different and the nucleation varies as the cube of the inverse diameter.

Wilson's views of the nature of the phenomena are quite different and lead to enormous nucleation, even as compared with the improbable $n_{2,1}$. He says (*loc. cit.*, p. 301):

> When all diffraction colors disappear and the fog appears white from all points of view, as it does when [the expansion] v_2/v_1 amounts to about 1.44, we can not be far wrong in assuming that the diameter of the drops does not exceed one wave-length in the brightest part of the spectrum, that is, about 5×10^{-5} cm. That the absence of color is not due to the inequality of the drops is evident from the fact that the colors are at their brightest when v_2/v_1 is only slightly less than 1.44 and from the perfect regularity of the color changes up to this point.
>
> Taking the diameter of the drops as 5×10^{-5} cm., we obtain for the volume of each drop about 6×10^{-14} c. cm., or its mass is 6×10^{-14} gram.
>
> Now, we have seen that when the expansion is such as produces the sensitive tint (when $v_2/v_1=1.42$), the quantity of water which separates out is about 7.6×10^{-6} gram in each cubic centimeter. With greater expansions rather more must separate out. We therefore obtain as an inferior limit the number of drops, when $v_2/v_1=1.44$, $7.6\times10^6/6\times10^{-14}=10^8$ per cubic centimeter.

In my data the smallest green corona corresponds to a diameter of particles of about $d_4=0.00052$ cm., the next to $d_3=0.00040$ cm., the next to $d_4=0.00023$, the first (which I have not been able to produce by any means whatever, however large the nuclei) should correspond to $d_1=0.00013$ cm., and even this calls for particles nearly three times as large as Wilson's estimate (0.00005 cm.). In a small tube but 2 cm. in diameter, like Wilson's test-tube apparatus, it is improbable that the d_2 green corona, which is about 27° in angular diameter, could look otherwise than greenish white, whereas the filmy disk of the large crimson coronas (the largest producible, $d_1=0.00016$, with an angular diameter of about 39°) would be mistaken for colorless. I shall venture to believe, therefore, that Wilson's large greenish-white coronas corresponded to about 0.9×10^6 rather than to 10^8 nuclei per cubic centimeter, and that the maximum nucleation would not exceed 10^7 even if colors of the unapproachable first order were produced.

36. Longer intervals between observations. Conclusion.—Finally, experiments were made with longer intervals of time, 2 minutes and 3 minutes, between the observations. The object in view was the avoidance of distortion of the higher coronas due to the absence of homogeneous nucleated wet air in the fog chamber. But the longer intervals did not improve the coronas and the data were for this reason discarded.

Using the method of successive equal exhaustions for standardization and a single spot of light as the source of diffractions, the coronas of cloudy condensation were overhauled in the above chapter with special reference to the use of an efficient plug-cock fog chamber. The ratio of the section of the exhaust to the section of the fog chamber was about one to six. The useful equations are summarized. The chief difficulty encountered is the extreme sensitiveness of the coronas produced to any lack of homogeneity in the nucleation of the air.

Given types of coronas, like the green pattern, for instance, seem to recur for the ratios of 4, 3, 2, 1 in the diameters of the fog particles. The results as a whole show fairly good agreement with the earlier results below the middle green-blue-purple corona, but above this the divergence of values has not been much improved. In the definite region specified, corrections need be made for subsidence only. The fiducial value of the nucleations of normal coronas has been accepted as heretofore.

It does not seem probable that fog particles as small as 0.0001 cm. are ever measurably encountered in the fog chamber. This is larger than Wilson's estimate made in terms of the wave-length of light; but detailed comparisons are unsatisfactory, because of the difficulty of identifying his colors as to their place in the observed cycles of colors.

DISTRIBUTION OF VAPOR NUCLEI AND OF IONS IN DUST-FREE WET AIR. CONDENSATION AND FOG LIMITS.

37. Introductory.—It will, in the first place, be desirable to gather certain of the older data together for the comparison of fog limits. There is, in fact, quite a serious discrepancy between Mr. Wilson's results and mine when reduced to the same scale. Mr. Wilson's supersaturations for negative ions and cloud are distinctly higher, which seems to mean nothing less than that my fog chamber, instead of being inferior, is in these regions superior to his own. Thus, in moderately ionized air my condensations begin at a drop of about 18.5 cm. from 76 cm. as compared with 20.5 in Wilson's apparatus; similarly, my fogs begin at the drop 20.3, Wilson's at 27.7. Furthermore, at low ionization even the vapor nuclei of dust-free wet air become efficient in the presence of ions. It seems impossible, therefore, that any positive ions should fail of capture.

38. Notation.—The whole case may best be represented graphically, but the tables will also be given. In my apparatus, however, the adiabatic volume expansion v_1/v is a troublesome datum to compute accurately; it appears as

$$\frac{v_1}{v}=\frac{p}{p_3-\pi}\;\frac{(p'/p)^{1-c/k}(1-\pi'_1 p_1^{1-c/k})+[v/V]\;(1-\pi_1/p_1^{1-c/k})}{1+[v/V]}$$

where p and p' are the pressures in the fog and vacuum chambers before exhaustion, p_3 their common pressure when in communication after exhaustion, always at the same temperature. The volume ratios of the chambers is $[v/V]=0.064$; the π's denote the different vapor pressures and k and c the specific heats. With a large vacuum chamber the approximation

$$v_1/v=(p/p_1)^{c/k}=(p/p_3)^{c/k}$$

may be used, so that if $\delta p=p-p_3$, the convenient variable for the comparison of exhaustions is the relative drop $\delta p/p_3$. This is used in the diagram with the approximate equivalent of the volume expansion v_1/v. (*Cf.* Chapter I.)

39. Data.—In table 25 results are given for the conditions observed near the fog limits of dust-free air, and of dust-free air weakly ionized by the beta and gamma rays (coming from a closed tube containing radium placed on the outside of the fog chamber) and strongly ionized by the X-rays (at a distance D from the fog chamber). The data for ionized air are nearly coincident, but dust-free air requires higher supersaturation. The notation is as above, p, $p-\delta p'$ being the pressures of the fog and vacuum chambers before, $p-\delta p_3$ the common pressure after exhaustion. The relative drop in pressure is x, the angular diameter of the coronas $s/30$, the number of nuclei per cubic centimeter n, the volume

TABLE 25.—Fog limits of non-energized air, of air energized by weak radium, and by intense X-rays. $D=35$ cm., anticathode to axis of fog chamber.

	$\delta p'$.	δp_3.	s.	$\delta p_3/p$.	$n\times 10^{-3}$.	v_1/v.
Bar. 76.2 cm.; temp. 26° to 28° C.						
Radium	21.1	19.7	4.5	0.259	22	1.237
	21.3	19.8	4.2	.260	18	1.238
	20.0	18.4	[1]r	.242	0.2	1.217
	20.2	18.9	1.5	.248	0.6	1.224
Air	23.3	21.5	1.7	.282	1.2	1.265
	22.8	(21.1)	1.2	.277	0.4	1.259
	21.9	20.3	[1]r	.266	0.2	1.246
	21.3	19.6	0.0	.257	0.0	1.234
X-rays	20.4	19.4	4.1	.255	17	1.232
	18.9	17.2	0.0	.226	0.0	1.199
	19.6	18.0	0.0	.236	0.0	1.211
	20.0	18.4	1.8	.242	1.3	1.217
	20.4	19.2	3.8	.252	1.3	1.228

Radiation.	δp_3.	s.	$\delta p_3/p$.	$n\times 10^{-3}$.	v_1/v.	$n_{27}\times 10^{-3}$.
Bar. 75.8 cm.; temp. 18.6° C.						
Radium	20.6	6.2	0.272	60	1.252	50
	18.6	r	.245	0.2	1.221	0.2
X-rays, $D=150$ cm.	18.6	r	.245	0.2	1.221	0.2
X-rays, with radium	18.6	[2]r	.245	0.2	1.221	0.2
X-ray, $D=50$ cm. and radium, $D=50$ cm.	18.4	[2]r	.243	0.2	1.218	0.2
	18.7	1.9	.247	1.5	1.223	1.3
Radium	18.7	r	.247	0.2	1.223	0.2
Do	21.6	[3]7.0	.285	89	1.269	7.5
X-rays, $D=50$	20.7	[4]9.5	.273	210	1.254	176

[1] No corona visible; scattered rain. [2] Coronas gradually increasing. [3] w y. [4] w c.

TABLE 26.—Dust-free wet air energized by weak radium acting from $D=35$ cm. Bar. 75.8 cm.; temp. 27° C. Wet glass walls.

$\delta p'$.	δp_3.	s.	$\delta p_3/p$.	$n\times 10^{-3}$.	v_1/v.
25.6	24.1	4.3	0.318	23	1.312
24.6	23.0	3.9	.304	17	1.293
23.2	21.8	3.9	.288	16	1.273
21.8	20.5	3.8	.271	14	1.252
21.1	19.8	2.5	.261	3.6	1.239
20.2	18.8	r	.248	0.2	1.224
20.1	18.8	0	.248	0.0	1.224
21.9	20.6	3.8	.272	14	1.253
24.0	22.3	3.7	.294	14	1.280
25.5	23.9	3.8	.315	17	1.308
27.5	25.7	4.6	.339	28	1.342
29.2	27.5	5.5	.363	50	1.377
31.2	29.0	[1]7.5	.383	133	1.408

[1] w o.

expansion on exhaustion v_1/v. Tables 26 and 27 contain corresponding results for air energized by the weak radium at a distance $D=35$ or 40 cm. from the fog chamber. The difference observed in the curves of successive identical experiments was found to be referable to the wet or dry condition of the inside of the glass walls of the fog chamber. Freshly wet walls are apparently essential.

TABLE 27.—Dust-free wet air energized by weak radium acting from $D=40$ cm. Supplementary data. Bar. 76.2 cm.; temp. 24° C. Dry glass walls.

$\delta p'$.	δp_3.	s.	$\delta p_3/p$.	$n\times 10^{-3}$.	v_1/v.	$n_{27}\times 10^{-3}$.
25.6	24.0	3.9	0.315	17	1.308	16
26.1	24.5	3.9	.322	17	1.318	16
26.7	25.0	3.9	.327	17	1.325	16
27.2	25.5	3.9	.334	18	1.335	17
28.1	26.5	4.2	.346	23	1.352	21
28.9	27.2	5.2	.356	41	1.365	39
30.1	28.3	6.5	.371	86	1.389	81
28.6	27.1	5.0	.354	37	1.364	35
28.5	26.8	4.9	.350	34	1.357	32
21.8	20.6	3.6	.270	12	1.250	11
21.1	19.9	2.0	.261	2	1.239	2
20.6	19.4	r 1.0	.255	0.2	1.232	0.2
20.6	19.6	r 1.0	.257	0.2	1.234	0.2
Repeated. Glass vessel clean and wet.						
27.2	25.7	4.5	0.337	27	1.339	26
28.3	26.7	5.0	.349	36	1.356	34
26.4	24.7	4.2	.323	21	1.319	20
25.7	24.0	4.2	.315	21	1.308	20
24.5	23.2	4.0	.304	18	1.293	17
24.0	22.3	3.8	.292	15	1.278	16
22.0	20.6	3.6	.270	12	1.250	12
21.0	19.9	2.4	.261	3	1.239	3

In table 28 the ionization is slightly intensified by affixing the radium tube to the outside of the walls of the fog chamber. In table 29 there is further intensification, obtained by acting upon the fog chamber with the X-rays at $\delta=50$ cm.

TABLE 28.—Dust-free wet air ionized by weak radium (10 mg. 10,000×) on glass fog chamber. Bar. 74.9 cm., 75.0 cm.; temp. 17.7° C.

δp_3.	s.	$\delta p_3/p$.	$n\times 10^{-3}$.	v_1/v.	δp_3.	s.	$\delta p_3/p$.	$n\times 10^{-3}$.	v_1/v.
20.5	6.5	0.273	69	1.254	24.1	6.9	0.321	92	1.316
19.4	3.4	.259	10	1.237	26.0	6.8	.347	93	1.352
17.9	.0	.239	0	1.214	29.4	6.9	.392	106	1.423
18.3	r 1.0	.244	0.2	1.219	32.5	6.9	.433	112	1.496
19.9	5.5	.265	40	1.244	39.4	Diffuse	.525	....	1.695
22.3	6.9	.297	86	1.284	42.8	Diffuse	.571	....	1.823

Fog limit below $\frac{p_1}{p}=0.756$ at 18°, equivalent to $\frac{v_1}{v}=1.22$, equivalent to a drop (adiabatically) of $\delta p=18.6$ cm. (about) at 76 cm., 2 cm. below Wilson's $\delta p=20.5$ cm.

TABLE 29.—Dust-free wet air ionized by X-rays at $D=50$ cm. Bar. 75.9 cm.; temp. 21.3° C.

δp_3.	s.	$\delta p_3/p$.	$n\times 10^{-3}$.	v_1/v.	δp_3.	s.	$\delta p_3/p$.	$n\times 10^{-3}$.	v_1/v.
18.4	1	0.242	0.2	1.218	20.2	[1]8.1	0.266	125	1.245
18.9	2.4	.249	3.3	1.225	19.4	5.0	.255	29	1.232
19.6	5.2	.258	32	1.236	19.0	1.9	.250	1.5	1.226

[1] w p corona.

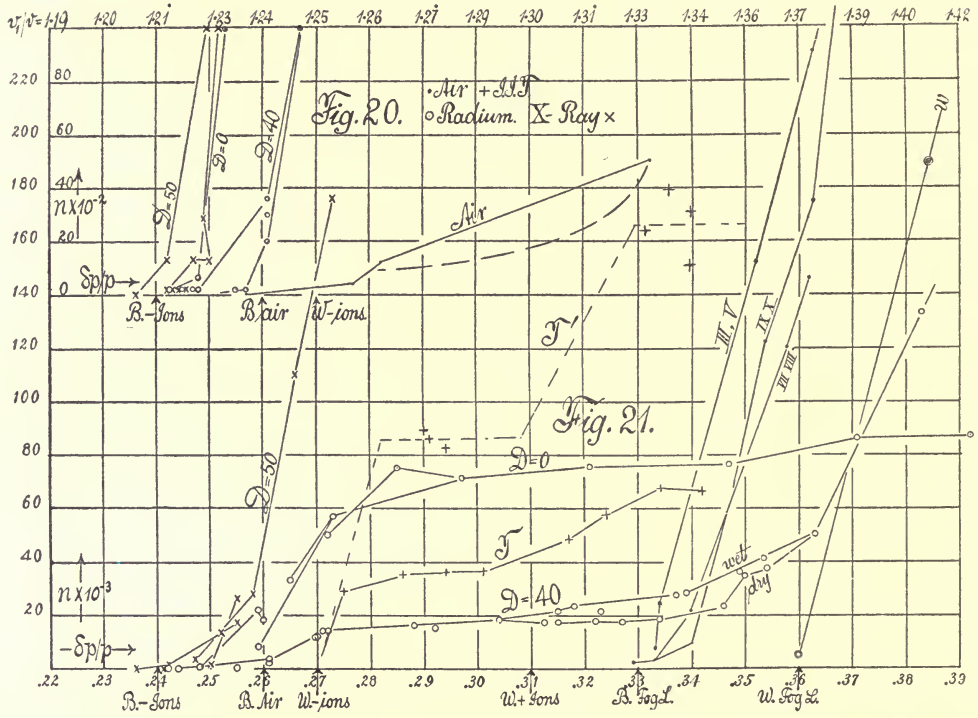

FIG. 20.—Nucleation n of dust-free air and of ionized air in terms of relative adiabatic drop in pressure $\delta p/p$ and of volume expansion v_1/v. Enlarged scale for n. Region for ions.

FIG. 21.—Nucleation n in terms of relative adiabatic drop of pressure $\delta p/p$, and of volume expansion v_1/v for dust-free air not energized, and for dust-free air acted on by the *beta* and *gamma* rays of radium and by the X-rays from different distances D. W refers to C. T. R. Wilson's condensation and fog limits, B to my own; T shows J. J. Thomson's results referred to scale of the diagram. Several older series, V to X, are given for dust-free air.

40. Graphs. Dust-free air.—The charts (figs. 20, 21, and 22) contain a number of curves showing the nucleation in different scales (computed from the angular diameter of coronas) in terms of the exhaustion. In figs. 20 and 21 typical cases are given, in their lower parts only. Fig. 22 contains full curves on a smaller scale. Thus the curve for the vapor nuclei of dust-free air begins appreciably below $\delta p/p=0.26$ ($v_1/v=1.24$,

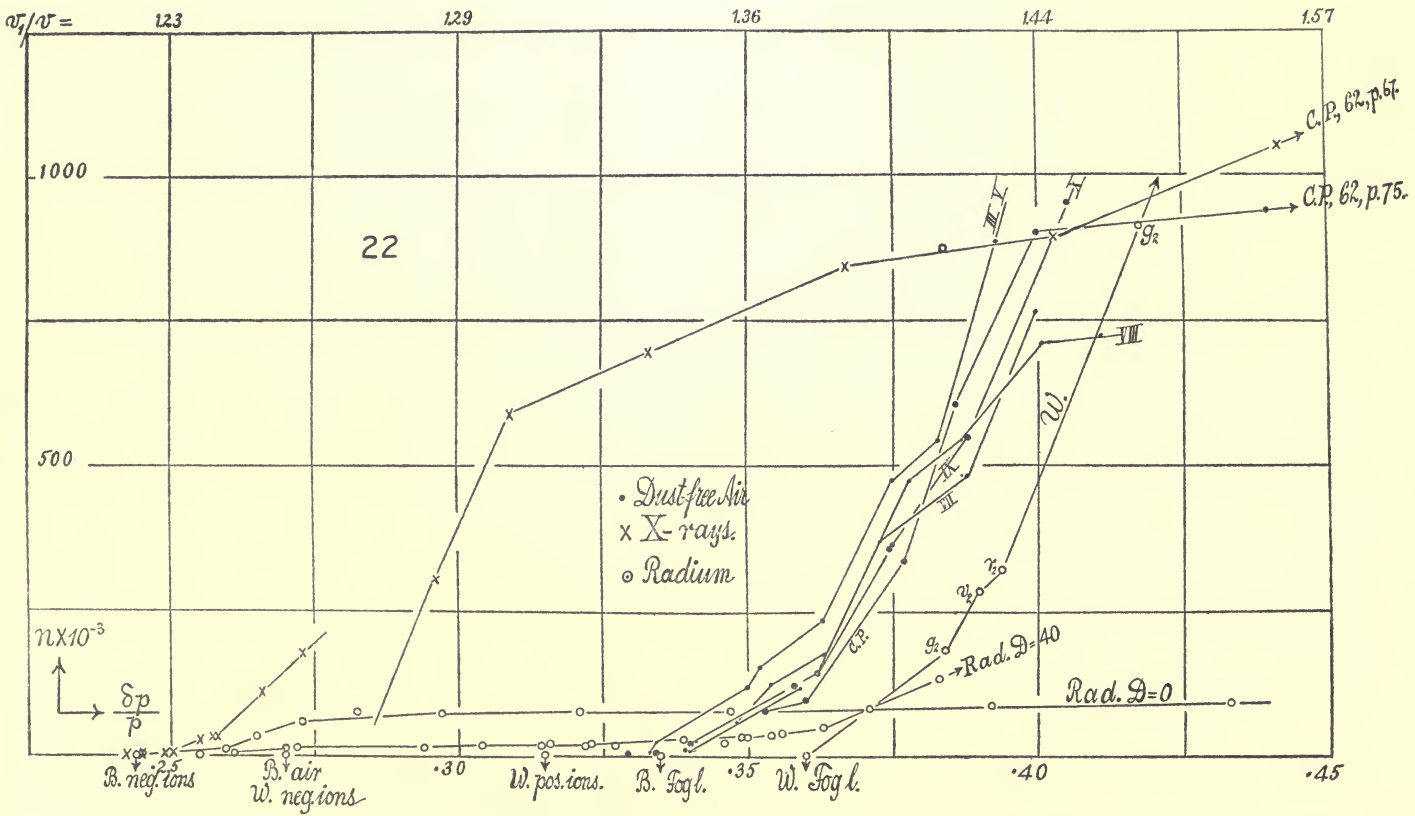

FIG. 22.—Results similar to preceding but in a different scale. *C. P.* is taken from the Carnegie Institution of Washington Publication No. 62. *W* indicates the probable position of Wilson's line, so far as can be made out.

adiabatic drop from 76 cm., 19.8 cm.), but it hugs the axis until about 0.33, after which it sweeps upward far beyond the chart into the hundred-thousands. The position of Wilson's negative ions and positive ions is indicated at 0.27 and above 0.31. Wilson's fog point would lie at 0.36 in the chart and there would be an air curve to the right beyond. Series III to X are taken from my earlier report (Carnegie Institution of Washington Publication No. 62, 1907, p. 67). The serial number is marked on the curve.

41. Weak radiation.—If a weak ionizer (radium 10,000×, 100 mg., sealed in an aluminum tube) is placed at $D=40$ cm. from the glass fog chamber, the air curve rises slightly above $\delta p/p=0.25$, becomes nearly constant slightly above 0.27 until above 0.35, after which it also begins to sweep with great rapidity into the hundred-thousands of nuclei. That is, at weak ionization the vapor nuclei of dust-free wet air become efficient in the presence of ions. There are but two steps in the curve, the initial one scarcely leaving the axis, the other at about $n=15{,}000$ to 20,000.

42. Moderate radiation.—Let the radium tube be attached to the outer surface of the fog chamber. The curve which is obtained begins appreciably slightly above $\delta p/p=0.24$ ($v_1/v=1.21$, adiabatic drop from 76 cm. about 18.4 cm.), but it scarcely rises until above 0.25. From this point it also sweeps upward but can not get much above 70,000 to 80,000 nuclei per cubic centimeter, which condition is reached at about 0.28. To make this curve rise into the hundred-thousands, *i. e.*, to make the vapor nuclei of dust-free wet air efficient in the presence of the ions, the exhaustion must be carried to about 0.50, much beyond the lateral limits of the diagram; but the fog is then intense and without coronas. Again there are but two steps, one very near the axis not appreciably influenced by the greater ionization and the other above $n=70{,}000$. Persistent nuclei are not produced, however long the exposure.

43. Strong radiation.—If an ordinary X-ray bulb (4-inch spark) is placed at a distance of about 50 centimeters from the fog chamber, the condensation produced begins appreciably somewhat below 0.24 ($v_1/v=1.21$; adiabatic drop from 76 cm. about 18 cm.); but the graph scarcely rises until nearly 0.25, when the upward sweep into the hundred-thousands begins. Exposure of a few seconds produces fleeting nuclei only; exposure of one or more minutes produces persistent nuclei. In spite of intense ionization, the first step near the axis has scarcely risen; the other is indefinitely high beyond the reach of coronas.

44. Other nucleations.—I have ventured to place the data of J. J. Thomson (Phil. Mag., vol. v, 1903, p. 349) at T in the same chart. They must be interpreted, however, relatively to Wilson's points (nega-

tive ions $v_1/v = 1.25$, positive ions 1.31, cloud 1.38). In relation to the other curves of the chart Thomson's graph must be shifted bodily toward the left until the lower and upper steps of the curve correspond with the other cases. In none of the experiments made with my apparatus does the initial step (which should correspond to the branch for negative ions) rise much above the horizontal axis, no matter how intense the ionization. This rise begins at about 0.25 in the chart and continues thereafter in a way to correspond with the ionization. The diagram also shows J. J. Thomson's second group of experiments, in which the initial step ($v_1/v < 1.33$) lies at an average height of $n = 85 \times 10^3$ and the second step at an average height about twice as large.

Fig. 22, which contains most of the earlier results reduced to the present scale, shows the variation of nucleation obtainable at different times to which reference has already been made. The high position of the X-ray curve is particularly noticeable. All data except C. T. R. Wilson's are given as if the coronas had been observed at 27°, for which case the least amount of reduction was needed. The Wilson line should therefore be depressed about $8 \times 2 = 16$ per cent in nucleation to be comparable with the others.

45. Temperature effects.—It was demonstrated in Chapter II that the vapor nucleation of dust-free air varies in marked degree with temperature, if the relative drop in pressure be computed as $x = (\delta p_3 - [\pi - \pi_1])/(p - \pi)$. Computed relatively to $\delta p_3/p$, there is a much more moderate variation with temperature outstanding, suggesting that the apparent variation may be associated with the occurrence of the vapor density π in x. To throw light upon this subject from a different point of view, the condensation limits of dust-free air and of ionized air were determined at temperatures between 13° and 30° and table 30 contains the results. The notation being as above, it is only necessary to refer to the final column for $\delta p_3/p$ and the volume expansion $v_1/v = (p/[p - \delta p_3])^{1/\gamma}$, computed therefrom.

The results of table 30 being summarized by giving expansions corresponding to the fog limits both for $[v_1/v] = (1 - x)^{1/\gamma}$ and $v_1/v = (1 - \delta p_3/p)^{1/\gamma}$, show clearly that v_1/v, computed from $\delta p_3/p$, is independent of temperature, whereas the other datum $[v_1/v]$ varies with temperature in a way referable to the values of π involved. It follows that the fog limits are not changed by temperature in a way found by the nucleation itself in Chapter II. The mean fog limit for dust-free air $v_1/v = 1.252$ agrees with Wilson's data. The fog limit for ionized air is, however, decidedly below this, and thus below Wilson's value. Finally, $[v_1/v]$ is always less than v_1/v and under ordinary temperatures from 1 to 2 per cent less.

TABLE 30.—Temperature comparisons. Radium on top of fog chamber. $D=0$.

$\delta p'$.	δp_3.	s.	$n\times10^{-3}$.	Temperature and barometer.	v_1/v $\delta p_3/p$.
Ions due to radium.					
22.6	21.6	6.8	80	14.0°	1.226
21.5	20.1	5.1	31	76.1 cm.	0.250
20.3	19.0	0.0	0.1	....	....
20.6	19.5	2.1	2.0	....	....
22.5	21.5	6.6	74	30.0°	1.222
21.5	20.1	5.0	29	75.7 cm.	0.246
20.1	18.4	1.7	1.0	....	0.243
....	18.6	<1.0	0.1	....	....
....	18.4	0.0	0.0	....	....
....	19.4	3.2	7.5	....	....
18.6	17.5	0.0	0.0	13.2°	....
19.2	18.0	0.0	0.0	76.8 cm.	1.220
20.0	18.8	0.5	0.1	....	0.245
Vapor nuclei.					
21.8	20.4	0.5	0.1	14.0°	1.247
22.4	21.1	1.0	0.2	76.0 cm.	0.268
....	20.3	0.0	0.0	....	0.267

$\delta p'$.	δp_3.	s.	$n\times10^{-3}$.	Temperature and barometer.	v_1/v $\delta p_3/p$.
Vapor nuclei. Wet dust-free air.					
....	25.6	4.6	28.6	30.0°	....
....	24.6	3.6	13.9	75.7 cm.	....
....	22.7	3.6	13.1	....	....
....	21.1	2.5	3.8	....	1.247
....	20.1	0.0	0.0	....	0.265
....	20.3	<1.0	0.1	....	0.268
20.0	18.7	0.0	0.0	13.2°	....
21.9	20.3	0.0	0.0	76.8 cm.	....
22.9	21.6	0.0	0.0	....	....
23.8	22.1	>1.0	0.2	....	1.263
23.3	21.9	>1.0	0.2	....	0.285
22.8	21.5	0.5	0.1	....	0.280
Ions due to radium.					
19.2	18.1	0.0	0.0	14.0°	1.226
19.8	18.6	0.0	0.0	76 cm.	0.245
20.6	19.4	strong	0.1	....	0.255

SUMMARY OF RESULTS.

	Ionized air.			Dust-free air.		
	v_1/v.	v_1/v.	Difference.	v_1/v.	v_1/v.	Difference.
14°	1.226	1.214	0.012	....	....	....
30	1.220	1.196	.24	1.247	1.222	0.025
13	1.220	1.212	.08	1.263	1.252	.011
14	1.226	1.214	.12	1.247	1.257	.010
Mean..	1.223	....	....	1.252	....	....

46. New investigations.—In tables 31, 32, and 33 data were investigated for X-rays of different strengths and for dust-free air. In the latter case the coincidence of data is not as close as was anticipated, different apparatus showing a somewhat different behavior. The results are all given in fig. 23. The drop in the upper X-ray curve is probably due to a breakdown in the X-ray bulb, as it is not sustained by the other curves.

Fig. 23 also contains Wilson's series, under the supposition that the coronas begin with the green of the third and end with the green of the second series. In such a case the present results lie in a region of lower supersaturation than Wilson's. The slopes throughout are similar. If Wilson's colors are of the second and first series, the green alone will appear in the diagram, the other nucleations being too high. In such a case Wilson's line will intersect the graphs of the present paper, as shown by the graphs of the point $g_{2,1}$.

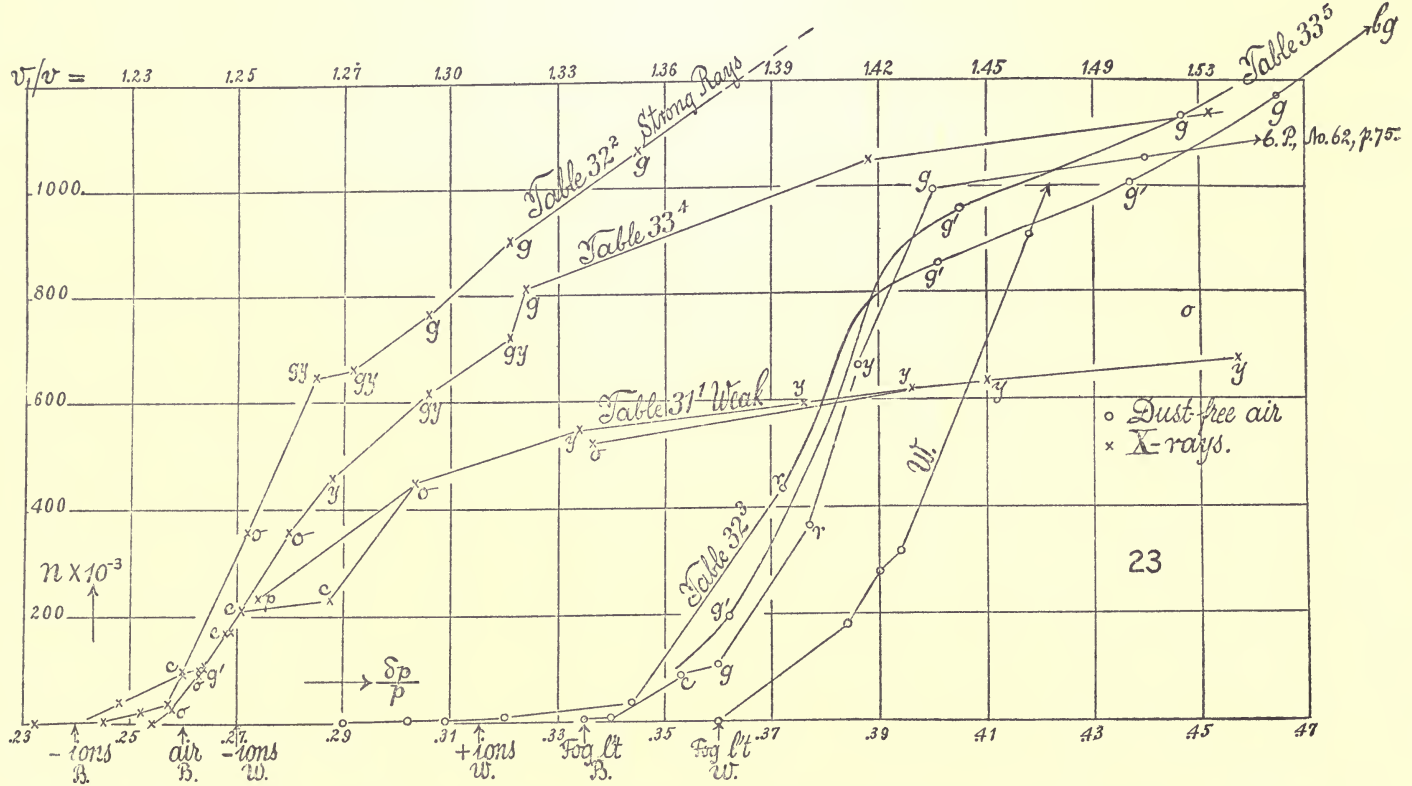

FIG. 23.—Results similar to the preceding. Nucleation of non-energized dust-free air and of air energized by X-rays, at different distances and at different exhaustions. The letters refer to colors of disks or first annuli of coronas.

TABLE 31.—Weak X-rays. App. II. Bar. 75.68 cm., 75.86 cm. . . . . 75.8 cm; temp. 25.0° C. February 18, 1907.

δp.	s.	Cor.	$\delta p_3/p$.	$n \times 10^{-3}$.	Corrected $n \times 10^{-3}$.	δp.	s.	Cor.	$\delta p_3/p$.	$n \times 10^{-3}$.	Corrected $n \times 10^{-3}$.
(1) 17.6	0	....	0.232	0	0	(1) 34.6	11.0	....	0.457	594	677
18.6	2.5	cor	.245	3	4	31.1	11.1	y	.410	562	638
19.5	5.2	o	.257	32	35	28.5	11.4	y	.376	529	598
19.7	7.0	c	.260	83	92	25.3	11.5	y	.334	490	549
19.9	7.0	o	.263	90	100	23.0	11.0	o	.303	403	450
20.0	7.4	g y	.264	97	108	20.8	9.5	p	.274	211	234
20.5	9.2	c	.271	191	212	19.1	3.9	cor	.252	14.6	16.1
21.8	9.3	c	.287	207	230	19.9	7.0	o	.263	84	93
25.5	11.0	o	.336	467	523	20.0	7.3	g	.264	94	104
30.0	11.0	....	.396	550	622	20.4	8.7	p	.269	155	172

TABLE 32.—Strong X-rays. App. II. February 21, 1907. Bar. 75.1 cm.; temp. 27.4° C.

δp.	s.	Cor.	$\delta p_3/p$.	20° C. $n \times 10^{-3}$.	Corrected $10 \times n^{-3}$.	δp.	s.	Cor.	$\delta p_3/p$.	20° C. $n \times 10^{-3}$.	Corrected $10 \times n^{-3}$.
(2) 18.6	2.4	cor	0.248	3.2	4	X-rays off. Dust-free air. Bar. 75.5; temp. 27.2° C.					
19.5	7.0	....	.260	83	96						
20.4	10.8	w o	.272	307	357						
21.4	12.	g y	.285	557	648	(3) 37.6	13	b g	0.500	1130	1380
21.9	....	g y	.292	566	662	34.9	13	g	.465	969	1170
23.0	....	g	.306	654	765	32.8	....	g′	.437	834	1007
24.1	....	g	.321	766	902	30.1	13	g to g y	.401	713	856
25.9	....	g !	.345	904	1071						
33.7	13	w o	.449	650	784	27.9	10	r	.372	367	437
33.6	12	w o	.448	650	784	25.8	4.7	cor	.344	30.8	36
39.9	smaller	w o	.532	640	782	24.0	3.2	cor	.320	8.9	10
						22.7	2.5	cor	.302	4.2	5

TABLE 33.—Strong X-rays. App. I. Bar. 76.5 cm. temp. 22.5° C. February 22, 1907.

δp.	s.	Cor.	$\delta p/p$.	20° C. $n \times 10^{-3}$.	Corrected $n \times 10^{-3}$.	δp.	s.	Cor.	$\delta p/p$.	20° C. $n \times 10^{-3}$.	Corrected $n \times 10^{-3}$.
(4) 19.4	0	....	0.254	0	0	X-rays off. Dust-free air. Bar. 76.7; temp. 22.4° C.					
19.7	4.9	....	.258	28	29						
20.5	8.8	c	.268	161	170						
21.4	10.7	w o	.280	357	357						
22.0	12.8	y o	.288	436	460	(5) 34.2	....	g	0.447	1060	1134
23.4	13.5	g y o	.306	584	617	31.0	....	g	.405	899	960
24.5	....	g y	.321	680	721	27.7	8.5	w/bg	.362	187	199
24.8	....	g′	.324	766	812	25.6	2.5	....	.335	4.5	5
29.7	....	g	.388	988	1052	23.6	1.8	....	.309	1.5	1.6
34.6	....	g	.452	1066	1140	22.2	1.2	....	.290	.4	.4

47. Conclusion.—The new results lead to about the same conclusions as the older data given above. The endeavor to obtain the negative and positive steps of the ionization fails in my apparatus. Sometimes there are suspicious breaks in the nucleation curve supporting such a tendency; but it is not sustained.

What I always get is division of the totality of ions into two groups—a numerically small group with large nuclei, and a numerically large group with relatively small nuclei containing all the ions. This occurs even in such cases where I catch the vapor nuclei of dust-free air in presence of the ions (radium at $D=40$ cm.), and hence all ions, positive and negative, must have been caught in an earlier stage of the exhaustion.

The slopes of the air graph and the strong X-ray graph represent the initial branches of a general law of distribution of molecular aggregates such as is given by the theory of dissociation. They may therefore be expected to be similar in their slopes, as they actually are. The results therefore bear on the molecular structure of vapors.

The question is finally to be asked why I catch the negative ions, etc., at an apparently much lower supersaturation than C. T. R. Wilson. I have entertained doubts whether the inertia of the piston in his apparatus is *initially* quite negligible; whether in any apparatus the computed adiabatic temperatures were actually reached. Nobody has proved it, and the case should be worst for small tubes. Moreover, in every apparatus there must be a limit at which the smaller nuclei of a graded system can no longer be caught in the presence of the larger nuclei. There is a remote possibility that, whereas in the plug-cock fog chamber the exhaustion starts rapidly but ends off with retardation, in Wilson's apparatus it may start with relative slowness but finish with accelerated rapidity. If the lower limits of condensation were due to emanations of metallic or other material coming from the vessel, the effect should vary with the intensity of the ionization, which it does not. If it were due to the use of filtered air in place of stagnant air, as in Wilson's apparatus, it should be equally evident with non-ionized air, where the limit of condensation agrees with Wilson's point for negative ions.

The chief results of this section will be found in the charts, corresponding points of which have been connected with straight lines with no attempt at smoothing. In case of the air lines, results made at long intervals of time apart have been summarized.

CHAPTER IV.

THE NUCLEATION CONSTANTS OF CORONAS—CONTINUED.

ON A METHOD FOR THE OBSERVATION OF CORONAS.

48. Character of the method.—In the usual practical experiments with the large coronas of cloudy condensation (the largest types having angular diameter of nearly 60°), the source of light is placed in the equatorial (vertical) plane of the fog chamber and remote from it. The eye and goniometer are put as near it as possible whenever sharp vision is essential. The diffracted rays in such cases come from the fog particles at the ends of the chamber, as in fig. 24, *a*, and are liable

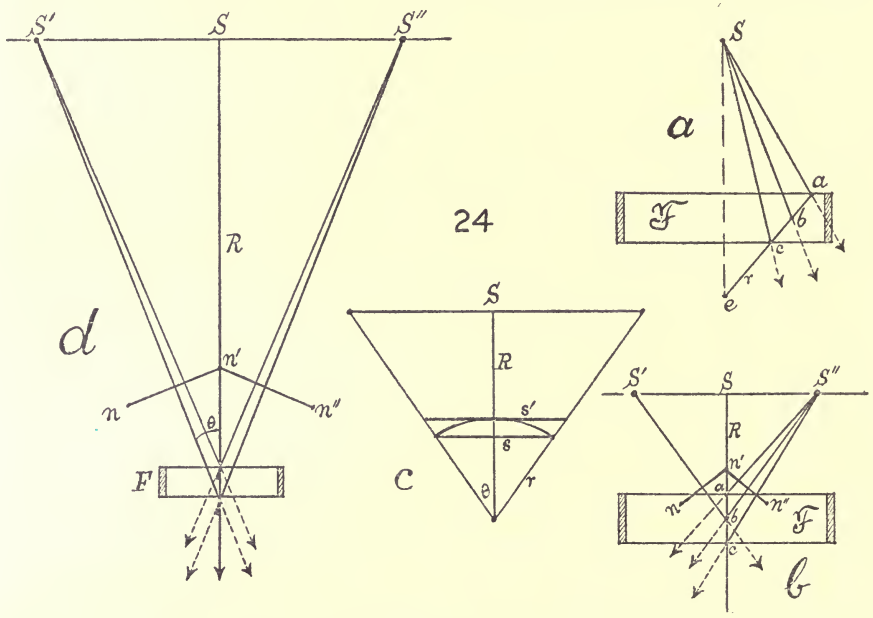

FIG. 24.—(*a*) Diffractions from fog particles at *a*, *b*, *c*, and a single source *S*, reaching the eye at *e*. (*b*) Diffractions from fog particles at *a*, *b*, *c*, and two sources *S'*, *S''*, with coronas *n n'* and *n' n''*, in contract at *n'*, reaching the eye at *c*. (*c*) Diagram showing the relation of *S*, *s'*, *s*, *R*, *r*, *θ*. (*d*) Case of two sources and coronas in contact at *n'* drawn to scale.

to be seriously distorted by the refraction of the glass walls. Furthermore, the limit will be reached sooner or later, in which the fog particles, to which the diffractions are due, lie at or beyond the ends of the fog chamber, after which the features essential to the measurement will no longer appear. Moreover, one eye only can be used in the measurements. In fig. 24, *a*, with a source at *S* and an eye at *e*, the diffractions of the fog particles *a*, *b*, *c* overlap.

It occurred to me, therefore, to invert the phenomenon by using two sources, which may be moved symmetrically towards or from the equatorial plane, as in fig. 24, *b*, and to observe the contact in this plane of the two identical coronas produced. In this way the oblique refractions are diminished as far as possible, coronas of all sizes are observable, and both eyes are available for observation, increasing sharpness of vision and lessening the eye strain. The contact method is in itself more sensitive, seeing that the eyes may be placed all but in contact with the fog chamber. In fig. 24, *b*, with two sources at S' and S'' and the coronas nn' and $n'n''$ in contact at n' at the edge of a given annulus, the diffractions of the fog particles *a*, *b*, *c* overlap.

49. Apparatus.—Fig. 24, *d*, shows a general disposition of the apparatus. S' and S'' are the two circular sources of light lying in the same horizontal, and movable in opposite directions in equal amounts, at the control of the observer at the fog chamber F. S' and S'' are therefore always symmetrical with respect to the vertical plane SR. The diffraction of rays due to the fog particles in F produces coronas seen at nn' and $n'n''$, and the lamps $S'S''$ have been adjusted at a distance S, so that the selected annuli of the coronas are in contact at n'. The angular radii of the coronas, marked θ or shaded in the diagram, are nearly equal and $2R \tan \theta = S$, where R is the distance of the axis of the fog chamber from the track S.

On a double track, at S, the two carriages for the lamps $S'S''$ are moved with sprocket and chain or in a similar manner, and provided with a scale stretched between them, reading to centimeters. This scale is a lath of wood about 3 meters long, with one end fastened at S', the other free, while the scale moves across an index at S''. A pole at R, with the end in the observer's hand, moves the two central sprockets and at the same time serves for the measurement of R, should this vary.

50. Errors.—Fig. 24 shows clearly that the angle of diffraction corresponding to the fog particles *a*, *b*, *c*, nearer and farther from the eye, will not be the same, and that this effect will vanish as the coronas are smaller, as the diameter or thickness of the fog chamber is less, and as the distance R from the source is greater. Slightly different annuli overlap; but the effect is much less here than in the case of a single source, where the active fog particles lie oblique to the axis. (See fig. 24, *a*, and fig. 24, *b*, at *a*, *b*, *c*.) In practice this effect is probably negligible if the dimensions of apparatus and disposition of parts are properly chosen, particularly so since the fog particles themselves are not usually so nearly of a size as to imply less overlapping. In fact the true corona, if large or even of moderate size, is seen but for an instant immediately after exhaustion. It thereafter shrinks rapidly, as may be gathered from

the incidental data shown in table 34, obtained with fog particles about 0.0002 cm. in diameter, belonging to the large yellow-blue corona.

TABLE 34.—Contraction of coronas during subsidence. Bar. 75.2 cm.; temp. 27° C.; $\delta p_3 = 30.7$; $\delta p_3/p = 0.408$; factor 1.56; temp. factor 0.027.

	t.	S.	s.	$n \times 10^{-3}$.		t.	S.	s.	$n \times 10^{-3}$.
I.	sec.	....	....	....	II.	sec.	....	....	....
	0	12.0	14.4	920		0	12.5	15.0	1140
	30	10.2	12.2	600		30	10.8	13.0	730
	60	8.4	10.1	350		60	8.8	10.6	400
	90	7.3	8.8	220		90	7.4	8.9	230

The coronas shrink as the fog particles increase in number and decrease in size at an accelerated rate. The initial rates must be estimated at a decrement of number greater than 1.4 per cent per second, supposing that no water is added from other sources than the evaporation of smaller particles. In 100 seconds about 80 particles have escaped out of each 100. The case is much more serious for larger coronas, so that these are characteristically fleeting and must be observed at once. It may not be impossible that rapidity of evaporation itself sets a limit to the largest coronas producible. The nuclei, however, are not lost as a rule. They occur as water nuclei and are available for the next coronas, if not removed.

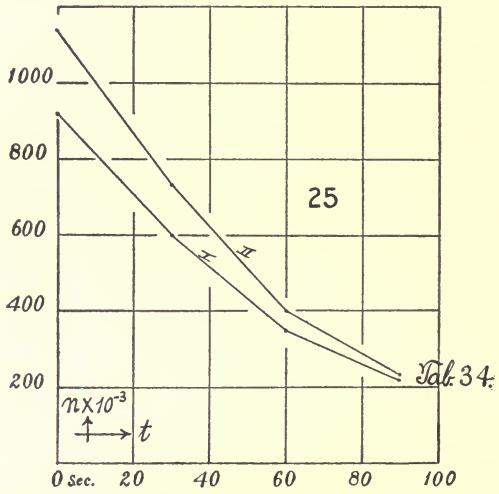

FIG. 25.—Nucleation n, computed from aperture s of the coronas, gradually shrinking during the subsidence within 100 seconds after exhaustion.

It follows, then, that for these cases the method of subsidence is not applicable, as the corona changes totally before measurable subsidence is recorded. Hence an instantaneous procedure like the goniometer method or the present method is alone available.

51. Data.—In table 35 I have inserted results obtained with phosphorus nuclei, leaving out the initial fogs. It is seen at once that large coronal diameters are actually measurable, a result not possible hitherto. Reduced to the goniometer method, the present results may be written $0.12\ S = s'$, for small coronas; but for large coronas, if θ is the an-

TABLE 35.—New apparatus. Two coronas in contact. Bar. 75.6 cm.; temp. 24.7° C.; $S = 2R \tan \theta$; $R = 250$ cm.; cock open 5 seconds; interval 1 minute. $\delta p_3 = 17.6$; $[\delta p_2] = 16.8$; phosphorus nuclei, $y = 0.771$; $\delta p_3/p = 0.233$; $m = 4.2$ g/cm^3; $a = 0.0032$; $S' = 6.5$.

Exp.	No.	S.	Cor.	s.	$10^{-3}n' = 0.244s^3$.	$n_1 \times 10^{-3}$.	$n \times 10^{-3}$.	$s = 0.16 \times n^{1/3}$	$s' = 0.12S$.
		cm.							
1.	1	?210	o′	19.3	....	....	3660	24.6	....
	2	185	o	16.7	....	....	2770	22.4	....
	3	165	r o	15.4	....	....	2080	20.5	....
	4	145	c	14.3	....	....	1560	18.6	....
	5	130	stone bl.	13.3	....	....	1160	16.8	....
	6	120	g′	12.5	....	....	862	15.4	....
	7	113	g y	11.9	....	....	636	13.8	....
	8	104	g y	11.1	....	....	467	12.4	....
	9	97	y o	10.5	....	....	341	11.2	....
	10	90	o	9.9	....	....	247	10.0	....
	11	78	c	8.8	....	....	178	9.0	....
	12	65	g	7.4	98.8	2880	125	8.0	....
	13	60	g y	6.9	80.0	3430	85.1	7.0	....
	14	55	r	6.4	63.9	4130	56.5	6.1	....
	15	45	cor	5.3	36.4	3633	36.6	5.3	....
	16	36	cor	4.3	19.4	3265	21.7	4.5	....
	17	30	cor	3.6	11.4	3830	10.9	3.6	....
	18	23	cor	2.8	5.4	4720	4.2	2.6	....
	19	18	cor	2.2	2.6	1750	.5	1.3	....
	20	o	absent	0.0	0.0	....	0.0	....	....
2.	1	?210	o′	19	....	....	2201	20.8	25.0
	2	198	o	18.6	....	....	1679	19.0	23.8
	3	185	c	17.9	....	....	1278	17.3	22.2
	4	174	w′	18.1	....	....	973	15.8	22.1
	5	158	st. bl.	16.1	....	....	740	14.5	19.0
	6	135	g	14.3	....	....	559	13.1	16.2
	7	118	g y	12.8	....	....	420	12.0	14.2
	8	101	o	11.2	....	....	313	10.9	12.1
	9	88	r	10.0	....	....	230	9.8	10.6
	10	75	r	8.6	....	....	167	8.8	9.0
	11	65	g y o	7.6	....	....	118	7.9	7.8
	12	58	r	6.8	84.0	2269	81.5	6.9	7.0
	13	51	cor	6.0	55.6	2250	54.4	6.1	6.1
	14	45	cor	5.3	38.5	2452	34.6	5.2	5.4
	15	35	cor	4.2	18.1	1927	20.7	4.4	4.2
	16	28	cor	3.4	9.6	2106	10.0	3.5	3.4
	17	21	cor	2.5	3.8	2462	3.4	2.4	2.5
	18	?15	very small	1.8	1.4	2680	1.1	1.6	1.8
3.	1	?210	o′	19.0	....	....	2010	20.1	25.0
	2	195	o	18.4	....	....	1534	18.4	23.4
	3	175	w′	17.2	....	....	1167	16.8	21.0
	4	158	v	16.1	....	....	885	15.4	19.0
	5	145	g	15.0	....	....	670	14.0	17.4
	6	133	g y	14.1	....	....	505	12.7	16.0
	7	120	y o	13.0	....	....	379	11.5	14.4
	8	106	o	11.7	....	....	282	10.6	12.7
	9	88	c	10.0	....	....	209	9.4	10.6
	10	74	g	8.5	....	....	151	8.5	8.9
	11	60	g	7.0	91.0	1708	107	7.6	7.2
	12	57	r	6.6	76.6	2133	72.2	6.7	6.8
	13	49	cor	5.7	50.0	2105	47.8	5.8	5.9
	14	40	cor	4.7	27.0	1813	29.9	5.0	4.8
	15	33	cor	4.0	15.6	1898	16.5	4.1	4.0
	16	27	cor	3.2	8.0	2104	7.5	3.1	3.2
	17	21	cor	2.5	3.8	3881	2.1	2.0	2.5
	18	....	just visible	....	....	....	.6	1.0	....

gular diameter, $S=2R \tan \theta$, $s=2r \sin \theta$, or $S=8.3\, s/\sqrt{1-s^2/4r^2}$, $s=0.12\, S/\sqrt{1+S^2/4R^2}$, $R=250$ cm., $r=30$ cm. Fig. 24, *c*, shows the relation of these quantities. Since the elementary diffraction equation may be put

$$\sin \theta = 1.22\ \lambda/d$$

for the first minimum

$$S=(2.44\, R\ \lambda/d)/\sqrt{1-(1.22\ \lambda/d)^2}$$

and S would therefore appear to be less immediately adapted for the equation than s. It does not follow, however, that this s and the one observed at the goniometer work are the same. In fact they are not, the latter being larger for reasons involved in the more recondite theory of the experiment, or else due to irregular refractions at the remote ends of the chamber. In practice S will usually be preferred to s.

In table 35, $y=0.771=(p-[\delta p_2]-\pi)/(p-\pi)$; $\delta p_3/p=0.233$; $10^6 m=3.80$ at 20°; therefore at 25°, 10 per cent higher or $10^6 m=4.18$ grams per cubic centimeter. Hence $n'=6ms^3/\pi a^3=0.244\, s^3/10^3$. The value of

TABLE 36.—New apparatus. Two coronas in contact. Bar. 76.4 cm.; temp. = 27° C; $S=2R \tan \theta$; $R=250$ cm.; cock open 5 seconds; interval 1 minute. $\delta p_2=9.9$. $[\delta p_2]=9.2$. Phosphorus nuclei. $\delta p_3/p=0.120$; $y=0.875$; $10^6 m=2.33$; $S'=6.5$.

Exp.	No.	S.	Cor.	$s'=12S.$	$10^3 n'=0.136 s^3.$	$n_1 \times 10^{-3}.$	$n \times 10^{-3}.$	$s=0.194 n^{1/3}.$
4.	1	>210	o-fog	25.0	....	....	1888	24.0
	2	201	o	24.1	....	....	1635	23.0
	3	194	o	23.3	....	....	1414	21.8
	4	188	o	21.4	....	....	1222	20.9
	5	173	r	20.8	....	....	1053	19.9
	6	160	c	19.2	....	....	907	18.9
	7	146	c	17.5	....	....	779	17.9
	8	131	v'c	15.7	....	....	667	17.0
	9	116	v'	13.9	....	....	567	16.2
	10	105	v' g	12.6	....	....	479	15.2
	11	98	v' g	11.8	....	....	402	14.4
	12	98	v' g	11.8	....	....	335	13.5
	13	98	g	11.8	....	....	280	12.8
	14	95	g y	11.4	....	....	233	12.0
	15	94	y o	11.3	....	....	194	11.3
	16	94	y o	11.3	....	....	161	10.6
	17	88	w r	10.6	....	....	133	9.9
	18	88	w c	10.6	....	....	110	9.4
	19	80	w p	9.6	....	....	90.3	8.8
	20	72	cor	8.6	....	....	73.2	8.2
	21	67	g'	8.0	....	....	58.5	7.6
	22	61	g y	7.3	....	....	46.1	7.0
	23	54	w r	6.5	37.4	1995	35.4	6.4
	24	48	r	5.8	26.5	1913	26.1	5.8
	25	42	cor	5.0	17.0	1748	18.4	5.2
	26	37	cor	4.4	12.0	1895	12.0	4.5
	27	28	cor	3.4	5.2	....	7.0	3.7
	28	22	cor	2.6	2.5	....	2.5	2.7
	29	17	cor	2.0	1.2	....	0.9	1.9
	30	0	....	0.0	0	....	0.3	1.4

the subsidence constant $S'=6.5$ is taken as the mea value of the above data. To compute $s=an^{1/3}/(6m/\pi)^{1/3}$, the reduced values are $s=0.16n^{1/3}$.

In table 36 the exhaustion $y=0.771$ is smaller and the temperature 27°. The constants have the corresponding values shown at the head of the table.

52. Remarks concerning the tables, and conclusion.—The first series in table 34 contains data both for S, $0.12\ S=s'$ and s, and leads to a curious consequence. The computed chords of the coronas, $s=a(\pi n/6m)^{1/3}$, is not proportional to $s=2r\sin\theta$ but to $S=2R\tan\theta$, where 2θ is the angular diameter of the coronas. This implies a diffraction equation reading $\tan\theta=1.22\ \lambda/d$.

These results are shown in fig. 26, where $s\propto n^{1/3}$ is laid off as the abscissas and $0.12\ s\propto\tan\theta$ and $0.12S/\sqrt{1+S^2/4R^2}\propto\sin\theta$, as ordinates. If we confine our attention to values within $s=14$, where the readings are more certain, and where there is less accentuated overlapping of coronas, the graph $0.12\ S$ oscillates between two straight lines as the coronas change from the red to the green types. The slopes of these lines are respectively as $1.08=73.2\ \lambda_1/a$ and $0.99=73.2\ \lambda_2/a$, whence $\lambda_1=0.000047$ and $\lambda_2=0.000043$ cm. These should be blue and violet minima.

Fig. 26 shows, moreover, that compared with the graph for $0.12\ S=60\tan\theta$, the curve for $\sin\theta$ is in series 1 quite out of the question, as already specified. Hence in the remaining series of observations in tables 35 and 36, $0.12\ S$ was used in place of s. The results for the series 2, 3, 4, are also given in fig. 26, in the same way. Curiously enough, series 2 and 3, which should be identical with 1, fail to coincide with it in the region of higher coronas. In these series the graph $s\propto\sin\theta$ would more nearly express the results, though the agreement is far from satisfactory. Series 4 again corroborates series 1, needing the $s'\propto\tan\theta$ graph for its nearest expression; but in this series there is a curious horizontal part corresponding to observed coronas of the fixed type in the middle region of green coronas ($s=10$ to 12), showing that the periodicity has been exaggerated.

It is exceedingly difficult to account for this difference of behavior. One may suppose that the phosphorus nuclei, which are here solutional water nuclei, are not quite of the same size. This may happen if the air is unequally saturated, for instance. In such a case the coronas would be largest when the air is most nearly homogeneous and the nuclei gradient within narrow limits (series 2 and 3), whereas in less favorable cases (series 1 and 4) smaller coronas would appear. As the abscissas, $s=a\ (n\pi/6m)^{1/3}$, where $n_z=y^{z-1}\Pi$ and the ordinates s (observed) are independent of each other, the equality of s' and s will in a measure check the work apart from the constant a which determines n_0. This is actually the case for the lower series of coronas below $s=10$.

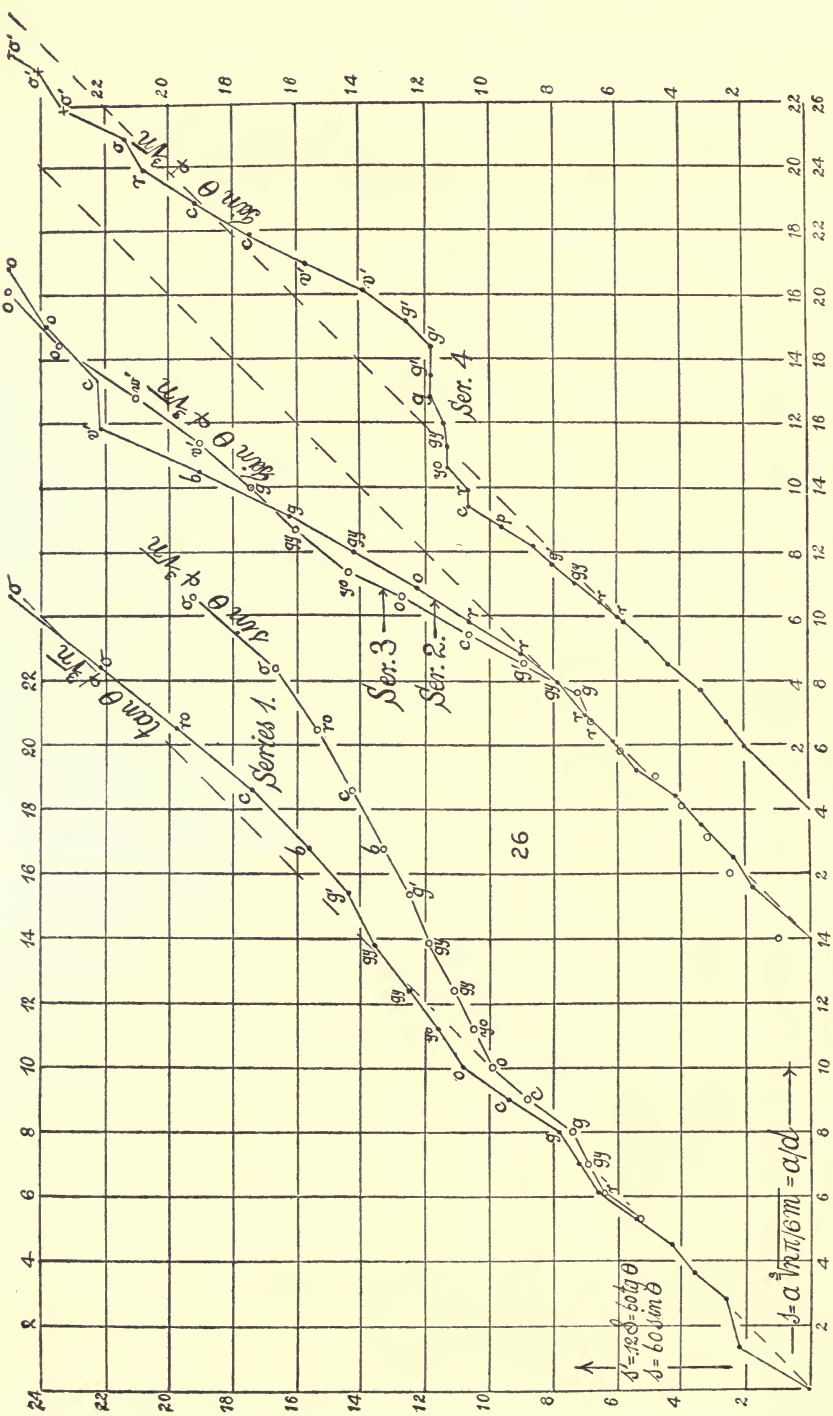

FIG. 26—Comparison of observed and computed angular diameter of coronas for the different series in table 34.

On the other hand, it is the *observational* value of the aperture of the given coronas which varies. Thus in fig. 26 the green coronas vary from $s=12$ to $s=17$ in the different series. Very probably mixed coronas are being observed. To this must be added the subjective error or personal equation which enters into the determination of contacts. Finally, the tendency of a corona to shrink at once after the formation of droplets makes it difficult to catch the time at which coronas should be observed soon enough. Under other circumstances there is even liable to be an oscillation of the coronal aperture in the lapse of time. All these difficulties are accentuated as the coronas become larger, for here not only are the droplets more volatile, but the coronas overlap, and there is an unlooked-for tendency for them to flatten at the point of contact. The dark rings are liable to invade the bright.

The green coronas in table 34, series 1 and 2, and table 35, series 3, show the following average values:

Series	Computed.		Observed.		Computed.		Observed.	
	s_3.	s_2.	s_3.	s_2.	$10^6 d_3$.	$10^6 d_2$.	$10^6 d_3$.	$10^6 d_2$.
1	8	16	8	14	400	200	400	230
2	8	14	8	15	400	230	400	210
3	8	13	8	13	400	250	400	260

Mean values are thus

$s_3=8.0$ $10^6 d_3=400$ $s_2=14.3$ $10^6 d_2=230$

agreeing pretty well with the above data (Chapter III, section 33), where

$s_3=8.1$ $10^6 d_3=398$ $s_2=14.0$ $10^6 d_2=228$

I may summarize, in conclusion, that the present section has developed the method of observation by which data are obtained from the distance apart of two sources of light when certain fiducial rings of the coronas are put in contact. This method is superior to the above method with a single source of light, although its full value has not been evidenced, because of the extreme sensitiveness of the coronas to differences in the distribution of the density of the nucleation. There is a second difficulty inherent in the phenomenon itself, viz, the shrinkage or oscillation in the size of coronas following the instant of their formation. It is probable that the number of fog particles actually decreases by evaporation, though the phenomenon is complicated by the coincident variation of temperature. After relatively long waiting, a somewhat similar shrinkage takes place throughout the period of subsidence, and in case of large coronas the apparent nucleation may thus be reduced to one-fifth of its original value.

DISTRIBUTIONS OF VAPOR NUCLEI AND OF IONS IN DUST-FREE WET AIR.

53. Behavior of different samples of radium. New fog chamber.—It was my hope to be able to obviate the need of using the troublesome and inconstant X-ray bulb by replacing it by a strong sample of radium. It also seemed possible that the fog chamber might be standardized in this way; but the attempts proved quite abortive, as indeed might have been expected. The coronas were but slightly increased on intensifying the original activity of radium I, 100 mg. 10,000×, equivalent to say 10^6, by adding radium II, 10 mg. 200,000×, equivalent to 2×10^6; radium III, 100 mg. 10,000×, equivalent to 1×10^6; radium IV, 100 mg. 10,000×, equivalent to 1×10^6; radium V, 100 mg. 20,000×, equivalent to 2×10^6; on the whole, therefore, about seven times. Obviously the radium must be kept sealed in tubes of aluminum or of very thin glass, as otherwise the fog chamber would become infected, which would be fatal to experiments of the present character.

The reason of the relative inefficiency of the radium is given by the equation $-dn/dt=a-bn^2$, where a is the number of ions generated per second and bn^2 the number which decay per second. Hence for the case of equilibrium $a/b=n^2$, where a varies as the activity of the radium.

If the five samples in question be taken together, therefore, the equilibrium nucleation n would be, for any fixed distance of the radium from the fog chamber,

$$n=\sqrt{n_1^2+n_2^2+\ .\ .\ .\ .\ n_5^2}\ =\sqrt{\Sigma(a/b)}$$

Now, n varies as S_3 (if S be the angular diameter of the coronas) in a general way, and therefore the resultant

$$a \propto S^6$$

Consequently enormous increases of the nucleation bring about but slight changes of the angular diameter of the coronas. This estimate is not quite correct if the values of b vary, as seems to be the case, with the nucleation; but for the larger nucleations here in question such an effect is not observable. If it can be controlled a new method of standardizing the fog chamber for moderate coronas would be suggested.

54. Data—Results of this character are given in table 37, where S is the double tangent of the corona on a radius of 250 cm., n the nucleation corrected for the exhaustion $v_1/v=1.287$. In addition to the effect of aggregating the radium tubes, their position on the outside of the fog chamber is indicated as follows: a denotes that the tubes are placed on the outside of the walls of the horizontal glass cylinder, above its middle or equatorial parts; b that they are similarly placed near the brass cap at the exhaust end; c that they are placed near the remote

TABLE 37.—Radium I, 100 mg. 10,000×, and radium II, 10 mg. 200,000× compared. Bar. 76.7 cm.; temp. 20° C.; $\delta p_3 = 22.9$ cm.; $\delta p_3/p = 0.299$; $v_1/v = 1.287$.

	S.	$0.12S = s'$.	$n \times 10^{-3}$.	$10^{-6}n^2$.	Σn^3.
(1) II	44, 45, 42	5.3	39	1,520	....
I	46, 45	5.4	42	1,810	....
I and II at *a*	50, 52	6.1	61	3,720	3,330
(2) The same, on different parts of chamber. Bar. 76.3; temp. 18° C; $\delta p_3/p = 0.299$.					
II at *c*	61, 62	7.3	104	10,820	....
I at *c*	60, 60	7.2	101	10,200	....
I and II at *c*	65, 67	7.9	129	16,640	21,000
II at *b*	44, 44	5.3	39	1,521	....
I at *b*	41, 38	4.7	29	841	....
I and II at *b*	47, 49	5.7	50	2,500	2,360
I and II at *b*	46	5.5	44	1,936	....
at *a*	57, 55	6.7	80	6,400	....
at *c*	65, 67	7.9	129	16,640	....
(3) II kept in old place *a*; I placed on chamber at *c* nearer glass end; observation at *c*. Bar. 76.3 cm.; temp. 19° C; $\delta p_3 = 22.9$; $\delta p_3/p = 0.300$; $\frac{v_1}{v} = 1.288$.					
V at *c*	66, 66	7.9, 7.9	129, 129	16,600	....
IV at *c*	62, 59	7.4, 7.1	92, 89	8,300	....
III at *c*	59, 59	7.1, 7.1	89, 89	7,900	....
III and IV at *c*	66, 66	7.9, 7.9	129, 129	16,600	16,200
III, IV, and V at *c*	71, 71	8.5, 8.5	162, 162	26,400	32,800

glass end. Observations were made with both eyes below *c*, as this position showed the largest coronas. The marked reductions of size for the other positions of the eyes are probably distance effects, though there are necessarily a variety of complications. Table 37 shows, however, the extreme need of placing all the radium as nearly as possible on the same spot, the importance of which was not at first adequately appreciated (compare series 2). Radium placed at *c* produces over eight times as

TABLE 37—Continued.

	S.	0.12S=s'.	$n\times 10^{-3}$.	$10^{-6}n^2$.	Σn^2.
(4) Further comparisons, all at *c*. Bar. 76.2; temp. 20° C; $\delta p_3/p=0.300$.					
II	66 68	8.0	135	18,200	....
I	69 71	8.4	157	24,600	....
V	67 71	8.3	152	23,100	....
III	60 65	7.5	111	12,300	....
IV	62 61	7.4	107	11,400	....
I+II+III+IV+V	82 85	10.0	266	70,800	89,600
I+III+IV+V	72 75	8.8	175	30,600	71,400
III+IV+V	73 69	8.5	162	26,200	46,800
III+IV	72	8.6	166	27,600	23,700

many nuclei than when placed at *b* and over twice as many than when placed at *a*, and the rate of production of ions would be as the square of these numbers. The effect is enhanced by the fact that the lateral rays have to pass obliquely through the glass; but this appears to be a minor disturbance. In all the experiments an aluminum gutter was cemented to the top of the fog chamber and the sample tubes of radium placed between given marks within it.

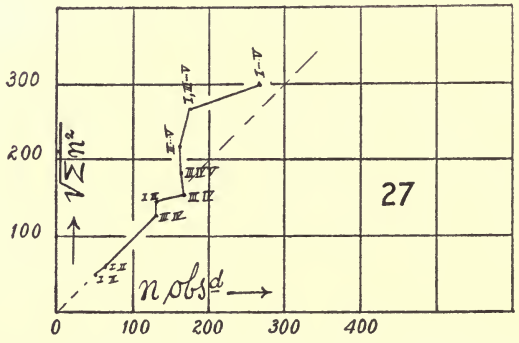

FIG. 27.—Aggregated effect of beta and gamma rays of different samples of radium, I, II, III, IV, and V, observed and computed in terms of nucleation *n* produced.

Table 37 contains the values of Σn^2 for the four series of experiments given, and in fig. 27 these data are additionally shown by mapping out the observed *n* as abscissas and the computed $n=\sqrt{\Sigma n^2}$ as ordinates. There is considerable divergence from the straight line which ought to

appear, reasons for which are outstanding. As a rule smaller values of n are observed than should occur, particularly for the larger coronas. As a means of standardizing the fog chamber, therefore, this method is again inapplicable; moreover, strictures are cast on the present theory by Chapter VI, where $-dn/dt = a - bn^2$ is called in question.

55. Distributions of vapor nuclei and of ions.—In tables 38 and 39 I have collected data for the number of nuclei and of ions found in apparatus II, under different conditions. Not only is a new fog chamber used here, but the method employed is the one described in the present chapter. Contact is therefore made between the fiducial annuli of two coronas, and the distance apart of the sources of light or the double tangent S, on a radius of 250 cm., at which contact occurs, is measured. Special work was also done to determine the fog limits; and in case of the vapor nuclei of dust-free air, the initial region of ions is explored in detail (table 39). The table contains the adiabatic expansion v_1/v and the relative adiabatic drop dp_3/p.

TABLE 38.—Certain distributions in apparatus II. Bar. 76 cm.; temp. 18° C.

	δp_3.	S.	$0.12S = s'$.	$^1n \times 10^{-3}$.	v_1/v.	$\delta p_3/p$.
(1) Radium I+II.....	22.8	72	8.6	167	1.288	0.300
	26.6	70	8.4	176	1.357	.350
	26.6	71	8.5	182	1.357	.350
	24.7	67	8.0	144	1.322	.325
	23.0	72	8.6	166	1.292	.303
	21.1	65	7.8	119	1.260	.278
	19.2	10	1.2	0.4	1.230	.253
	19.2	10	1.2	0.4	1.230	.253
Fog limit. Radium I+II and X-rays. Bar. 76.1 cm.; temp. 21° C.						
(2) Radium I+II.....	18.5	0.0	0.0	0.0	1.218	0.243
	19.5	0.0	0.0	0.0	1.233	.256
	20.4	(?)	(?)	(?)	1.247	.268
	20.4	17	2.0	2.5	1.247	.268
Bar. 76.0 cm.; temp. 21° C.						
(3) Radium I+II.....	18.3	0	0	0.0	1.216	0.241
	18.8	0	0	0.0	1.222	.247
	19.3	9	11	0.3	1.231	.254
	19.3	9	11	0.3	1.231	.254
(4) X-rays; $D=35$.....	19.5	22	26	4.6	1.234	.257
	18.9	10	12	0.3	1.225	.249
$D=10$.....	19.1	13	16	0.9	1.227	.251
	18.5	0	0	0.0	1.219	.243

[1] Ions under radiation not lost by exhaustion.

TABLE 39.—Distributions of vapor nuclei in dust-free air. Bar. 75.9 cm.; temp. 21.5° C

	δp_3.	S.	s'.	n.	$\delta p_3/p$.	v_1/v.
(1)	19.3	0	0.0	0.0	0.254	1.231
	20.3	13	1.6	0.9	.267	1.246
	20.8	14	1.7	1.2	.275	1.256
	21.2	14	1.7	1.2	.279	1.262
	21.7	15	1.8	1.4	.286	1.270
	22.0	14	1.7	1.2	.290	1.275
	22.3	15	1.8	1.5	.294	1.280
	22.8	15	1.8	1.5	.300	1.288
	23.3	17	2.0	2.0	.307	1.297
	23.6	19	2.3	3.3	.311	1.302
	24.4	19	2.3	3.4	.322	1.318
	25.3	26	3.1	8.6	.333	1.333
	26.4	30	3.6	14.7	.348	1.354
	27.1	52	6.2	74.0	.357	1.368
	26.9	45	5.4	47.0	.355	1.365
	27.6	y 69	8.3	176	.364	1.378
	28.1	72	8.6	194	.370	1.388
	28.9	81	9.7	289	.381	1.405
	29.1	c 97	11.6	480	.383	1.408
	29.5	r 102	12.2	560	.389	1.418
	30.5	y 129	15.5	1210	.402	1.440
	31.0	g' 128	15.4	1225	.410	1.454
	32.0	g' 140	16.8	1533	.422	1.476
	32.0	g 136	16.3	1431	.422	1.476
	33.5	g 147	17.6	1780	.442	1.513
	35.4	v'? 140	?17.0	1670	.466	1.561
	38.0	v'? 140	?18.0	2090	.500	1.635

	δp^3.	S.	s'.	n.	$\delta p_3/p$.	v v.
Radium removed from the room. Bar. 75.1; temp. 22° C. Vapor nuclei.						
(2)	19.4	0	0	0.0	0.258	1.235
	20.1	10	1.2	0.4	.268	1.248
	20.3	10	1.2	0.4	.270	1.250
X-rays. $D=10$; bar. 75.1 cm.; temp. 22° C.						
(3)	18.5	? 10	1.2	0.4	0.246	1.222
	19.5	26	3.1	7.1	.260	1.238
	20.8	r 89	10.7	303	.277	1.259
	20.9	y b 115	13.8	654	.278	1.260
	21.7	g'o 135	16.2	1074	.289	1.274
	21.9	g 130	15.6	959	.292	1.278
	22.4	g 131	15.7	1017	.298	1.285
	23.0	g' 136	16.3	1130	.306	1.296
	23.4	131	15.7	1058	.312	1.304
	25.0	132	15.8	1107	.333	1.333
	30.0	134	16.1	1317	.400	1.437
	35.1	136	16.3	1486	.467	1.563

56. Remarks on the table.—These results are constructed in figs. 28 and 29 in different scales, the nucleation of fig. 29 being on a scale 100 times greater, so that it may be in keeping with the very low nucleations. As a whole the figures are very closely like the above, though a different apparatus was used. The line for dust-free air and vapor nuclei here showed a tendency to transcend large green coronas, distinctly entering the violet of the first series; but as the coronas are filmy the measurement is correspondingly difficult. Over 2,000,000 vapor nuclei are registered by the present method in the extreme case.

In general, however, apparatus II shows fewer nuclei than apparatus I under like conditions of exhaustion. Thus at $\delta p_3/p = 0.375$, $n = 250{,}000$ for I and $n = 500{,}000$ for II; at higher exhaustions, $\delta p_3/p = 0.39$, $n =$ 800,000 to 900,000 for I, $n = 600{,}000$ for II; at $\delta p_3/p = 0.40$, $n = 900{,}000$ to 1,000,000 for I and $n = 1{,}200{,}000$ for II; but here apparatus I is already losing efficiency.

Fig. 28 also shows the small nucleations due to radium I+II and radium I to V, as compared with the enormous effect of X-rays in proper positions. In the case of the intense X-rays, the striking rapid upward sweep of the curve is noticeable in case of apparatus I as compared with apparatus II. The asymptote is reached much more

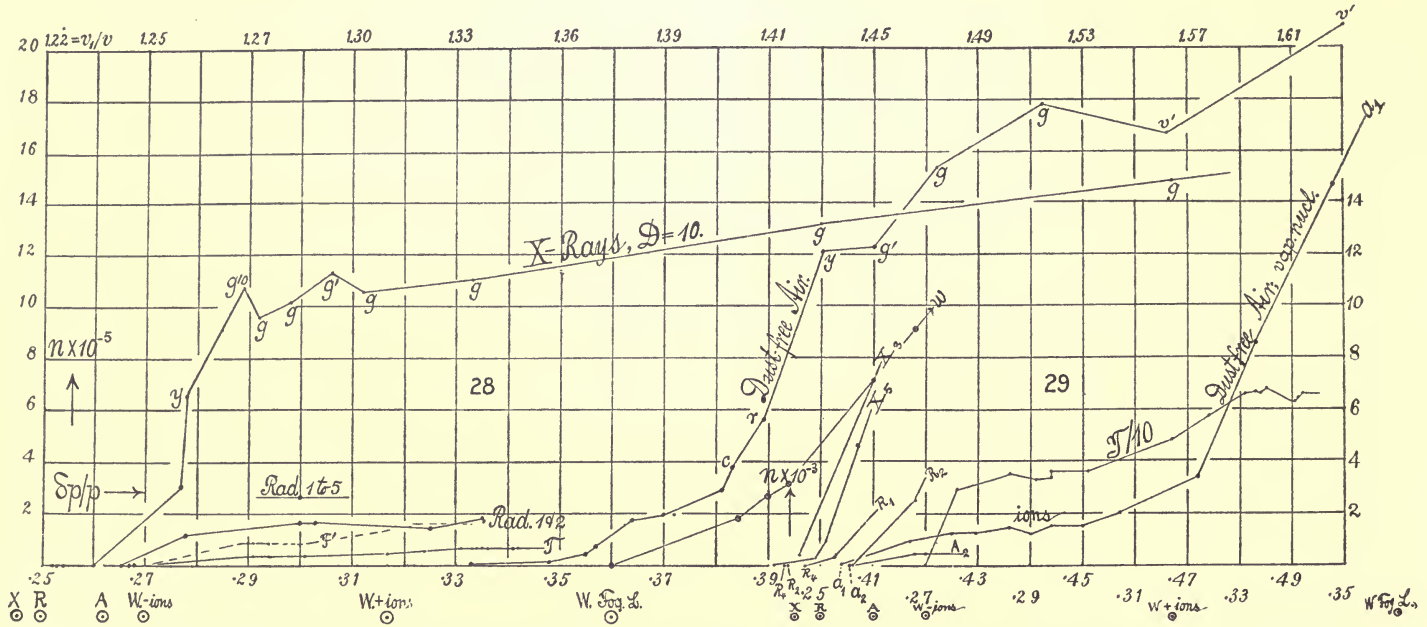

FIG. 28.—Nucleation n, in terms of adiabatic drop of pressure $\delta p/p$, and the volume expansion v_1/v, in case of non-energized wet dust-free air, and of the same acted on by radium and the X-rays from different distances D. The letters refer to colors of coronas. T shows J. J. Thomson's result adapted to the same scale; W refers to Wilson's condensation and fog limits. The scale of nucleation is compressed ($n \times 10^{-5}$). (Note the low radium asymptote [I to V] as compared with the X-rays.)

FIG. 29.—The same in the region of ions; nucleations laid off on a larger scale.

suddenly in case of the new results, and it is perhaps higher than in the old. No progress above the green corona could be obtained, but on the other hand there was no decrement of nucleation at very high exhaustions, such as is often obtained.

57. Condensation limits and fog limits. Conclusion.—The condensation limits, or the exhaustions at which condensation begins, are best gathered from fig. 29, which also shows the nearly constant low nucleation (due, as C. T. R. Wilson has proved, to ions), which precedes the region of vapor nuclei in the case of dust-free wet air.

	Series.	Condensation limit.	
		v_1/v.	$\delta p_3/p$.
Radium I+II	II	1.240	0.262
X-rays, $D=10$ cm	II	(higher)	....
Radium I+II	IV	1.226	.250
X-rays, $D=35$ cm	V	1.225	.249
$D=10$ cm	V	1.223	.247
Vapor nuclei	I	1.238	.261
Do	II	1.241	.263
X-rays, $D=10$ cm	III	1.222	.246

D is the distance from which the X-ray tube acts.

It appears certain from these results that the condensation limit decreases slowly as the intensity of radiation increases; also that it is lower for ionized air, even under weak radiation, than for dust-free normal air. Coronas may be obtained in succession, in these instances, after they have completely vanished in the preceding case of weaker radiation. Rain is naturally accompanied by a definite corona. If we reckon the intensity of the radiation as the square of the maximum radiation producible, or the height of the asymptote, the following data may be adduced from figs. 28 and 29:

	$n\times 10^{-3}$.	n^2.	Ratio.	$\delta p_3/p$.	v_1/v.	$\delta(v_1/v)$.
Wet air (dust-free)	1.5	2	1	0.26	1.240	0.0
Radium I+II	100 to 150	1 to 2×10^4	10^4	.25	1.225	.015
X-rays, $D=0$	1000	10^6	10^6	.245	1.220	.020

Thus, while the intensity of radiation changes from the natural radiation in dust-free air, 1, to 10^4 for beta-gamma radiations, and from 1 to 10^6 for X-rays, the volume expansion at which condensation takes place shifts over decrements of 0.015 and 0.020 or 15/1240 and 20/1240, *i. e.*, 1.2 per cent and 1.6 per cent.

In conclusion, it may be interesting to adduce mean values for the condensation limits as obtained in Chapter III, with the former apparatus I. They are shown in the table below, and they agree well with the present set, remembering that the values would be slightly below these data if taken from the chart.

	$\delta p_3/p.$	$v_1/v_1.$
Air alone	0.265	1.243
Air actuated by radium	.246	1.223
Air actuated by X-rays	.243	1.220

The results of the chapter may be summarized as follows. The endeavor to standardize the fog chamber by a number of distinct but similar samples of radium, used in succession, runs counter to a great difficulty, inasmuch as the effect produced at the line of vision depends upon the position of the radium tubes on the outside of the fog chamber. Moreover, the aperture of the coronas varies only with the sixth root of the rate of production and is therefore not a sensitive criterion.

The results for vapor nuclei and ions are best seen from the chart. The deductions are similar to those already given at the end of Chapter III. The positions of the condensation and the fog limits have just been stated. These terminal points, as well as the graph as a whole, are reached at lower exhaustions than was the case in Wilson's experiments.

CHAPTER V.

RESIDUAL WATER NUCLEI.

PROMISCUOUS EXPERIMENTS.

58. Historical.—A nucleus obtained from a partial evaporation of fog particles will be called a residual water nucleus or, briefly, a water nucleus.

C. T. R. Wilson,* in his experiments with ultra-violet light, found that nuclei were spontaneously producible on long exposure of dust-free air saturated with water vapor to the radiation. He explained this as being due to the probable production and solution of hydrogen peroxide, wherefore the vapor pressure at the surface of the minute solvent water droplets would be diminished. Such droplets would therefore grow in the saturated environment. Wilson also encountered water nuclei produced by evaporation, but he expressed no opinion of their nature, merely treating them as an impurity to be removed to make the air dust-free.

J. J. Thomson,† in his famous experiments, encountered similar difficulties with water nuclei. He states that

> When . . . . the number of ions is large, experience shows that they are not all brought down by the first cloud formed by sudden expansion . . . . . after the first cloud has subsided, [and] . . . . . another expansion be made, a second cloud is formed . . . . .

On page 531, moreover,

> The first expansion . . . . though it does not bring all the ions down, seems to increase the size of those left and makes them more permanent, ... these modified ions are able to cause a cloud to settle with an expansion of less than 1.25 . . . . secondary clouds . . . . are but little affected by the electric field, ...

From this it seems that Thomson did not regard these secondary clouds as precipitated upon water nuclei derived from the evaporation of the fog particles of the first cloud.

In 1902,‡ and more at length in my memoir on the structure of the nucleus,§ I gave a detailed account of the behavior of the residual water nuclei and showed by direct experiment that the merest trace of solute in the fog particle evaporated left a persistent water nucleus behind. The water nuclei of pure water seem by comparison to be evanescent. The reduction of vapor pressure due to solution compensated the increased vapor pressure due to curvature.

---

*Phil. Trans., p. 428, vol. 192, 1889.
†Phil. Mag. (5), 1898, vol. 46, p. 528 (*cf.* pp. 529 and 531).
‡Phil. Mag. (6), IV, pp. 262–269, 1902.
§Structure of the Nucleus, Smithsonian Reports, No. 1373, 1903, Washington.

In 1903 J. J. Thomson* gave a general account of condensation nuclei, at the end of which he formulates succinct reasons for the persistence of water nuclei, even when derived from the evaporation of fog particles of pure water. He says "on the view of the relation between surface tension and the thickness of water films, to which Reinold and Rucker were led by their experiments with very thin films, drops of pure water of a definite radius might be in equilibrium with saturated water vapor even if they were not charged," a proposition which is thereafter proved. A further deduction of J. J. Thomson's which may be of use below is that "the efficiency of an ion as a nucleus for condensation depends upon the maximum size of the aggregation, while the velocity of the electric field depends upon the average size." Thus the "average size of a negative ion may easily be less than that of a positive ion, ..." while the negative nucleus is larger than the positive, other things being equal. I may also add that J. J. Thomson computes the radius of a vapor nucleus to be $10^{-7}/1.9$ cm., whereas the radius of the ionized nucleus is $10^{-7}/3.1$, so that the vapor nuclei are slightly larger than the ions.

Furthermore, Thomson shows that vapor nuclei are probably aggregations of water molecules, and elsewhere that "in a space far from saturated with water vapor, ... drops will be formed, and that the size of these drops diminishes only very slowly as the quantity of water vapor in the surrounding air diminishes . . . ."

In 1905 the Transactions of the St. Louis International Electrical Congress were published, which gave a review of the present state of our knowledge of condensation nuclei by C. T. R. Wilson.† This contains the most recent contributions relating to water nuclei. In view of the investigations of Langevin and of E. Bloch‡ on the occurrence and behavior of slow-moving ions, Wilson finally summarizes the results bearing on nuclei as follows:

> (1) The ions proper, requiring a fourfold or sixfold supersaturation to cause water to condense on them, and having a mobility exceeding 1 cm. per second in a field of one volt per second. (2) Loaded ions, requiring little or no supersaturation to make water condense on them, and having a mobility generally less than a thousandth part of that of the ions proper. (3) Uncharged nuclei, resembling the second class and requiring little or no supersaturation in order that visible drops may form upon them.

59. Purpose, plan, and method.—My purpose in the present paper is to determine whether there is any difference in the sizes of residual water nuclei obtained in the evaporation of fog particles under different conditions; for instance, whether the fog particles of large coronas

*Conduction of Electricity through Gases, Chapter VII, Cambridge, 1903.

†Trans. of International Electrical Congress of 1904, p. 365 (*cf.* p. 378), St. Louis, 1905.

‡Recherches sur la conductilité électrique de l'air, etc., Paris, 1904 (quoted by Wilson).

evaporate to the same nucleus as the fog particles of small coronas; or, more pertinently, whether the fog particles precipitated on ions evaporate to the same nucleus as the fog particles precipitated on the vapor nuclei of wet dust-free air. A number of allied questions will be treated.

A variety of methods were tested, as follows:

I. The endeavor was made to find if from fogs characterized by identical coronas the number of residual nuclei was the same after the natural evaporation during subsidence, no matter whether the original precipitate occurred on ions or on the vapor nuclei of dust-free air.

II. Identical coronas were produced on ions and on vapor nuclei, respectively; but the evaporation of fog particles was accelerated by keeping the influx valve open by a definite amount. The number of residual nuclei was then tested by a second exhaustion, the amount of which was varied. This was done both by starting with different pressures in the vacuum chamber for full barometric pressure in the fog chamber and by starting with different partial exhaustions in the fog chamber for the same pressure in the vacuum chamber.

III. The persistence of the residual nuclei was studied by measuring their decrease in number in the lapse of time. Incidentally the loss due to evaporation was estimated and the distribution of sizes considered. Finally, in the second part of this chapter the method of successive exhaustion, which is found to be most productive, is brought to a definite conclusion.

In all cases the ions were produced by a weak sample of radium in a sealed aluminum tube, attached to the top of the fog chamber. This was removed during the examination for water nuclei, inasmuch as the ions are efficient in the presence of the latter. The corona obtained from the radium was always the same, care being taken to precipitate all residual water nuclei in these cases, and to have a pressure difference sufficiently high to catch all the ions, or at least the same fraction of the total number. To produce the same given corona with the vapor nuclei of dust-free air is easily accomplished after a short preliminary trial. Moreover, these coronas may be obtained at the same pressure whenever the asymptote for the ions has been reached. The eye is always 40 cm. and the source of light 250 cm. from the axis of the fog chamber.

60. Residual water nuclei after the natural evaporation of fog particles.—The results obtained from these experiments are given in table 40. Here $p=76$ and $p-\delta p'_a$ are the initial pressures of the fog and vacuum chambers; $p-\delta p_a$ the final pressure, when in communication after exhaustion; $s_a/30$ the angular diameter of the corona, observed for ions and vapor nuclei in dust-free air, as specified. Again, $p=\delta p'_b$; $p-\delta p_b$ denotes the initial pressure of the fog chamber and vacuum chamber before exhaustion; $p-\delta p_c$ the final common pressure after

exhaustion, when the fog particles corresponding to s_a have subsided, leaving (by natural evaporation) the residual water nuclei corresponding to the corona of any diameter $s_b/30$, behind.

TABLE 40.—Experiments with residual water nuclei. Bar. 76 cm.; temp. 14° C. Natural evaporation.

Precipitation on—	$\delta p'_a$.	δp_a.	s_a.	$\delta p_a/p$.	$n_a \times 10^{-3}$.	$\delta p'_b$.
Vapor nuclei	28.3	26.7	3.5	0.351	14	27.5
I.	29.3	27.5	[1]6.9	.385	106	....
	29.3	27.8	[2]6.9	.385	106	27.8
Rad. ions	29.3	27.7	[1]6.9	.385	106	27.7

Precipitation on—	δp_b.	δp_c.	s_b.	$\frac{\delta p}{p} = \frac{\delta p_c - \delta p_b}{p - \delta p_b}$	$n_b \times 10^{-3}$.
Vapor nuclei	....	26.5	2.3	0.349	3.6
I.	....	....	....	....	....
	11.9	26.8	2.7	.232	4.2
Rad. ions	11.9	26.7	3.0	.231	5.6

[1]wo; [2]gbp.

Table 40 shows that for initial coronas of the same size, $s = 6.9$, the residual coronas $s = 2.7$ and 3.0 do not differ sufficiently to make the evidence decisive. Less than one-tenth the original number of ions are represented by water nuclei, the remainder having vanished by subsidence with the fog particles or otherwise. There does not seem to be any certain difference between the behavior of vapor nuclei and of ions, so far as these experiments go. The large number surviving in the first instance (small initial corona), as compared with a smaller number in larger coronas, is striking.

61. Rapid evaporation of fog-particles.—In table 41 the filter cock is left slightly open in order that the water nuclei may be increased. The fog-chamber is initially at barometric pressure. The initial pressures of the vacuum chamber are $p = 76.7 - 23.6$ cm., to catch the ions produced by weak radium and numbering about 100,000. The pressure-differences are then reduced successively to the values to catch the water nuclei left after the accelerated evaporation specified. The exhaustion drops from p and $p - \delta p'$ as initial pressures in fog chamber and in vacuum chamber to $p - \delta p_3$, the final common pressure in both, while $x = \delta p_3/p$ is a convenient datum for the comparison of the water nucleations n. These have been corrected for the temperature t of the fog chamber, more water being precipitated as t is higher and for volume expansion from v at t to v_1 at t_1.

TABLE 41.—Sizes of water nuclei. Radium ionizer. Slightly open filter cock; t several minutes.

	$\delta p'$.	δp_3.	s_2.	$\delta p_3/p$.	$\frac{mv_1}{m'v}$.	$n_2 \times 10^{-3}$.	At 20°. $n_2 \times 10^{-3}$.
Ions originally; $s=7.0$ (w o): $n=115{,}000$. Bar. 76.7 cm.; $p'=53.1$ cm.; temp. 21.0° C.							
I.	23.6	22.2	4.5	0.289	....	30.2	31
	23.6	22.2	[1]5.0	.289	....	40.3	[1]41
	23.6	22.2	[2]4.4	.289	....	28.7	[2]29
	23.6	22.2	4.6	.289	....	32.1	33
	13.0	12.4	[3]5.4	.162	....	27.8	28
	16.7	16.0	[4]5.2	.209	....	32.5	33
	17.0	16.2	[4]5.2	.211	....	32.8	33
	6.0	5.9	[5]7.1	.077	....	30.2	31
	23.6	22.2	4.7	.289	....	34.4	35
	23.6	22.2	[4]5.5	.289	....	54.2	55
Ions...	....	22.2	7.0	.289	....	114.7	117
Bar. 75.9 cm.; temp. 26° C. Original corona, $s=6.4$; $n=95{,}000$; $\delta p'=22.1$ cm.							
II.	5.0	4.9	[5]7.5	0.065	....	30.3	32
	1.9	1.9	[6]9.2	.025	....	23.1	24
	22.1	20.8	[3]6.4	.214	....	83.5	95
Ions...	10.3	10.0	[3]5.4	.132	....	22.5	24
Bar. 76.2 cm.; temp. 25.5° C.; ions, $n=115{,}000$.							
III.	1.0	1.0	[7]8.6	0.013	....	9.5	10.1
	18.0	17.0	3.3	.223	....	9.2	[7]10.3
	....	2.2	[8]7.5	.029	....	13.0	13.8
	....	22.1	2.2	.290	....	3.6	[7]4.1
	....	1.9	[8]7.5	.025	....	12.3	13.0
	....	17.0	2.8	.223	....	5.5	[7]6.2
	....	3.0	7.5	.039	....	18.3	19.4
	....	22.2	2.2	.291	....	3.6	[7]4.1

[1]Radium not removed. [2]Cock open late. [3]g b p. [4]w o. [5]g y o. [6]w c. [7]Subsequent exhaustion to catch the water nuclei left after first exhaustion. w c to g b p, very faint. [8]g b p.

The data are given in fig. 30, n in terms of the relative drop in pressure, $x=\delta p_3/p$. Though the experiments were made with great care and apparently satisfactory, the results are disappointing; but this is probably to be expected when the water nuclei are only obtainable by evaporations lasting as much as a fraction of a minute, during which there must be both subsidence and probably also a washing-out of nuclei by the disturbance produced during the influx of air. In the first series, where there are 115,000 ions, not more than 30,000 or 40,000 water nuclei (about one-third), are obtainable. On opening the filter cock

wider and as wide as permissible to insure filtration, the number of water nuclei was increased to over 50,000, or to about one-half the number of ions. In the second series about 90,000 ions were available, because of the lower drop δp_3, and less than 30,000 were represented by water nuclei, again about one-third.

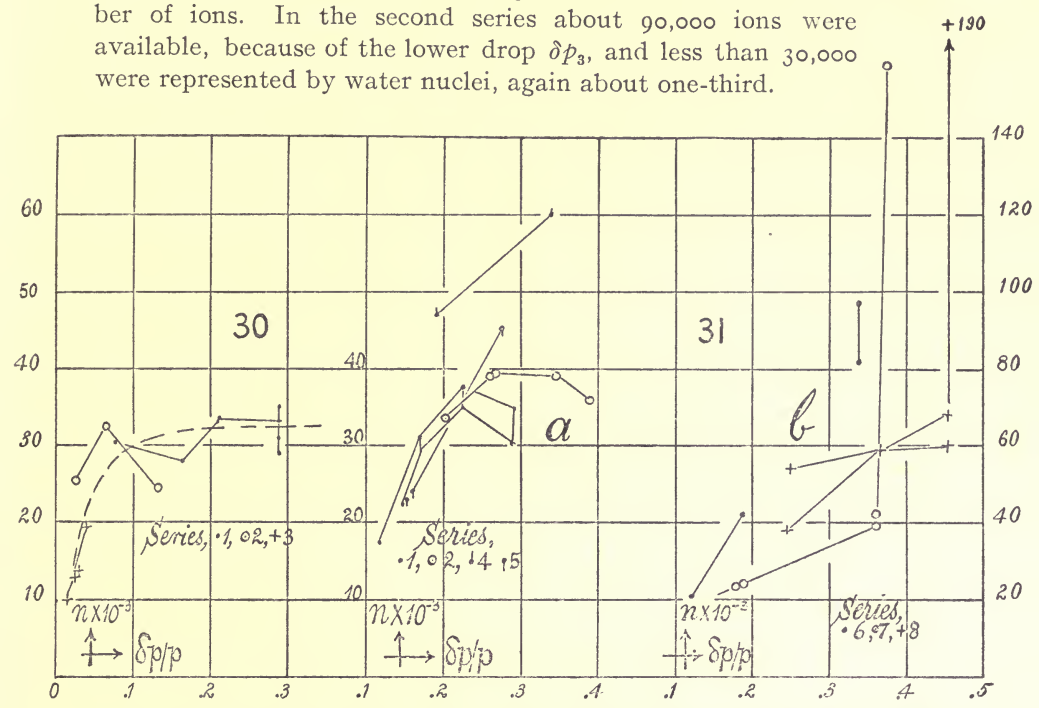

FIG. 30.—Number of residual water nuclei obtained from rapid evaporation of fog particles and found at different small adiabatic drops of pressure $\delta p/p$.

FIG. 31.—Number of residual water nuclei obtained from rapid evaporation of fog particles in a partially exhausted fog chamber and caught at different small adiabatic drops of pressure $\delta p/p$.

When the drop δp_3 is as low as 2 cm., the number of water nuclei is relatively small, though at 5 cm. the maximum is already reached. Unfortunately, therefore, the range of marked variation of n lies below a few centimeters of δp_3, wherefore the coronas are too filmy and large to admit of easy identification, unless a special immense fog chamber is constructed for small exhaustions. So far as these experiments go, however, the appearance is rather such as recalls the distribution curves for ions and for dust-free air; in other words, the water nuclei are probably of all sizes within certain limiting dimensions, like the ions.

In the third series of table 41 the attempt is made to further study these large, filmy coronas. They may be recognized with certainty here and are throughout of the green-blue-purple type, corresponding to about 100,000 nuclei under normal expansions. At the low exhaustions used, however, they correspond to 10 or 15 thousand nuclei per cubic

centimeter, since but little water is precipitated. In this series a second large exhaustion was made to catch the nuclei left by the first exhaustion in each of the four cases. But few nuclei were found, however, perhaps because considerable time (5 minutes) was needed between the exhaustions; but the reason for this is not clear. One may notice in conclusion that the numbers found for the nucleation depend essentially upon computation, as the coronas are large. There is one correction, m/m_{27}, to allow for the small quantity of water precipitated; another for the volume increase on exhaustion; a third for temperature, etc. The coronas themselves naturally increase as the expansion is larger, but they do not keep pace with the corrections.

62. Continued.—In the experiments of table 42 the filter cock was again left slightly open; but the vacuum chamber was kept at the same initial pressure $p-\delta p'$. The low drops of pressure were secured by successively reducing the pressure of the fog chamber, as shown under $p-\delta p_a$. This is a much more convenient method of experiment, though the computation is more troublesome. The final common pressure after exhaustion is $p-\delta p_3$. All other data have the same meaning as before and corrections are added for the precipitation of water, m'/m; for the volume expansion v_1/v and for temperature. The table contains six series of results for different exhaustions and differently opened filter cock. Data are reproduced in fig. 31.

Naturally the same evaporation difficulties are again obtained, but the curves as a whole are more definite. In series I and II the number of ions which survive in the water nuclei is again about a third in each case; but if the filter cock is opened wider, about half as many water nuclei occur relatively to the original number of ions. If radium is left in place (series III, VI) the ions are still efficient in presence of the increased number of nuclei.

The curves corresponding to the distribution of water nuclei in series I again suggest the distribution curve of ions and of vapor nuclei in dust-free air. In other words, all sizes of nuclei within a certain range of dimension seem to be present. Series II has not been carried far enough, for the experiment places a lower limit at which the method necessarily breaks down. Series VI, however, is of a similar character to series I.

The distinctive feature of these experiments is the occurrence of reduced nucleation at very much higher drops of pressure than above. One would naturally associate this with the fact that the water nuclei are stored before the precipitation of fog upon them, in a partially exhausted vessel. Yet the evidence is not clear on this point. The smallest nucleation occurs at the lowest pressure attainable, viz, 59.8 to 61.9; but in series II higher values of n appear at 62.0 to 62.4 cm. A larger drop of pressure is here applied adapted to catch the smaller nuclei.

TABLE 42.—Sizes of residual water nuclei.

	p.	δp_a.	δp_3.	s_2.	$\delta p_3/p$.	p_3.	p'.	$n_2 \times 10^{-3}$.	At 24° $n_2 \times 10^{-3}$.
I. Cock open 30°. Bar. 76 cm.; temp. 24.2° C.; $p' = 52.4$ cm. Original ions,[1] $s = 6.9$; $n = 110{,}000$.									
	76.0	0.0	22.1	4.5	0.291	59.9	54.4	....	30.4
	76.0	0.0	22.2	4.7	.292	53.8	....	....	34.8
	63.9	12.1	22.9	5.5	.169	53.1	....	....	31
	64.0	12.0	22.9	5.4	[2].170	53.1	....	....	29.3
	68.7	7.3	22.9	5.3	.227	53.1	....	....	37.5
	68.8	7.2	22.6	5.2	.224	53.4	....	....	34.8
	59.8	16.2	23.2	5.2	.117	52.8	....	....	17.4
	61.9	14.1	23.2	5.2	.147	52.8	....	....	22.3
II. Higher exhaustions. Ions, $n = 130{,}000$.									
	76.0	0.0	26.3	4.6	0.346	49.7	48.9	....	38.9
	62.0	14.0	26.5	5.3	.202	49.5	....	....	33.5
	67.9	8.1	26.2	[2]5.1	.267	49.8	....	....	39.3
	67.8	8.2	26.2	5.1	.266	49.8	....	....	39.0
	76.0	0.0	25.8	4.5	.339	50.2	....	....	35.9
III. Miscellaneous. Ions, $n = 137{,}000$.									
Cock open 60° ..	76.0	0.0	25.9	5.1	0.341	50.1	48.9	....	50.9
Cock open 90° ..	76.0	0.0	25.9	5.1	.341	50.1	....	....	50.9
Radium in place	76.0	0.0	25.9	5.6	.341	50.1	....	....	67.9
Ions.....	76.0	0.0	25.9	7.0	.341	50.1	....	....	129.0
IV. Bar. 75.9 cm.; temp. 26° C. $\delta p' = 27.1$ cm.									
Cock open 60° ..	75.9	0.0	25.7	5.3	0.339	50.2	48.8	57	60
	61.1	14.8	26.5	6.0	.191	49.4	....	46	47
V. Low pressure. $\delta p = 22.1$ cm. Original corona, $s = 6.4$; $n = 86{,}000$.									
	75.9	0.0	20.7	[2]5.3	0.273	55.2	53.8	45	47
	64.7	11.2	21.5	[3]5.2	.159	54.4	....	24	86
	64.0	11.9	21.5	[3]5.2	.150	54.4	....	23	81
VI. Bar. 76.0 cm.; temp. 14° C. Original corona on radium ions, $s = 6.9$; $n = 97{,}000$. Cock open 30°. $\delta p' = 27.5$ cm.									
	60.6	15.4	26.8	6.2	0.188	49.2	48.5	51.5	42
	55.9	20.1	26.9	5.6	.122	49.1	....	24.9	21
Radium in place	76.0	0.0	25.7	6.5	.338	50.3	....	108	82
Ions.....	76.0	0.0	25.7	6.9	.338	50.3	....	127	97

[1] Loss by subsidence. [2] w o. [3] g b p.

TABLE 42.—Sizes of residual water nuclei—Continued.

	p.	δp_a.	δp_3.	s_2.	$\delta p_3/p$.	p_3.	p'.	$n_2 \times 10^{-3}$.	At 24° $n_2 \times 10^{-3}$.
VII. Bar. 75.7 cm.; temp. 29.5° C.									
Ions.....	75.7	0.0	28.1	6.9	0.371	47.6	46.7	141	159
	75.7	0.0	27.1	[1]6.2	.358	48.6	....	[5]102	115
	75.7	0.0	27.4	[2]4.3	.362	48.3	....	[6]34.5	39
	58.2	17.5	28.0	4.7	.180	47.7	....	20.9	23
	58.8	16.9	28.0	4.7	.189	47.7	....	22.2	24
	75.7	0.0	27.4	4.4	.362	48.3	....	36.8	42
VIII. Same. Lower pressures. Bar. 75.7 cm.; temp. 29.5° C.									
	75.7	0.0	34.4	4.8	0.454	41.3	39.3	59.7	68
	53.8	21.9	35.2	5.0	.247	40.5	....	34.3	38
	75.7	0.0	34.4	4.6	.454	41.3	....	52.6	60
	64.0	11.7	35.1	5.0	.366	40.6	....	52.0	59
	53.6	22.1	35.5	5.6	.250	40.2	....	49.1	54
(Ions).....	75.7	0.0	34.4	6.9	.455	....	....	176	201

[1] Radium in place; ions active in presence of water nuclei. [2] Radium off.

When the relatively large nuclei are caught at the very low drop of pressure, a higher drop applied in turn always reveals a relatively large number of water nuclei, apparently too small to have been caught in the first exhaustion. This evidence must also be used with caution, because evaporation in the filmy coronas, observed in the first instance, is liable to be a marked feature.

If the graphs of fig. 31 be prolonged until they intersect the axis at about $x = 0.05$, the limiting superior diameter of water nuclei may be estimated from the Kelvin-Helmholtz equation. Regarding the supersaturation to be about $S = 1.15$, the amount of adiabatic cooling as far as 9°, the maximum diameter for the present series would be about $d = 2 \times 10^{-6}$ cm. In the above cases where the condensation began below 2 cm. (say at about 1 cm.) the maximum diameter than $d = 25 \times 10^{-6}$ cm.

One may notice, however, that the effect of temperature enters absolutely into Helmholtz's equation, so that if the minimum volume of expansion could be found it would be worth while to compute d carefully. S decreasing rapidly implies a corresponding rapid increase of d.

In series VII and VIII, made at a somewhat later date, high exhaustion and (incidentally) relatively high temperatures occur. The data are also given in fig. 2, but they show no definite tendency. There remain for discussion series IV and V, in each of which the filter cock was open as widely as permissible and in which the number of water nuclei resulting from more rapid evaporation is often twice as large as heretofore. In each of these cases the nucleation decreases very definitely and rapidly with the exhaustion, as the numbers of nuclei were not only large, but their sizes distributed over a wide range of values.

The values of table 42 refer to different numbers of initial ions. The initial coronas are usually the same (w y o); but being obtained at different exhaustions, this corona implies greater nucleation as the exhaustion is higher. The number of ions in the tables has been computed by supposing the exhaustion to be faster than the reproduction of ions; *i. e.*, the number of ions found for the exhausted vessel is always multiplied by the volume expansion, apart from the correction for the increased quantity of water precipitated. It may be questioned whether this hypothesis is justified, but there is no way of testing it. It is also very difficult to understand why the corona remains constant, while the exhaustion, after all ions are caught, continually increases over enormous ranges.

In table 43 the data of table 42 are summarized, but without referring them to the same initial ionization, as these reductions would be uncertain. $X=\delta p_3/p$. Notwithstanding the care given the work, the results are far from satisfactory. All series show, however, that the number of residual water nuclei present after the evaporation of a fog originally containing about 100,000 ions per cubic centimeter is smaller as the exhaustion is smaller, as if the water nuclei within certain ranges were of all sizes.

TABLE 43.—Summary of table 42. Filter cock open 30°. Data referred to 125,000 ions, originally present.

$X\times 10^{-3}$.	$n\times 10^{-3}$.
Series I. Ions 110,000. Bar. 76.0 cm.; temp. 24° C.; $p'=52.4$ cm.	
291	30
292	35
169	31
170	29
227	37
224	35
117	17
147	22
Series II. Ions 130,000. Bar. 76 cm.; temp. 24° C.; $p'=48.9$ cm.	
346	39
186	45
202	33
267	39
266	39
339	36
Series VI.[1] Ions 97,000. Bar. 76 cm.; temp. 14° C.; $p'=48.5$ cm.	
188	42
122	21
Series VII. Ions 160,000. Bar. 75.7 cm.; temp. 30° C.; $p'=46.7$ cm.	
362	39
180	23
189	24
362	42
Series VIII. Ions 200,000. Bar. 75.7 cm.; temp. 30° C.; $p'=39.3$ cm.	
454	68
247	38
454	60
366	59
250	54

[1]Made at an earlier date. The filter cock may have been too widely open.

The effect of the low pressure under which the water nuclei are stored does not clearly appear; nor can the effect of temperature be stated. The most consistent results are those of series I, in which the lowest exhaustions were applied. One-third to one-half of the original ions or vapor nuclei are represented by the residual water nuclei, the number

TABLE 44.—Decay of residual water nuclei.

Exciter.	δp_3 and $\delta p_3/p$.	s.	$n \times 10^{-3}$.	t.	δp_3 and $\delta p_3/p$.	s'.	$n' \times 10^{-3}$.	Ratio.
I. Bar. 76.2 cm.; temp. 15° C.; radium and water nuclei, $\delta p' = 24.0$ cm.; vapor nuclei, $\delta p' = 29.3$ cm.; $\delta p/p = 0.297$ and 0.362; $v_1/v = 1.284$ and 1.375; not corrected for temperature.								
Radium..	22.6	6.9	86	90	22.6	4.6	26	0.30
	$\delta p/p = 0.297$		86	90	.297	5.0	32	.37
			86	180	....	5.0	32	.37
			86	180	....	5.0	32	.37
			86	300	....	3.7	14	.16
			86	600	....	3.9	16	.19
II. Wet air.								
None.....	27.6	[1]7.5	150	120	22.6	5.3	38	0.25
	0.362	[2]6.2	88	180	.297	4.2	20	.23
		[3]6.9	117	300	....	5.1	34	.29
		[3]6.9	117	600	....	4.8	29	.25
III. Repeated. Identical pressures ($\delta p' = 28.3$ cm.) throughout. Always same rate of influx (partially open cock). Temp. 22° C.; bar. 76 cm.; $v_1/v = 1.363$.								
None.....	26.9	6.3	91	600	26.9	4.2	27	0.30
Radium..	.354	6.4	94	600	.354	[4]6.3	(91)	.97
		6.6	102	600	....	3.6	17	.17
IV. Repeated. Bar. 75.2 cm.; temp. 19° C.; $v_1/v = 1.362$; $\delta p' = 28.3$ cm.								
None.....	26.5	[2]6.7	107	660	26.5	3.4	14	0.13
	.352				.352			
None.....	26.7	[3]6.9	116	720	26.7	3.5	16	.14
	.355				.355			
Radium..	....	[3]6.7	107	600	....	3.5	16	.15
Radium..	....	6.6	102	600	....	3.3	13	.13
None.....	....	[1]6.9	116	690	....	3.8	20	.18

[1]g b p. [2]w r. [3]w o g. [4]Radium in place.

increasing with the rapidity of evaporation. As the evaporation is accentuated, the graduation of sizes lies within larger ranges. Ions are efficient in the presence of water nuclei, indicating the small bulk of the latter.

63. Persistence of water nuclei.—If there is a difference between the water nuclei obtained after evaporation of fog particles precipitated upon ions and those precipitated upon vapor nuclei, this should show itself in a corresponding difference in the length of life of the types of water nuclei in the two cases. Incidentally the number of nuclei dissipated upon evaporation must appear in the graphs.

The data of the experiments are given in table 44, where n shows the number of nuclei in the original fog precipitated upon ions or on vapor nuclei and n' the number of residual water nuclei after the evaporation of the first fog. In series I the filter cock was open after the measurement of the first corona and the exhaustion used in the precipitation upon vapor

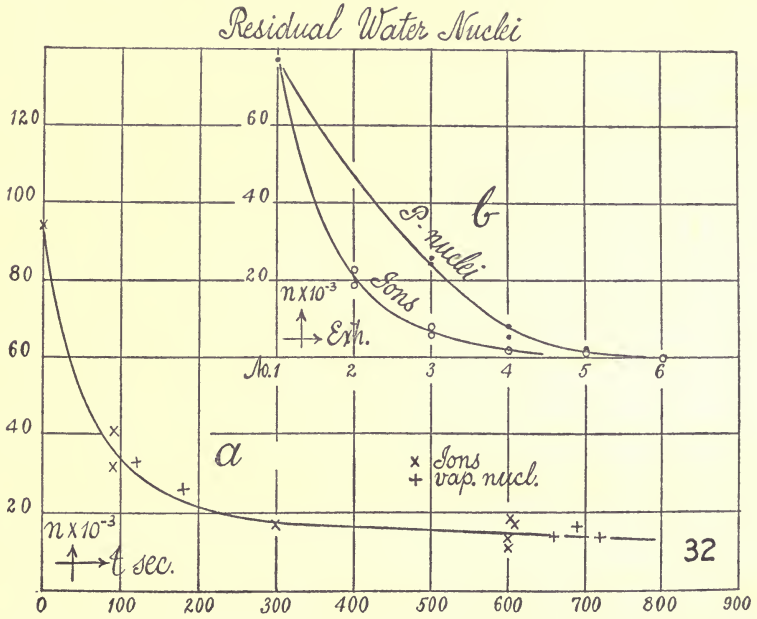

FIG. 32.—(*a*) Persistence of residual water nuclei obtained from the evaporation of fog particles precipitated upon ions and vapor nuclei. The curve shows the number n of water nuclei left t seconds after evaporation. (*b*) Comparison of water nuclei obtained from evaporation of fog particles precipitated upon phosphorus nuclei and ions, in successive identical exhaustions. (Note the conspicuous loss in evaporation between the first and second precipitations.)

nuclei was greater than it was in the corresponding case for ions. These objectionable features were removed in the second and third series, where identical exhaustions occur throughout and the graduated filter cock (fine screw-valve) was opened to a definite number of degrees (30°). After about 60° the resistance of the long filter prohibited a more rapid influx.

The results are all shown in fig. 32, *a*, with the series suitably distinguished by crosses, and they are referred throughout to an initial nucleation of 86,000 per cubic centimeter. The data show, in the first place, that somewhat more than one-third of the original number of ions or of vapor nuclei are represented by these residual water nuclei,

the remainder having been dissipated during the first evaporation. This agrees with the above results. The loss of nuclei in the lapse of time is thereafter relatively slow, not more than one-half vanishing in the ensuing 10 minutes. From the nature of the experiments it is idle to endeavor to make out a numerical value for the rates, but they are of the value of those obtained on shaking very dilute solutions, for instance.

Under the influence of radium, about the same number of water nuclei occur after 10 minutes, no matter whether the initial δp_3 is 26.7 or 22.6. Temperature corrections would not modify the conclusions drawn. When the fog is precipitated under the same exhaustions with identically initial coronas (this is possible because the vapor nuclei are efficient in the presence of the ions), on either ions or vapor nuclei, the persistence of the water nuclei obtained on identical evaporation is about the same. From this one may argue that the water nuclei which persist, *cæt. par.*, are roughly independent of the nature of the original nuclei. Finally in fig. 32, *b*, the persistence of water nuclei in successive exhaustions is shown for comparison, the data being anticipated from the next section. Water nuclei precipitated on ions vanish much more rapidly than for the corresponding case of phosphorus nuclei.

64. Summary.—Fogs when characterized by identical initial coronas evaporate naturally, or under compression, to about the same number of residual water nuclei, no matter whether the precipitation takes place on ions or on vapor nuclei. The method, however, is rough. In the most favorable cases about one-half of the original number of ions are represented by the residual number of water nuclei. If the drop of pressure is continually decreased the number of residual water nuclei caught decreases with the pressure, rapidly below $\delta p/p = 0.1$ to 0.2. In view of the small amount of water precipitated and of the extremely filmy coronas obtained as a consequence, measurement is difficult. There is a lower limit to which the drop of pressure may be reduced unless a huge fog chamber is constructed specially for these experiments. For small exhaustions, coronas are liable to remain of the same type even though $\delta p/p$ decreases over wide ranges.

The persistence of residual water nuclei is not appreciably different when this precipitation of fog particles to be evaporated takes place on ions or on water nuclei. It is, however, enormously different, *cæt. par.*, from the case of phosphorus nuclei. It appears that this difference is not of the nature of a time loss, but of a true evaporation loss. When water nuclei are obtained from fog particles precipitated upon ions or upon vapor nuclei, the chief loss of water nuclei accompanies each evaporation of the fog particles, and over one-half of the total number of ions may fail of representation in the number the nuclei present after the first evaporation. This incidental observation will be systematically considered in the next section.

THE PERSISTENCE OF WATER NUCLEI IN SUCCESSIVE EXHAUSTIONS.

65. Standardization with ions.—A curious behavior appeared in an attempt to standardize the coronas by aid of the ions due to gamma rays penetrating the fog chamber. These were obtained from a sealed sample of radium of strength 10,000× and weighing 100 mg. The coronas were produced by successive exhaustions of the same value, the fogs being dissipated by evaporation as soon as possible. The data given in the above way in table 45 show an enormously rapid initial loss. To obtain large coronas, the exhaustion to catch the ions was higher (drop of pressure $\delta p_3 = 22.6$) than to catch the water nuclei resulting from the evaporation of fog particles ($\delta p_3 = 17.1$). Hence, in the two cases $\delta p_3/p = 0.293$, volume expansion $v_1/v = 1.28$, and $\delta p_3/p = 0.227$, $v_1/v = 1.20$, whence $n \times 10^{-3} = 0.268 s^3$ and $n \times 10^{-3} = 0.215 s^3$.

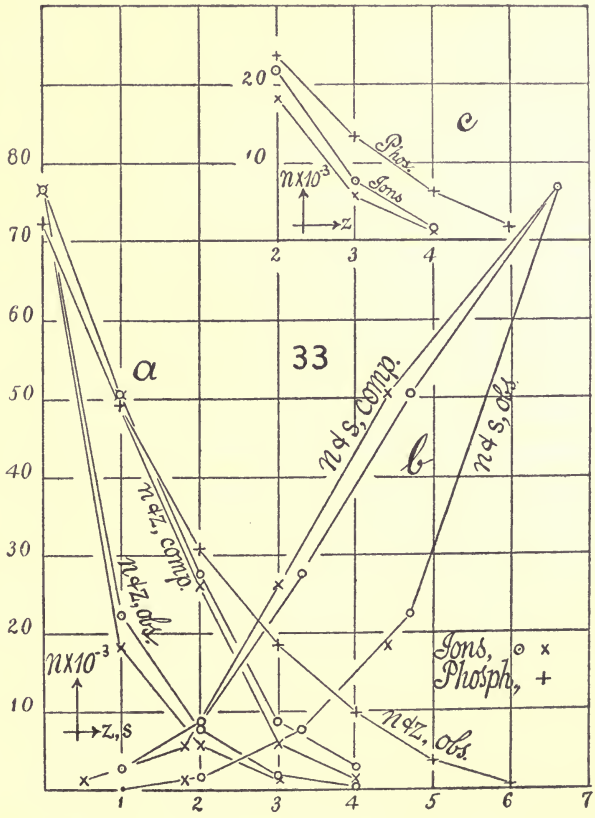

FIG. 33.—Residual water nuclei obtained from evaporation of fog particles precipitated upon ions. Curve (*a*) shows number of nuclei computed and observed found in successive identical exhaustions; curve (*b*) the corresponding relations of nucleation n and coronal diameter s; (*c*) the corresponding behavior of phosphorus nuclei compared with the ions.

The attempt to find the subsidence constant S fails; as, for instance,

s=	4.7	3.3	2.0	1.0	4.4	3.0	1.8
S=		12.2	7.9	3.4		11.5	6.6

showing a well-marked progression of data. Similarly, the attempt to find n_0 in the table fails, as the progression is here equally manifest. In other words, with the evaporation of the first fog (on ions) more than half the nuclei are lost, whereas in subsequent evaporations the behavior of the remaining nuclei is more like phosphorus nuclei.

TABLE 45.—Coronas standardized. Ions from gamma rays (radium). Bar. 75.2 cm.; temp. 25° C.; 90 seconds between observations. Cock open 5 seconds. For ions $\delta p' = 23.6$ cm.; $\delta p_3 = 22.0$ cm.; $y' = 0.71$; $\delta p_3/p = 0.293$ (factor, $0.268s^3$); for water nuclei, $\delta p = 18.1$; $\delta p_3 = 17.1$; $[\delta p_2] = 16.5$; $\delta p_3/p = 0.227$; $y = 0.774$. Assume $S = 6.5$.

No. of exhaustion.	Corona.	s.	$n' \times 10^{-3} = 0.215s^3$.	No. of exhaustion.	Corona.	s.	$n' \times 10^{-3} = 0.215s^3$.
(Ions) 1	w r	6.6	176.9	(Ions) 1	w r	6.6	176.9
(Water nuclei) 2	....	4.7	22.3	(Water nuclei) 2	....	4.4	18.3
3	....	3.3	7.7		....	3.0	5.8
4	....	2.0	1.7		....	1.8	1.2
5	....	1.0	0.2		....	0.0	0.0
6	....	0.0	0.0				

$n' = 0.268s^3$.

These data are shown in fig. 33, where $10^{-3}n' = 0.215s^3$ indicates the number of nuclei actually present in the exhausted fog chamber and n the number which presumably ought to be present. The discrepancy is obvious and in large measure due to the losses in the first evaporation. Thus, taking the second residue ($n \times 10^{-3} = 50.6$) as the initial number the results, in thousands per cubic centimeter, show that over one-half are lost on first exhaustion.

	Nuclei present.	Should be present.		Nuclei present.	Should be present.
Ions	76.9	76.9	Ions	76.9	76.9
After 1 evaporation	22.3	50.6	After 1 evaporation	18.3	50.6
After 2 evaporations	7.7	8.0	After 2 evaporations	5.8	6.2
After 3 evaporations	1.7	0.9	After 3 evaporations	1.2	0.4
After 4 evaporations	0.2	0.1	After 4 evaporations	0.0	0.0

The same result may be inferred by laying off the nucleation in terms of the number of the exhaustion as in fig. 33. In fact, the phosphorus nucleation, as taken from table 20 for corresponding initial nucleations, vanishes per exhaustion more slowly throughout.

66. Further data.—Thus it appears that the water nuclei obtained by evaporating fog particles precipitated on ions vanish more rapidly, at least in the beginning, than may be accounted for as the combined result of the exhaustion applied and the subsidence. New results were

therefore investigated in table 46, by aid of the method of two sources, S being their distance apart on a radius $R=250$ cm., where $S=2R$ tan $\theta/2$, if θ is the angular diameter of the coronas. The number of water nuclei must be increased by the exhaustion, but not the initial number of ions in the exhausted fog chamber. The data for n are taken from the observed sizes of coronas as investigated above.

TABLE 46.—Fog chamber standardized with ions from radium. Bar. 76.0 cm.; temp. 20° C.; 60 seconds between observations; subsidence 5 seconds.

	Series and exhaustion number.	S.	$0.12S=s'$.	$n\times10^{-3}$ (exh.).	$n\times10^{-3}$.	Calculated $n\times10^{-3}$.
For ions, $\delta p'=24.0$ cm.; $\delta p_3=22.9$ cm.; $[\delta p_2]=22.4$ cm. For water nuclei, $\delta p'=24.0$ cm.; $\delta p_3=22.9$ cm.; $[\delta p_2]=22.4$ cm.; $\delta p_3/p=0.301$; $S=6.5$.						
1.	(Ions) 1	g y 72	8.6	....	166	....
	(Water nuclei) 2	39	4.7	28	36	....
	3	27	5.2	8.5	11	....
	4	21	2.5	4.1	5.3	....
	(Air) 5	y′ 17	2.0	2.2	2.8	....
2.	(Ions) 1	72	8.6	....	166	....
	(Water nuclei) 2	42	5.0	32	42	....
	3	30	3.6	13.1	17	....
	4	21	2.5	4.1	5.3	....
	(Air) 5	18	2.2	2.9	3.7	....
3.	(Ions) 1	y′ 70	8.4	....	157	....
	(Water nuclei) 2	40	4.8	29	38	....
	3	29	3.5	12	15	....
	4	20	2.4	3.7	4.8	....
The same.[1] For ions, $\delta p'=24.0$ cm.; $\delta p_3=22.9$ cm.; $[\delta p_2]=22.4$ cm.; $\delta p_3/p=0.301$. For water nuclei, $\delta p'=18.5$ cm.; $\delta p_3=17.7$ cm.; $[\delta p_2]=17.0$ cm.; $\delta p_3/p=0.233$; $y=0.771$.						
4.	(Ions) 1	71	8.5	....	162	162
	(Water nuclei) 2	47	5.6	....	45.7	114
	3	33	4.0	....	18.6	69
	4	24	2.9	....	6.3	32
	5	14	1.7	....	1.2	5.5
	6	0	0.0	....	0.0	0.9
5.	(Ions) 1	72	8.6	....	166	166
	(Water nuclei) 2	40	4.8	....	29.3	117
	3	30	3.6	....	13.1	64
	4	20	2.4	....	3.7	25
	5	13	1.6	....	1.0	9
	6	0	0.0	....	0.0	4
6.	(Ions) 1	72	8.6	....	166	167
	(Water nuclei) 2	42	5.0	....	33.6	117
	3	33	4.0	....	17.7	66
	4	25	3.0	....	6.9	30
	5	15	1.8	....	1.4	6.5
	6	0	0.0	....	0.0	1.4

[1]Water nuclei removed by exhaustion, but the ions are not.

TABLE 46—Continued.

Series and exhaustion number.	S.	$0.12S=s'$.	$n\times 10^{-3}$ (exh.).	$n\times 10^{-3}$.	Calculated $n\times 10^{-3}$.
The same, with ions from X-rays. Bar. 76.1; temp. 21° C. Ions, $\delta p'=24$ cm.; $\delta p_3=22.9$ cm.; $[\delta p_2]=22.4$ cm.; $\delta p_3/p=0.301$. Water nuclei, $\delta p'=18.5$ cm.; $\delta p_3=17.7$ cm.; $[\delta p_2]=17.0$ cm.; $\delta p_3/p=0.233$.					
7. (Ions) 1	0 102	12.2	....	475	475
(Water nuclei) 2	50	6.0	....	57	350
3	40	4.8	....	29	221
4	30	3.6	....	13	122
5	19	2.3	....	3.2	47
6	0	0.0	....	0.0	18
8. 1	0 102	12.2	....	475	475
2	54	6.5	....	74	350
3	41	4.9	....	30	228
4	30	3.6	....	13	128
5	17	2.0	....	2.2	49
9. (Ions) 1	g y 124	14.9	....	813	813
(Water nuclei) 2	63	7.6	....	115	607
3	46	5.5	....	44	415
4	33	4.0	....	17.6	245
5	23	2.8	....	5.7	112
6	13	1.6	....	1.9	16
7	0	0.0	....	0.0	2
10. (Ions) 1	g′ 123	14.8	....	813	813
(Water nuclei) 2	66	7.9	....	128	607
3	49	5.9	....	53	419
4	38	4.6	....	26	263
5	27	3.2	....	8.5	140
6	17	2.0	....	2.2	37
11. (Ions) 1	g′ 128	15.4	....	1100	1100
(Water nuclei) 2	66	7.9	....	128	823
3	47	5.6	....	46	568
4	35	4.2	....	20	348
5	26	3.1	....	8.0	174
6	17	2.0	....	2.2	50
12. (Ions) 1	128	15.4	....	1100	1100
(Water nuclei) 2	71	8.5	....	162	823
3	50	6.0	....	57	580
4	39	4.7	....	28	366
5	29	3.5	....	11.7	199
6	18	2.0	....	2.8	72
7	0	0.0	....	0.0	26

In the first, second, and third series the exhaustion was somewhat above the condensation limit of air, so that the coronas do not vanish. But as the vapor nuclei are relatively inactive as compared with the ions, the initial fall of nucleation is well brought out. The exhaustion is here identical for ions and for water nuclei.

In series 4, 5, and 6 the exhaustion for water nuclei is below the condensation limit of air and the coronas vanish in successive partial evacuations. It is necessary, therefore, to make the exhaustion for ions (only) above the fog limit of air, as otherwise too few would be caught. The observed march of data is, however, similar to the preceding experiments, as is shown in fig. 34.

These results were now varied by bringing to bear stronger radiation obtained from an X-ray bulb placed at successively decreasing distances D from the fog chamber. In series 7 and 8, $D=40$, in series 9 and 10, $D=20$ cm. and in series 11 and 12, $D=12$ cm. (about) from the axis of the fog chamber. The enormous initial radiations drop off rapidly in the same way as in the preceding case. All the series are consistent, except the eleventh, in which the initial drop is too large compared with the others. It was customary to keep the exhaust cock open for 5 seconds, after which the filter cock was opened to dispel the fog, 1 minute being allowed between the exhaustions. The results are shown in detail in fig. 34, *a*, *b*, *c*, together with similar data for vapor nuclei and for phosphorus nuclei.

TABLE 47.—Vapor nuclei. Fog chamber standardized.

Series and exhaustion number.		S.	$0.12\,S=s'$.	$n\times10^{-3}$.	Calculated $n\times10^{-3}$.
Bar. 76.0 cm.; temp. 20° C. For vapor nuclei, $\delta p'=33.1$ cm.; $\delta p_3=31.3$ cm.; $[\delta p_2]=30.8$ cm.; $\delta p_3/p=0.412$. For water nuclei, $\delta p'=18.5$ cm.; $\delta p_3=17.7$ cm.; $[\delta p_2]=17.0$; $\delta p_3/p=0.233$.					
1.	(Vapor nuclei) 1	y 117	14.0	[1]905	905
	(Water nuclei) 2	80	9.6	234	674
	3	67	8.0	135	482
	4	52	6.2	66	333
	5	39	4.7	27.7	214
	6	28	3.4	10.9	116
	7	19	2.3	3.3	39
	8	10	1.2	0.3	13
2.	(Vapor nuclei) 1	y 116	13.9	[1]905	905
	(Water nuclei) 2	p cor 72	8.6	166	673
	3	r 61	7.3	103	473
	4	50	6.0	57	319
	5	37	4.4	23.7	201
	6	26	3.1	8	103
	7	20	2.4	3.7	26
	8	10	1.2	0.3	6
Bar. 76.1 cm.; temp. 21° C. For vapor nuclei, $\delta p_3=28.3$ cm.; $\delta p_3/p=1.233$. For water nuclei, $\delta p_3/p=0.372$.					
3.	(Vapor nuclei) 1	6.8	8.2	172	172
	(Water nuclei) 2	5.2	6.2	66	120
	3	4.0	4.8	29	77
	4	2.7	3.2	9.1	42
	5	1.7	2.0	2.1	12
	6	0.0	0.0	0.0	4
4.	(Vapor nuclei) 1	7.1	8.5	191	191
	(Water nuclei) 2	5.1	6.1	61	134
	3	4.3	5.2	35	85
	4	3.3	4.0	17.7	49
	5	2.5	3.0	6.9	22

[1]Water nuclei removed by exhaustion, but not the vapor nuclei.

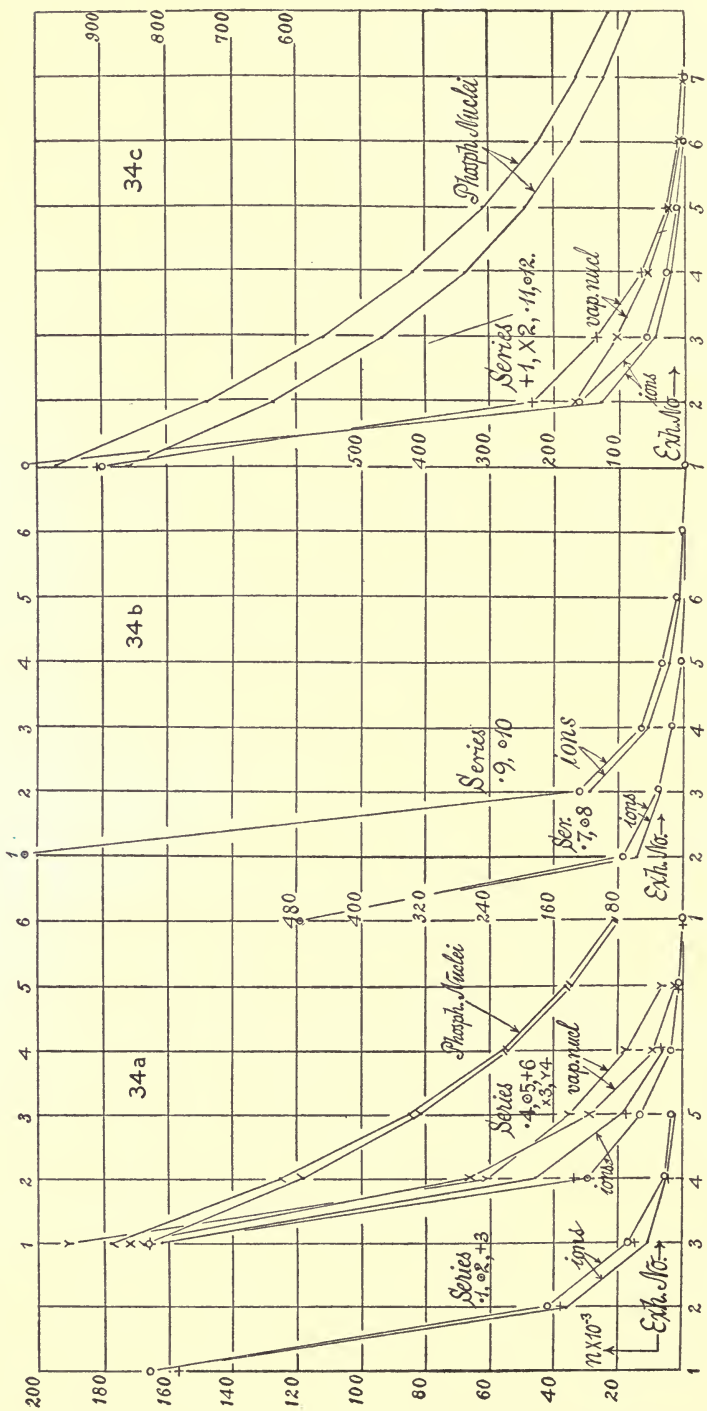

FIG. 34, *a*, *b*, *c*.—Showing number of residual water nuclei *n* per cubic centimeter found in successive identical exhaustions, after evaporation of fog particles precipitated upon phosphorus nuclei, vapor nuclei, and ions, respectively.

67. Data for vapor nuclei.—Table 47 contains similar data for the vapor nuclei of wet dust-free air. In series 1 and 2 large coronas or high nucleations are met with at the start, and they are compared in fig. 34, *c*, with a corresponding case for ions. In series 3 and 4 lower initial nucleations are contained, and these data are compared in fig. 34 with the corresponding cases of ions and phosphorus nuclei. Corrections for subsidence should have been added to the graphs for ions and for vapor nuclei, but these are not large enough to modify them materially, so far as the figures go.

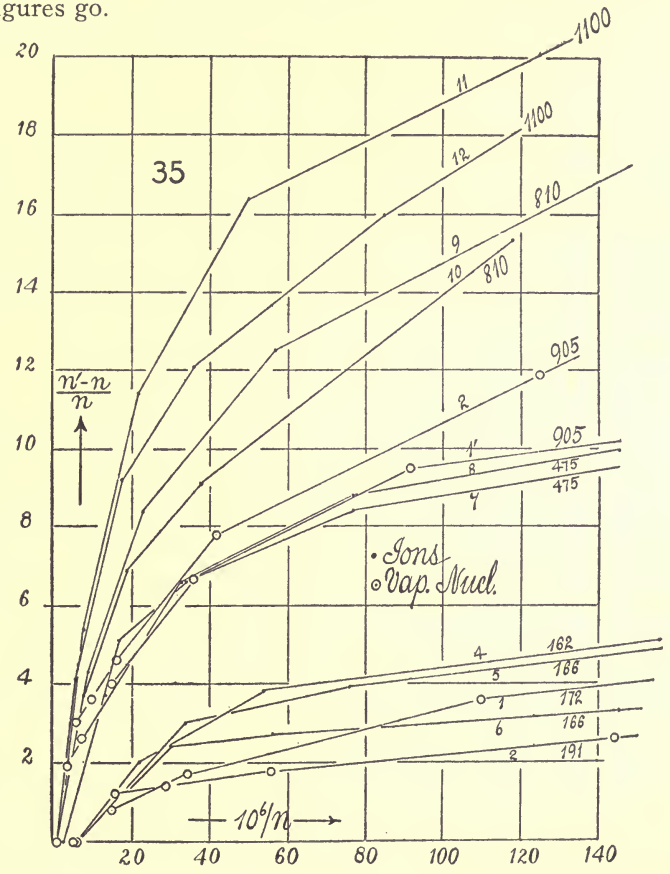

FIG. 35.—Relative difference of nucleation $(n' - n)/n$ of water nuclei from fog particles precipitated upon phosphorus nuclei and on ions, in terms of $1/n$. The serial number of the initial nucleation is attached to each curve.

68. Remarks on the tables.—The graphs in figs. 34, *a*, to 34, *c*, show unmistakably that the water nuclei obtained from the evaporation of fog particles precipitated on ions vanish in the successive exhaustions faster than in the corresponding case with the vapor nuclei of dust-free air; while the water nuclei from fog particles precipitated on vapor nuclei vanish much faster than is the case for the corresponding solu-

tional nuclei obtained with phosphorus emanation. It is thus necessary to examine in detail the three more obvious causes for the decrease in nuclei, which are as follows: (1) The exhaustions, applied alike in all cases; (2) the subsidence of fog particles during the short time of their suspension, *i. e.*, between the exhaustion and the evaporation by influx of air; (3) the occurrence of electrical charge in the case of ionized nuclei, whereby the charged water nuclei may be brought to coalescence.

Probably the best method of reaching a numerical result will consist in eliminating the effect of exhaustion and subsidence, as was done above for phosphorus nuclei, thus leaving the new losses of nuclei alone outstanding. If

$$n'_z = n_1 y^{z-1} \Pi (1 - S/s^2_{z-1})$$

where y is the exhaustion ratio and the product $\Pi(1-S/s^2_{z-1})$, the correction for subsidence, the data marked n' calculated in the table may be obtained. They are such as apply for solutional nuclei produced by phosphorus, but they are throughout enormously in excess of the values n observed for vapor nuclei and for ions. If we suppose that there is a second cause of dissipation with each exhaustion we may therefore write (abbreviating the products Π)

$$n'_z = n_1 y^{z-1} x^{z-1} \Pi$$

merely to get a numerical statement of the case. The values of the fraction or coefficient of survival x so found show a gradual increase of value as the numbers of exhaustions increase or the nucleations decrease, indicating that the greatest dissipation of nuclei is during the first exhaustion.

If these values of x, as summarized in table 48, be constructed in terms of n, they show that x is considerably in excess for vapor nuclei as compared with ions. Thus, at an average $(n_1+n_2)/2$, very roughly,

$$\frac{n_1+n_2}{2} = 100{,}000 \text{ vapor nuclei ions, } \begin{cases} x = 0.55 \\ .40 \end{cases}$$
$$= 50{,}000 \text{ vapor nuclei ions, } \begin{cases} x = .62 \\ .45 \end{cases}$$
$$= 10{,}000 \text{ vapor nuclei ions, } \begin{cases} x = .65 \\ .49 \end{cases}$$

results which are too irregular for further comparison.

A simple term like $(n'-n)/n$ is preferable in other respects, and in order to put the larger and more certain data on the diagram, $(n'-n)/n$ may be constructed in terms of $1/n$. If it were a question of time loss merely, some further theoretical progress might be made, but the results are not sufficiently smooth to give much assistance here. Hence in fig. 35, $(n'-n)/n$ is shown in terms of $10^6/n$, both for ions and for vapor nuclei. In both cases the curves rise higher as the parameter n is greater. The initial ascent is not very different for ions and for vapor nuclei. The dissipations up to (or due to) the first exhaustion are similar in amount. But thereafter the curves for ions rise more rapidly than the

corresponding curves for vapor nuclei, showing that the water nuclei in the latter case are more persistent under successive exhaustions and evaporation than the ions.

TABLE 48.—Summary of table 46. Ions.

Series.	Observed $n \times 10^{-3}$.	Computed $n' \times 10^{-3}$.	$10^6/n$.	$(n'-n)/n$.	$x \times 10^2$.	x, x', x'', etc.	$d' \times 10^5$.
4.	162	162	6	0	....	....	38
	46	114	22	2.0	40	0.40	57
	19	69	54	3.8	52	.68	80
	6	32	159	5.1	59	.71	110
	1	6	830	4.5	69	1.1	190
5.	166	166	6	0	....	....	37
	29	117	34	3.0	25	0.25	67
	13	64	76	3.9	45	.80	89
	4	25	267	5.7	53	.75	133
	1	10	1000	8.5	80	2.7	200
6.	166	167	6	0	....	....	37
	34	117	30	2.4	29	0.29	64
	18	66	56	2.7	51	.90	80
	7	30	145	3.3	61	.89	107
	1	6	690	3.6	68	.91	180
7.	475	475	2	0	....	....	26
	57	350	17	5.1	16	0.16	53
	29	221	34	6.6	33	.69	67
	13	122	77	8.4	45	.84	89
	3	47	312	14.0	51	.80	140
8.	475	475	2	0	....	....	26
	74	350	13	3.7	21	0.21	49
	30	228	33	6.6	33	.52	65
	13	128	77	8.8	44	.77	89
	2	49	450	....	46	.53	160
9.	810	813	1	0	....	....	21
	115	607	9	4.3	19	0.19	42
	44	415	23	8.4	48	.58	58
	18	245	57	12.5	52	.65	80
	6	112	175	18.5	47	.71	114
10.	810	813	1	0	....	....	22
	128	607	8	3.7	21	0.21	41
	53	419	19	6.9	51	.62	54
	26	263	38	9.1	56	.76	70
	8	140	118	15.4	50	.61	100
11.	1100	1100	1	0	....	....	21
	128	823	8	5.4	16	0.16	41
	46	568	22	11.4	43	.51	57
	20	348	50	16.4	49	.71	76
	8	174	125	21	46	.81	103
12.	1100	1100	1	0	....	....	21
	162	823	6	4.1	20	0.20	38
	57	580	17	9.2	46	.51	53
	28	366	36	12.1	53	.77	68
	12	199	85	16.0	49	.76	92

TABLE 48—Continued.—Summary of table 47. Vapor nuclei.

Series.	Observed $n\times10^{-3}$.	Computed. $n'\times10^{-3}$.	$10^6/n$.	$(n'-n)/n$.	$x\times10^2$.	x, x', x'', etc.	$d\times10^5$.
1.	905	905	1	0.0	....	....	23
	234	674	4	1.9	35	0.35	33
	135	482	7	2.6	53	.80	40
	66	333	15	4.0	58	.71	52
	28	214	36	6.7	60	.65	68
	11	116	92	9.5	....	.73	94
	3.3	39	300	11	....	.90	140
2.	905	905	1	0.0	....	....	23
	166	673	6	3.0	25	.25	37
	103	473	10	3.6	47	.88	44
	57	319	18	4.6	56	.82	53
	24	201	42	7.8	59	.67	73
	8	103	125	11.9	....	.65	103
	4	26	270	....	....	1.7	134
3.	172	172	6	0.0	....	....	39
	66	120	15	0.8	55	0.55	52
	29	77	34	1.7	62	.69	67
	9	42	110	3.6	60	.58	100
	2	12	450	4.8	66	.82	160
4.	191	191	5	0.0	....	....	38
	61	134	16	1.2	46	0.46	53
	35	85	29	1.4	64	.89	62
	18	49	56	1.7	71	.88	80
	7	22	145	2.5	75	.86	107

Finally, the best method of interpreting the above results is in terms of an equation of the form (if n_1 be the initial nucleation)

$$n_z = n_1 y^{z-1} x\ x'\ x'' \ \ldots\ \Pi$$

where n_z is the nucleation of the zth exhaustion, y the exhaustion ratio, Π the subsidence correction, and x, x', x'', etc., the successive coefficients showing the relative survival x, or the corresponding loss $1-x$, of nuclei, accompanying the evaporation of fog particles. This equation asserts that the loss is different in the successive evaporations, and this is actually the case, as has been fully shown in table 48. The data x, x', x'', etc., have been constructed in fig. 36, *a*, *b*, *c*, *d*, in terms of the number of successive identical exhaustions for the case where the nuclei are ions, and in fig. 36, *e*, *f*, for the case of vapor nuclei. The ordinates thus show the fraction of the total number of fog particles evaporated, surviving as nuclei after the particular evaporation given (in turn) by the abscissas. It is not probable that more than three or four successive data will be trustworthy, because with the rapidly decreasing size of coronas the errors are cumulative.

Fig. 36, *a*, *b*, *c*, *d*, shows that the effect of the first evaporation is always preponderating and that it is more destructive as the original

number of ions is greater. Thus when $n = 160{,}000$, $1 - x$ or 60 to 70 per cent are lost during the first, and only about $1 - x'$ or 20 per cent during the second and subsequent evaporations. If $n = 900{,}000$ to $1{,}100{,}000$ where the fog particles are very much smaller, the first destroys about

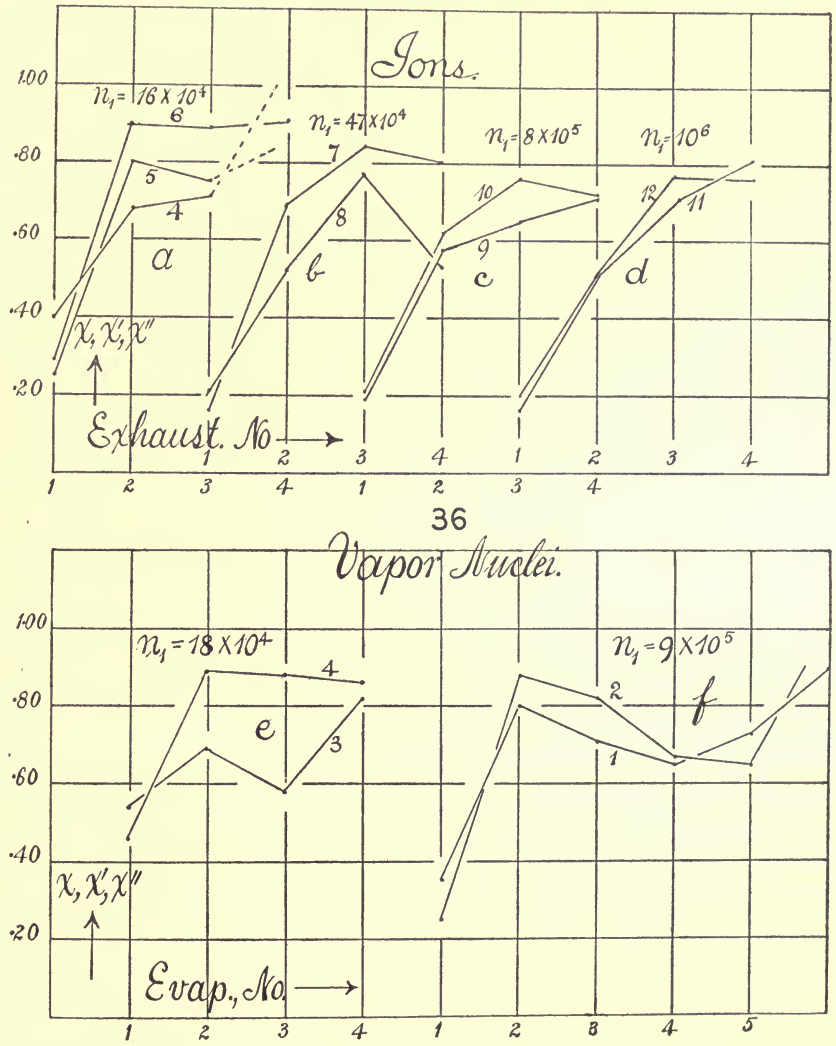

36

FIG. 36, *a*, *b*, *c*, *d* *e*, *f*.—Charts showing the rate of survival of nuclei in each successive identical evaporation of fog particles precipitated upon ions. x is the relation of the number of nuclei after the given evaporation of fog particles to the number of nuclei before it. The abscissas show the number of evaporation in the series.

80 per cent, the second 40 per cent, the third 30 per cent of the number which happen to be present just before the respective evaporation. Hence for large values of n the loss due to evaporation is appreciable throughout many repetitions.

The results (fig. 36, *e*, *f*) for fog particles precipitated upon the vapor nuclei of dust-free air are similar, but in no case does the coefficient of survival x increase after the second exhaustion, as was the case with

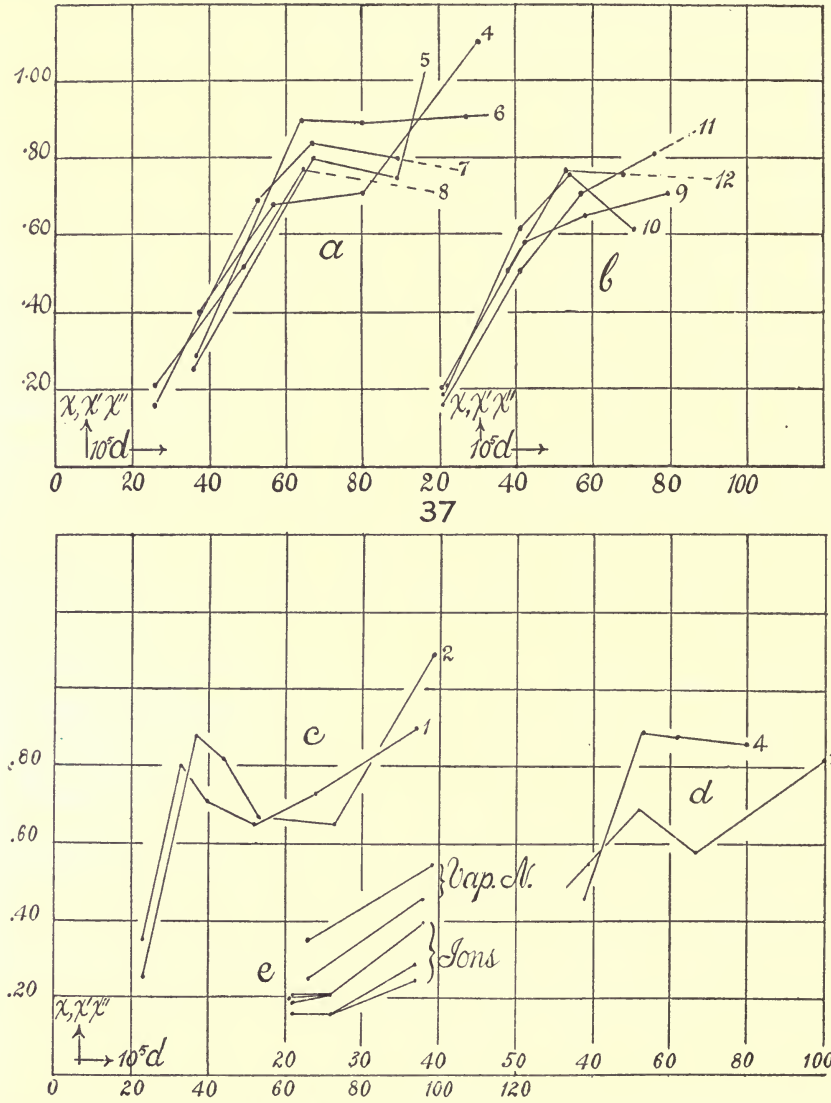

37

FIG. 37, *a*, *b*, *c*, *d*, *e*.—The same as fig. 36, showing x, x', x'', in terms of the diameters d of fog particles evaporated.

ions. (Compare fig. 36, *c*, *d*, with fig. 36, *e*, *f*, all of which apply for high original nucleations of about 10^6 per cubic centimeter.) Contrasting the case of ions with the case for vapor nuclei, by comparing *a* with *e* and *c*, *d* with *f*, in fig. 36, specifically, the coefficient of survival is always

decidedly smaller for ions in the first exhaustion than for vapor nuclei. The charged nuclei are therefore destroyed in greater number by the evaporation of fog particles precipitated on them. When the number of nuclei is large (10^6) this is also true in subsequent evaporations, though the contrast is less marked.

Another question which comes up for settlement is this: Whether the fog particles which are represented by nuclei after evaporation are above a certain critical size, and those particles which vanish are below it. This is hardly probable, because all the fog particles contributed to the same corona and because it implies an enormous inequality in the fog particles of the first exhaustion, considering that 45 to 85 per cent of these vanish in the different cases cited. For the present purpose it is sufficient to write $ds' = 0.0032$, where s' may be taken from tables 46 and 47. These results for the diameters of fog particles are given in table 48. They are constructed graphically in fig. 37, *a*, *b*, for ions, and in fig. 37, *c*, *d*, for water nuclei.

Fig. 37, *a*, containing series 4 to 8 for ions and small nucleations below 500,000, suggests that x may change abruptly when $d = 0.0006$ cm.; while fig. 37, *b*, for ions and large nucleations, 10^6 has the same appearance at $d = 0.0005$ cm. It is seen, however, that this is nothing more than the transition from the first to the second evaporation, the former being so much more efficient.

Fig. 37, *c* and *d*, for large and small nucleations of vapor nuclei, has the same character. In *c*, for instance, there is an abrupt change below 40,000 nuclei. But the case is again one instancing the paramount importance of the first evaporation. There is, however, no doubt of an outstanding effect due to the number or the size of nuclei. The coefficient of survival x decreases as the number of nuclei increases, or better, as their size diminishes. Thus, if the comparison be restricted to the first evaporation fig. 37, *e*,

Ions.....	$10^5 d =$	38	37	37	26	26	21	22	21	21	centimeters.
	$10^2 x =$	40	25	29	16	21	19	21	16	20	
Vapor nuclei..	$10^5 d =$	39	38		23	23	..	..	..	..	centimeters.
	$10^2 x =$	55	46		35	25	..	..	..	..	

from which the increase of x with the size of particles is put beyond question and the larger coefficient of survival for vapor nuclei as compared with ions is again apparent. Whether the peculiar features of the curve (fig. 37, *c*), which reappears in each case, have a definite meaning must be left to conjecture; but in most of the curves *a*, *b*, *c*, *d*, *e*, the occurrence of maximum x is in evidence.

69. The loss of nuclei actually due to evaporation.—It is finally to be shown that the peculiar loss of water nuclei resulting after evaporation of fog particles precipitated upon ions is due to this evaporation

(or its equivalent) and not due to the dissipation of the water nuclei in the lapse of time. It might be supposed, for instance, that water nuclei obtained from the fog condensed on the ions are smaller and therefore diffuse more rapidly than water nuclei obtained by other methods. If so, then if the time between the successive exhaustions is doubled, trebled, etc., the loss should be correspondingly increased.

TABLE 49.—Successive exhaustion after different time intervals. Ions due to gamma rays. Bar. 76.1 cm.; temp. 18° C.; $\delta p_3 = 22.9$ cm. For ions, $\delta p_3/p = 0.301$; $\delta p_3 = 17.7$ cm. For water nuclei, $[\delta p_2] = 17.0$ cm.; $\delta p_3/p = 0.232$; $v_1/v = 1.21$.

Series.	Time.	S.	Exhausted $n \times 10^{-3}$.	$n \times 10^{-3}$.
	min.			
I.	0	[1]73	175	175
	1	38	22	27
	2	26	6.6	8.0
	3	17	1.6	2.0
	4	0	0.0	0.0
II.	0	[1]72	166	166
	1	46	36	44
	2	30	11.6	14.0
	3	22	3.8	4.6
	4	12	0.5	0.6
III.	0	[1]72	166	166
	2	49	44	53
	4	30	10.8	13.0
	6	20	3.1	3.7
	8	10	0.3	0.3
IV.	0	[1]68	146	146
	3	42	27	33
	6	25	5.7	6.9
	9	15	1.2	1.4
V.	0	66	129	129
	4	32	12.7	15.4
	8	20	3.1	3.7
	12	12	.5	0.6
Radium left in place except during exhaustion.				
VI.	0	[1]0	170	170
	1	46	36	44
	2	33	14.6	17.7
	3	23	4.7	5.7
	4	12	0.5	0.6
Bar., 76 cm.; temperature 21° C.				
VII.	0	76	196	196
	4	38	22	27
	8	23	4.7	5.7
	12	12	0.5	0.6
VIII.	0	70	157	157
	6	39	23	28
	12	22	3.8	4.6
	18	12	0.5	0.6

[1] g to gy corona.

Table 49, constructed on the above plan but containing the time interval t, in minutes between the exhaustions, shows that the time effect is secondary. The table gives n with correction for the exhaustion or volume increase v_1/v.

The data are represented in fig. 38, the abscissa being the time in minutes, the ordinates showing the nucleation. The curves indicate a steady progression toward the right as the time interval increases, showing that the time losses, although not necessarily absent, are not of serious importance. In fact, in fig. 39 the group for 1-minute and 6-minute intervals constructed in terms of the number of exhaustions (ignoring lapse of time) are virtually coincident. Again, the curve for

2-minute intervals actually shows less loss (due to favorable exhaustion conditions) than the curve for 1-minute interval.

In series 6 radium was left in place except during the exhaustion, (for ions are efficient in presence of water nuclei). It is seen, however, that the water nuclei stored in this ionized field do not decay more rapidly than in ordinary dust-free wet air.

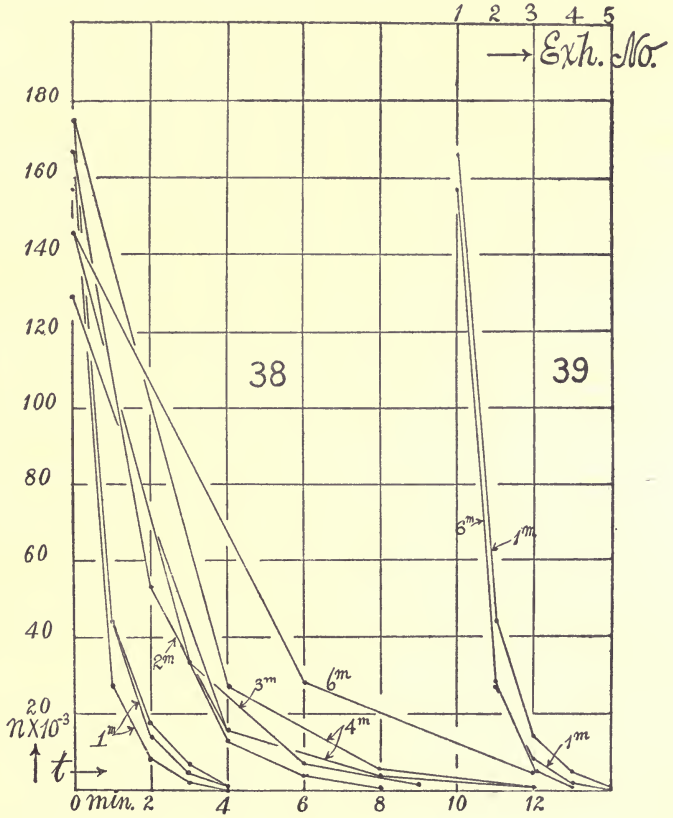

FIG. 38.—Nucleation of residual water nuclei in successive identical exhaustions made at different intervals of time apart. Fog particles precipitated upon ions.

FIG. 39.—The same, constructed for successive exhaustions and ignoring the time intervals.

All the results might be made more striking by reducing them to the same initial nucleation or ionization. Just how differences in these values arise is difficult to affirm, but all the after effects in the successive exhaustions are usually consistent. It does not follow, however, that the correction is to be made by proportionately increasing all the low nucleations by the amount required in the primary nucleation. Series 7 and 8 were therefore added specially with a view to normally large initial nucleations.

70. Conclusion.—When fog particles are precipitated upon solutional nuclei, like those of phosphorus, the losses in successive identical exhaustions are due to the magnitude of this exhaustion, to subsidence, and (in a small measure) to time losses or decay.

On the other hand, when fog particles are precipitated on ions or vapor nuclei, there is an additional and usually very large loss, accompanying the evaporation of the fog particles to water nuclei. Fully 50 to 80 per cent of the nuclei may be lost after the first evaporation. The time between the evaporations is of little consequence. More nuclei are lost for the cases of ions than for the cases of vapor nuclei, other things being equal. All this is very well brought out by the figures.

The loss decreases as the number of the exhaustion increases, or as the number of nuclei present is smaller, or better, as their size is larger. If, apart from subsidence, the nucleation n_z of the zth identical exhaustion of ratio y be put

$$n_z = n_1 y^{z-1} x\ x'\ x'' \quad . \quad . \quad . \quad . \quad .$$

the fractions x, x', x'', etc., make an increasing series and may be called the successive coefficients of survival characteristic of the sizes of fog particles in each of the successive evaporations. The values of x increase from about 0.2 for large and 0.5 for small ionization in the initial evaporation to about 0.8 in the latter evaporations. For particles of like size x is larger for vapor nuclei than for ions. The x values of the initial evaporation distinctly increase with the respective size of particles in all cases.

CHAPTER VI.

THE DECAY OF IONIZED NUCLEI IN THE LAPSE OF TIME.

71. Introduction.—The attempt was made in an earlier paper to standardize the coronas by aid of the decay curves of radium. The method is apparently very simple and requires the knowledge merely of the coronas appearing under given circumstances when the radium tube is in place d on the outside of the fog chamber, in comparison with the coronas observed under the same circumstances when the radium has suddenly been removed for different lengths of time before condensation. From electrical observations the equation

$$dn/dl = -bn^2 \qquad \text{or} \qquad 1/n = 1/n' + b(t-t')$$

is found to be adequate if n and n' denote the ionizations occurring at the times t and t', and the same would appear to be the case with the corresponding nucleations. Moreover, if the relative nucleations n'/n for two coronas obtained at a given exhaustion are known (for instance by the above method of geometric sequences) the absolute values of the nucleations will follow. With a radium ionization at t and t' seconds after its removal

$$n' = ([n'/n]-1)/b(t-t')$$

But the attempt to carry out this apparently straightforward method leads to grave complications. If n be reckoned in thousands per cubic centimeter, the electrical value of b may be taken as $b=0.0014$, while the value of b found from the decay of ions is more than two times as large as this, increasing, moreover, very rapidly as the nucleation is smaller. True, it is possible that the above method for finding the nucleations absolutely may be at fault. Relative values seem to be trustworthy, but absolute data are not to the same degree substantiated; but even if this were granted, the march in the values of b would be unaccounted for and seems to be a new phenomenon.

72. Data. Exhaustion above the fog limit of air.—In table 50 the adiabatic drop of pressure δp_3 is somewhat larger than the fog limit of dust-free air, as is shown in the second section of the table. The column s gives the angular diameter of the coronas at a time t in seconds after the sudden removal of radium from the outer walls of the glass fog chamber. The relative drop in pressure $x=\delta p_3/p$ and the nucleations n follow. The initial coronas are small, as the radium is weak (10,000×, 100 mg.).

TABLE 50.—Fog chamber standardized with radium. Bar. 76.2 cm.; temp. 25.7° C.; water nuclei precipitated. Exhaustions above the fog limit of dust-free air. $\delta p_3/p =$ 0.290 to 0.293; factor 1.22–1.23.

	δp_3.	s.	t.	$\delta p_3/p$.	$n \times 10^{-3}$.	Successive b.	Mean b.
	cm.	*cm.*	*sec.*				
Radium.....	18.4	0	0	0.242	0	....	....
	20.6	[1]6.4	0	.270	65	....	....
I.....	22.2	[1]6.9	0	.292	85	....	0.00331
	.3	[1]6.8	0	.293	82	0.0029	....
	.1	5.3	5	.290	38		
	.1	5.3	5	.290	38	.0021	....
	.1	4.7	10	.290	27		
	.1	4.7	10	.290	27		
	.1	3.8	20	.290	15.1	.0033	....
	.2	3.7	20	.292	13.9		
	.2	3.7	20	.292	13.9	.0042	....
	.2	3.3	30	.292	9.5		
	.2	3.2	30	.292	8.4	.0035	....
	.2	2.6	60	.292	4.6		
	.2	2.6	60	.292	4.6	.0150	....
	.1	1.6	120	.290	0.9		
	.1	1.6	120	.290	0.9	....	....
	.2	6.7	0	.292	79	....	....
	.2	6.8	0	.292	82	....	....
II. Air[2].....	22.1	1.9	....	.290	1.7	....	....
	.1	1.7	....	.290	1.2	....	....
	20.7	r′	....	.272	0.2	....	....
	20.4	r′	....	.268	0.1	....	....

[1]w r cor. [2]Radium removed. Corona glimpsed at $\delta p = 20.4$.

These data are given in fig. 40,* which also contains the observed values of $1/n$ and the corresponding computed values of $1/n$ if $b = 0.0014$. If the values of b are computed from the means of *successive* pairs of measurements at different times t, the data under b "successive" are obtained. A somewhat irregular increase is observed as n decreases. If the first observation be combined with the fourth, etc., the values are

$n = 0.29$	$b = 0.0029$
	34
	36
	41

or a mean value $b = 0.0033$, if the last observation be ignored, since the coronas are just visible here.

If the electrical datum $b = 0.0014$ be correct, the present nucleations n are to be increased on the average, $0.0003/0.0014 = 2.3$ times; if the last datum for b were included, much more. This is quite unreasonable. One must conclude, therefore, that b for nuclei is larger than b for ions or that an ion, acting as a nucleus in a saturated atmosphere, decays

*The data of fig. 40 are constructed from an earlier computation not differing essentially from table 50.

$(dn/dt = -bn^2)$ several times as rapidly as the same ion in a dry atmosphere when tested by the electrical conduction of the medium.

If but a part, n, of all the ions are captured, n' escaping, we may write

$$-dn/dt - dn'/dt = bn^2 + 2bnn' + bn'^2$$

so that both dn/dt and dn'/dt are larger than bn^2 and bn'^2. If $n = n'$,

$$-2dn/dt = 4bn^2 \quad \text{or} \quad -dn/dt = 2bn^2$$

If but one-third of all the ions, $3n$, are captured, $-dn/dl = 9\ bn^2$; etc. Hence if but $1/m$ of all the ions are captured, the coefficient of decay

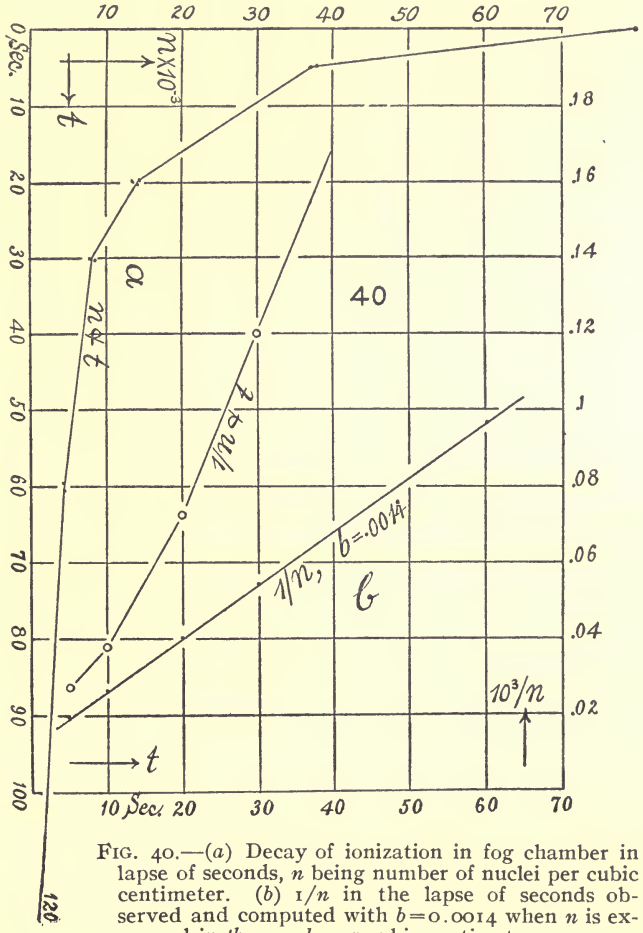

FIG. 40.—(*a*) Decay of ionization in fog chamber in lapse of seconds, n being number of nuclei per cubic centimeter. (*b*) $1/n$ in the lapse of seconds observed and computed with $b = 0.0014$ when n is expressed in *thousands* per cubic centimeter.

being as found should be about m times too large as compared with the true values. This does not explain, however, why the coefficient b increases when t is larger and n is smaller; if it were additionally assumed that the ions decrease regularly in size as they decay more and more,

so that they withdraw more and more fully beyond the given range of supersaturation applied, the second part of these occurrences would also be accounted for; but the assumption is not probable.

73. Exhaustions below the condensation limit of dust-free air.— It would follow from what has just been stated that if the drop of pressure is lower, the values of b obtained must be larger; for not only are few of the ions caught, but the diminution of bulk (virtually) which may accompany the decay would place them sooner out of reach of the given

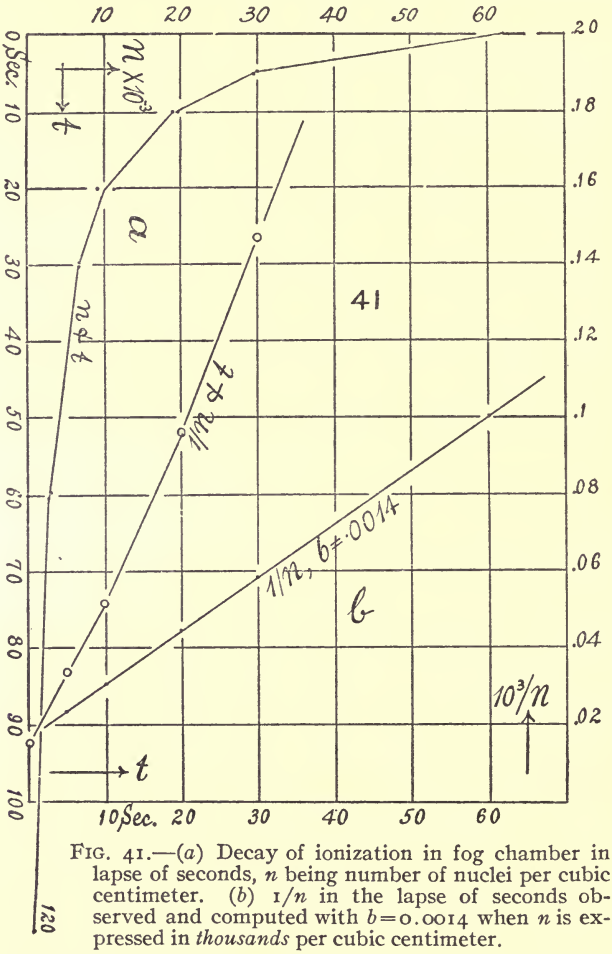

FIG. 41.—(*a*) Decay of ionization in fog chamber in lapse of seconds, n being number of nuclei per cubic centimeter. (*b*) $1/n$ in the lapse of seconds observed and computed with $b=0.0014$ when n is expressed in *thousands* per cubic centimeter.

exhaustion as the interval of decay increases. Table 51 contains experiments of this kind, and they are reproduced in fig. 41, the data, however, being again constructed from an older computation which suffices for the present purposes. The relative drop in the first series is about at the fog limit of dust-free air, while in the second series it is

much below. The successive values of b show an outspoken march into larger values as the time t increases.

If we combine the first observation with the fourth, etc., in series 1, $x=0.27$, $b=0.0038$, 0.0041, 0.0057, 0.0134, or a mean value of $b=0.0045$, if the last observation is ignored. But to ignore this value is here quite inadmissible, as the data for series 2, where $x=0.25$, viz, $b=0.021$, 0.177, fully show.

TABLE 51.—Fog chamber standardized with radium (10 mg. 10,000×). Bar. 76.1 cm.; temp. 25.1° C.; water nuclei precipitated. Exhaustions practically below the fog limit of dust-free air. $\delta p/p=0.268$ to 0.272; distances 40 and 250 cm.

	δp_3.	s.	t.	$n\times10^{-3}$.	Successive b.	Mean b.
	cm.	*cm.*	*sec.*			
I. Radium.....	20.7	6.4	0	66	....	....
	.6	6.3	0	63	0.0036	0.0045
	.6	5.0	5	30		
	.4	5.0	5	30	.0031	....
	.6	4.4	10	21.4		
	.5	4.2	10	19.5	.0042	....
	.5	3.6	20	12.1		
	.5	3.4	20	10.0	.0044	....
	.5	3.1	30	7.4		
	.5	3.1	30	7.4	.0066	....
	.5	2.3	60	3.0		
	.5	2.3	60	3.0	.0180	....
	.4	1.5	120	0.7		
	.6	1.5	120	0.7	....	....
Air.....	.6	0	....	0.0	....	....
Radium at 325 cm.	.6	1	....	0.2	....	....
Bar. 76.2 cm.; temp. 24.0° C.; $\delta p/p=0.254$–0.256.						
II.....	19.4	3.0	0	6.1	....	....
	.4	3.2	0	7.5	0.0206	0.021
	.5	2.5	5	3.9		
	.5	2.6	5	4.1	.1770	....
	.3	1.7	10	1.1		
	.3	1.7	10	1.1	....	....

74. Data for weak ionization. — In the above work the initial intensity of radiation was the same. It was suggested that the average size of a nucleus might decrease in the lapse of time. Thus a variety of further questions arise: (1) Whether weak radiation produces a smaller average nucleus; (2) whether a stronger radiation does the reverse; (3) whether the limit of b decreases as the exhaustion increases and finally approaches $b=0.0014$, etc. The experiments of the following tables show that b varies with the number of nuclei present, no matter whether a given nucleation is due to weak radiation or to decay from a stronger radiation, or finally to low exhaustion; or that the nuclei probably break to pieces as a whole.

TABLE 52.—Decay of weak ionization. Radium at $D=40$ cm. Bar. 76.3 cm.; temp. 24.0° C.; $\delta p_3=22.3$; $\delta p_3/p=0.292$. Above fog limit of air. $\delta p'=23.8$ cm.

	S.	s.	t.	Exhausted $n\times10^{-3}$.	$n\times10^{-3}$.	b.
		cm.	sec.			
1. Radium.....	[1]3.5	4.2	0	[1] 20.0	....	....
	[1]3.6	4.3	0	21.5	....	....
	[2]3.9	4.7	0	[2] 27.3	....	....
	[2]4.0	4.8	0	28.9	(24.4)	0.0017
	3.0	3.6	5	12.9	16.5	.0015
	3.1	3.7	5	13.9	17.8	.0052
	3.1	3.7	10	13.9	17.8	.0055
	3.0	3.6	10	12.9	16.5	
	2.8	3.4	15	10.7	13.7	....
	2.8	3.4	15	10.7	13.7	....
	2.6	3.1	20	7.9	10.1	
	2.4	2.9	20	6.3	8.1	
	2.2	2.6	30	4.6	5.9	.0041
	2.1	2.5	30	4.1	5.2	
	1.8	2.2	60	2.8	3.6	
	1.8	2.2	60	2.8	3.6	
Air.....	1.6	1.9	..	1.7	....	....

[1] Subsequent. [2] Initial.

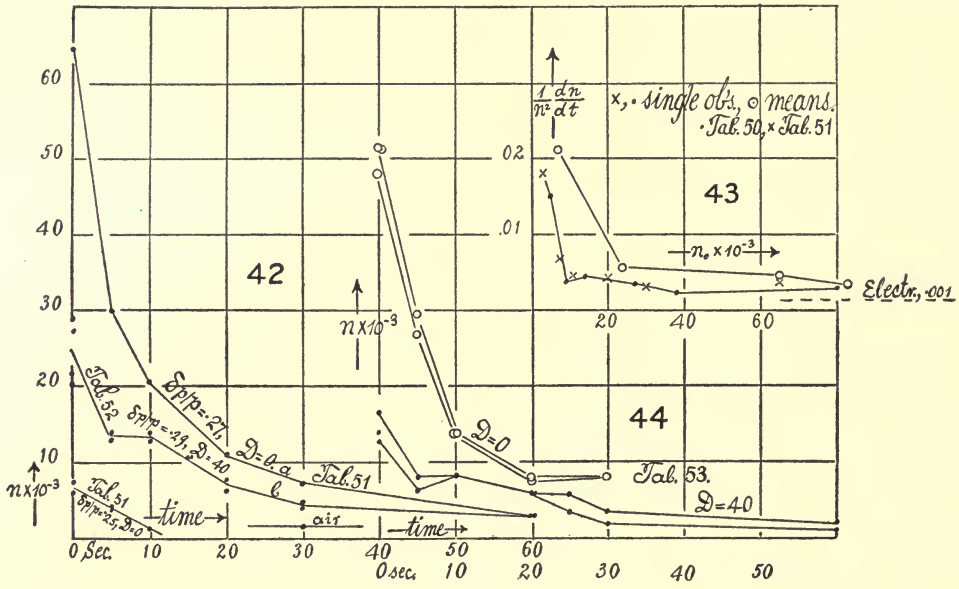

FIG. 42.—Decay of ionization n in fog chamber in lapse of seconds for different initial ionizations and different exhaustions.

FIG. 43.—Coefficients of decay referred to thousands of nuclei per cubic centimeter for different initial exhaustions n_0.

FIG. 44.—Decay of ionization in fog chamber in lapse of seconds for different initial ionization.

In table 52 weak ionization is obtained by placing the radium tube at 40 cm. from the fog chamber. The data, moreover, are investigated by the new method of two sources of light S cm. apart, at a distance R from the fog chamber. The number of nuclei n, computed for the exhausted fog chamber, is corrected by multiplying by the volume expansion $v_1/v = 1.25$. Finally, b is computed from pairs of observations about 20 seconds apart, as suggested by the brace. Water nuclei were always precipitated before each test. In table 52 the exhaustion is above the fog limit of air and the data are constructed in fig. 42 in comparison with cases for stronger radiation and of weaker radiation (by decay) in table 51. Together they form a coherent series of curves, since it is the number n present which determines the value of b, no matter whether the small number is due to low exhaustion ($\delta p_3/p$ near the fog limit); or to decay of ions in the lapse of time (exhaustion t seconds after removing the radium from the fog chamber), or due to

TABLE 53.—Decay of weak ionization. Radium at $D = 40$ cm. Bar. 76.9 cm.; temp. 18.0° C.; $\delta p_3 = 21.0$ cm.; $\delta p_3/p = 0.273$. Practically below fog limit of air. $R = 250$ cm. Exhaustion $1.25 = v_1/v$.

	S.	$0.12S = s'$.	t.	Exhausted $n \times 10^{-3}$.	Corrected $n \times 10^{-3}$.	b.
			sec.			
2. Radium.....	31	3.7	0	13.2	[1](16.5)	....
	29	3.5	0	11.1	[1](13.9)	....
	28	3.4	0	10.2	[1](12.8)	
	25	3.0	5	6.5	8.1	0.0043
	23	2.8	5	5.1	6.4	043
	25	3.0	10	6.5	8.2	131
	25	3.0	10	6.5	8.2	135
	22	2.6	20	4.7	5.8	
	22	2.6	20	4.7	5.8	
	18	2.2	25	2.7	3.4	....
	22	2.6	25	4.5	5.7	....
	18	2.2	30	2.7	3.4	....
	15	1.8	30	1.4	1.8	....
	15	1.8	60	1.4	1.8	....
	13	1.5	60	0.8	1.0	....
The same; stronger radiation. Radium at $D = 0$ from walls.						
3.....	45	5.4	0	38.3	[1](47.9)	....
	46	5.5	0	41.0	[1](51.3)	
	37	4.4	5	22.2	27.7	0.0047
	38	4.5	5	23.5	29.4	0.0053
	29	3.5	10	11.1	13.9	
	29	3.5	10	11.1	13.9	....
	25	3.0	20	6.4	8.0	....
	24	2.9	20	6.0	7.5	....
	25	3.0	30	6.4	8.0	....
	46	5.5	30	41.0	51.3	....

[1] Ions under radiation not lost by exhaustion like the rest.

lower radiation (radiation at some distance, 40 cm., from the fog chamber). Thus in fig. 42 curve *c* introduces low exhaustion $\delta p_3/p$, curve *b* low radiation, all of them the time effect.

In fig. 43 the results of tables 50 and 51 have in fact been summarized, the table giving $-b=(dn/dt)/n^2$ and the nucleation n from which the decay takes place. One may note the rapidly increasing values of b when n is smaller and their tendency towards constant values when n is larger, remembering always that the ionization is throughout *low*.

75. Further experiments.—Table 52, containing exhaustions above the fog limit of air, fails to show the usual high values of b, for the ionized nucleation eventually emerges into the vapor nucleation of dust-free air. In table 53, however, the exhaustion is low enough to catch but few vapor nuclei, while being high enough to insure large coronas due to ions. The data are shown in fig. 44. Series II for low initial nucleations is somewhat irregular, for reasons, as I afterwards learned, connected with the precise position of the radium tube on the top of the fog chamber. Series III for higher nucleations is smoother. Both, however, confirm the occurrence of large values of b associated with small values of n, no matter how the latter are obtained.

If the true equation of the decay curve, dn/dt, were known, it would be worth while to reduce all these data to a common scale. But fig. 43 shows that the values of b rather suddenly increase below $10^3 n_0=10$, so that a simple relation is not suggested for the reduction.

The question arises incidentally whether the ions may not vanish by accretion, *i. e.*, their number may be reduced because individual ions cohere. In such a case the fog limits should be reduced, which is contrary to the evidence. There seems to be a second cause for decay entering efficiently when the nucleation becomes smaller. We may therefore pertinently inquire whether for large nucleation the decay of ions in the fog chamber approaches the electrical value.

76. Case of absorption and decay of ions.—The most promising method of accounting for the above results has been suggested by the work in connection with the behavior of phosphorus nuclei.* There may be either generation or destruction of ions proportional to the number n present per cubic centimeter, in addition to the mutual destruction on combination of opposite charges. In other words, the equation now applicable now is

$$-dn/dt=a+cn+bn^2$$

where a is the number generated per second by the radiation, cn the number independently absorbed per second, and bn^2 the number decay-

*Barus, Experiments with Ionized Air, Smiths. Contrib. No. 1309, 1901, pp. 34–36.

ing by mutual destruction per second. Here c is negative for generation and positive for absorption. If a is zero,

$$-dn/dt = cn + bn^2$$

or

$$\frac{1}{n} = \frac{1}{n_0} + \left(\frac{1}{n_0} + \frac{b}{c}\right)\left(\varepsilon^{c(t-t_0)} - 1\right)$$

where the nucleation n and n_0 occurs at the times t and t_0, respectively. If $b = 0$,

$$n = n_0 \varepsilon^{-c(t-t_0)}$$

if $c = 0$, the equation reverts to the preceding case, where $-dn/dt = bn^2$. Hence when c becomes appreciable,

$$-\frac{dn/dt}{n^2} = \frac{c}{n} + b$$

or the usual decay coefficient increases as n diminishes, becoming infinite when $n = 0$. This is precisely what the above tables have brought out. The value of b does not appear, except when n is very large. Since b is of the order of 10^{-6}, if c is of the order of 3×10^{-2} (as will presently appear), c/n will not be a predominating quantity when n is of the order of 10^6 ($c/n = 3 \times 10^{-8}$); but it will rapidly become so as n approaches the order of 10^4 ($c/n = 3 \times 10^{-6}$), which again is closely verified by the above data.

Finally, if the decay bn^2 is temporarily ignored and if the ions are supposed to be absorbed with a velocity K at the walls of the cylindrical fog chamber of length l and radius r,

$$l \,.\, 2\pi r \,.\, K \,.\, n = l \,.\, \pi r^2 \,.\, cn \quad \text{or} \quad K = cr/2$$

if $c = 3.5 \times 10^{-2}$, $r = 6$ cm., $K = 0.1$ cm/sec., which is not an unreasonable datum. It is not improbable, however, that absorption occurs within the fog chamber in view of the presence of water nuclei. Finally, if the ends of the fog chamber be taken,

$$K = C \frac{r}{2(1 + r/l)}$$

quite apart from the effect of internal partitions. Hence K estimated at 0.1 cm./sec. is an upper limit.

Again, if $-dn/dt = -a + bn^2 + cn$, the conditions of equilibrium are modified and become (since $dn/dt = 0$)

$$a = cn + bn^2$$

where a measures the intensity of radiation. It no longer varies with n^2. Thus

$$n = \frac{c}{2b}\left(1 + \sqrt{1 + 4ab/c^2}\right)$$

The complicated relation of n and a was not suspected in my earlier work, where distance effects due to X-rays were observed.

77. The absorption of phosphorus nuclei.*—The method of the preceding paragraph applied to the data obtained in the given paper with phosphorus nuclei leads to striking results. It shows the possibility of computing nucleation by passing a current of highly ionized air through tubes of known length and section into the steam-jet apparatus there developed. In these experiments, made a long time ago, the value of the absorption velocity K was found to be 0.3 cm. per second, with the condition that decay by the mutual destruction of phosphorus nuclei is negligible. The equations here are

$$n = n_0 \varepsilon^{-2Kx/rv}$$

where v is the velocity of the air current bearing phosphorus nuclei and flowing through a tube of radius r, and where n_0 and n are the nucleations at the ends of the tube of length x.

If V and V' are the volumes of air in liters per minute of lengths x and 0, discharging equal numbers of nuclei per second into the steam jet,

$$K = 2.65\ (V/rx) ln(V/V_0)$$

If decay can not be ignored, as is now to be assumed, the equation is more complicated; for

$$-(v/K')dn/dx = 2Kn/K'r + n^2$$

or

$$n(\varepsilon^{2K(x-x_0)/rv}(2K + K'rn_0) - K'rn_0) = 2Kn_0$$

where K' is the decay coefficient; or since $v = 1000\ V/60\pi r^2$

$$\frac{1}{n} = \varepsilon^{Krx/2.65V}\left(\frac{1}{n_0} + Rr\right) - Rr$$

if $R = K'/2K = b/2c$.

For the same clear blue field seen in the steam-jet apparatus, the incoming volume per second of nucleation must be constant. Hence $nV = n'V'$, and if $x = 0$,

$$\frac{1}{V}\varepsilon^{Krx/2.65V}\left(\frac{1}{n_0} + Rr\right) - \frac{Rr}{V} = \frac{1}{V'}\varepsilon^{Krx'/2.65V'}\left(\frac{1}{n_0} + Rr\right) - \frac{Rr}{V'}$$

If $V' = V_0$ corresponds to $x' = 0$ (or the absence of the tube)

$$\varepsilon^{Krx/2.65V}\left(\frac{1}{n_0} + Rr\right) - Rr = V/V_0 n_0$$

The equation therefore reduces to

$$\varepsilon^{Krx/2.65V} = \frac{V/V_0 + 1}{1 + Rrn_0} + 1$$

whence

$$n_0 = \frac{1}{Rr}\left(\frac{V/V_0 - 1}{\varepsilon^{Krx/2.65V} - 1} - 1\right)$$

---

*Experiments with Ionized Air, Smiths. Contrib., 1309, pp. 34–36, 1901.

It is well worth while to compute n from the results stated, and this has been done in table 54. To do so it is necessary to accept the values

TABLE 54.—Initial phosphorus nucleation, n_0, from steam-jet measurements (Smithsonian Contrib. No. 1309, pp. 34–36, 1901). Assumed $b=10^{-6}$; $c=0.0356$; $b/2c=14\times10^{-6}=R$. V in liters per minute. $n_0=\frac{1}{Rr}\left(\frac{V/V_0-1}{\varepsilon^{krx/2.65V}-1}-1\right)$

x.	V.	$10^{-6}n_0$.	x computed.
I. Absorption pipe gray rubber. $2r=0.64$ cm.; $V_0=0.75$.			
cm.			
0	0.7	....	....
125	3.1	3.3	120
295	4.7	3.6	291
455	6.5	4.6	555
0	0.8	....	....
II. Same. $V=0.75$.			
cm.			
0	0.5	....	....
85	2.1	1.9	49
125	2.8	2.7	97
295	5.2	4.4	360
455	6.9	5.3	624
III. Absorption pipe brown rubber. $2r=0.35$ cm.; $V_0=0.6$.			
cm.			
0	0.5	....	....
100	1.3	4.6	....
150	1.7	4.7	....
200	2.2	5.9	....
250	2.6	6.4	....
300	3.3	9.0	....
350	4.2	13.0	....
IV. Absorption pipe glass. $2r=0.29$ to 0.32 cm.; $V_0=0.8$.			
cm.			
0	0.8	....	....
50	1.2	2.5	....
100	1.4	2.1	....
150	1.9	3.7	....
0	0.8	....	....

x.	V.	$10^{-6}n_0$.	x computed.
V. Absorption pipe brown rubber. $2r=0.35$ cm.; $V_0=6$.			
cm.			
0	0.7	....	....
50	1.5	7.1	....
100	1.9	6.4	....
150	2.3	6.6	....
200	2.8	7.8	....
250	3.1	7.7	....
300	3.5	8.4	....
0	0.6	....	....
VI. Absorption pipe lead. $2r=0.63$ cm.; $V=0.6$.			
cm.			
0	0.5	....	....
100	2.3	3.0	....
200	4.2	5.9	....
300	4.6	4.6	....
400	4.7	3.4	....
0	0.8	....	....
VII. Same.			
cm.			
0	0.5	....	....
34	1.2	1.6	....
68	2.0	3.2	....
100	2.6	4.1	....
200	3.8	4.6	....
300	4.3	3.9	....
0	0.6	....	....
VIII. Absorption pipe lead. $2r=3.2$ cm.; $V_0=0.7$.			
cm.			
0	0.7	....	....
50	1.4	4.8	....
100	1.7	4.1	....
150	2.0	4.4	....

for K' and K, and these are taken from section 79, where $b=K=10^6$ and $c=K=0.0356$, fairly reproducing the data obtained with ions in the fog chamber.

Naturally it is hazardous to accept the constants for ionized air and apply them to the case for phosphorus emanations. Hence the order of values of n in table 54 is surprisingly good. For similar values of n are obtained with the fog chamber where the initial nucleation has been found by the totally different method of successive exhaustions.

There is an observable increase of n with the volume of nuclei-bearing air (V liters per minute) passing through the tube in a given time. But this is not unreasonable, because when the velocity of the current is greater, fresher phosphorus emanation reaches the mouth of the absorption tube. Moreover, since the criterion of an efflux of fixed total nucleation (nV) per minute is the color of the field of the steam tube, a better general agreement must not be anticipated. Finally, the activity of phosphorus in producing ionized emanations varies with temperature and V_0 is very difficult to obtain closer than $V_0=0.5$ to 0.8. The constants b and c are thus provisional values.

The high results for brown rubber are clearly due to low values of V_0 found in the experiment. Thus if $V_0=0.8$ had been taken instead of $V_0=0.6$ the following values would have resulted:

III	$V=$	1.3	1.7	2.2	2.6	3.3	4.2	liters per minute.
	$10^6 n_0=$	2.0	2.4	3.6	4.0	6.0	8.8	
V	$V=$	1.5	1.9	2.3	2.8	3.1	2.5	liters per minute.
	$10^6 n_0=$	4.0	4.0	4.0	5.2	5.2	6.4	

These are much nearer the other values, showing that the great difficulty of finding V_0, the influx in the absence of an absorption tube, is the outstanding discrepancy which is principally responsible for the fluctuation of data. There seems to be no effect due to either diameter of tube or substance of walls.

In Series I and II, a few of the tube-lengths are computed for a mean constant $n_0=3{,}600{,}000$. The agreement is admissible in case of series I but not in series II, since a tube-length of 10 cm. makes an appreciable difference in V.

In the above equations, since $nV=n_0V_0$, it is therefore possible to pass at once to the nucleations by writing $C=n_0V_0$, or

$$\varepsilon^{Krnx/2.56C}-1=\left(\frac{n_0}{n}-1\right)/(1-Rrn_0)$$

It is therefore well worth while to try the experiment with dust-free air ionized by radium or the X-rays, in which case the complications met with in case of phosphorus nuclei will be avoided. The steam tube, which is ordinarily fed with atmospheric air, may, however, have to be modified.

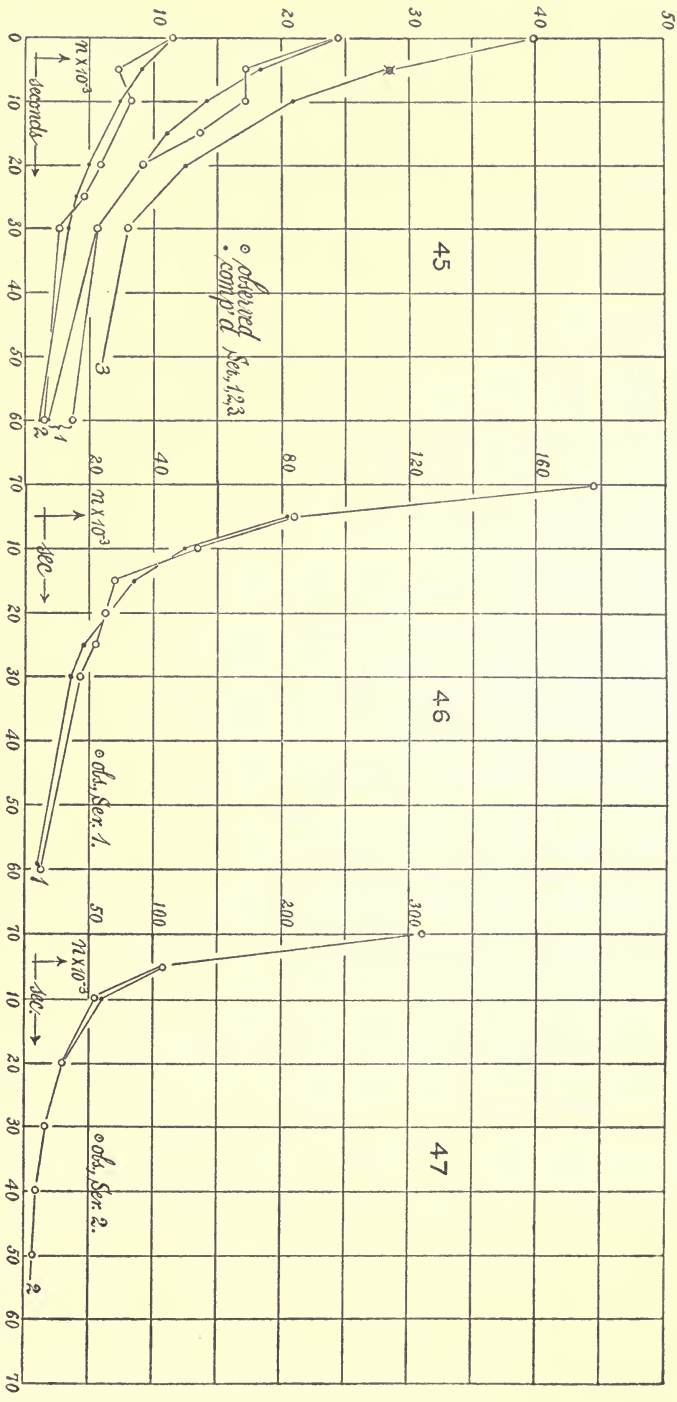

FIGS. 45, 46, and 47.—Decay of ionization n in fog chamber in lapse of seconds, observed and computed.

78. Data.—Experiments were made with special reference to the views just given and are found in table 55. It is not possible, however, from results of the character of the present, to discriminate sharply

TABLE 55.—Decay of ions under high ionization (strong radium and X-rays). $\delta p/p = 0.305$. Bar. 75.3 cm.; temp. 27° C.; $\delta p = 22.9$ cm.

Radium I–IV.

Time.	S.	$s' = 0.12S$	Corrected $n \times 10^{-3}$.	Successive $10^6 b$. 5 sec.	Successive $10^6 b$. 20 sec.	Time.	S.	$s' = 0.12S$	Corrected $n \times 10^{-3}$.	Successive $10^6 b$. 5 sec.	Successive $10^6 b$. 20 sec.
0	g'o 73	8.8	[1]178	....	....	20	33	4.0	23	....	....
0	g'o 73	8.8	[1]178	....	....	25	29	3.5	16	1.10	1.98
5	51	6.1	81	1.26	....	25	35	4.2	27	....	....
5	52	6.2	87	....	....	25	33	4.0	23	....	....
10	46	5.5	58	1.32	....	30	29	3.5	16	2.66	2.02
10	44	5.3	51	....	....	30	30	3.6	17	....	....
15	35	4.2	27	3.44	....	60	21	2.5	5.5	4.1	3.30
15	37	4.4	30	....	....	60	21	2.5	5.5	....	....
20	35	4.2	27	0.86	1.72	0	71	8.5	[1]165	....	[2]2.25

II. X-rays. $D = 100$. $\delta p/p = 0.300$. Bar. 75.6 cm.; temp. 27° C.

Time.	S.	$s' = 0.12S$.	Corrected $n \times 10^{-3}$.	Successive $b \times 10^6$.	Time.	S.	$s' = 0.12S$.	Corrected $n \times 10^{-3}$	Successive $b \times 10^6$.
0	w c 89	10.7	[3]321	1.50	40	25	3.0	8.9	2.40
0	87	10.4	[3]299	....	40	25	3.0	8.9	....
10	45	5.4	53	1.63	50	23	2.8	7.4	....
10	46	5.5	56	....	50	23	2.8	7.4	....
20	37	4.4	29.7	2.43	0	88	10.6	[3]316	....
20	36	4.3	28.1	....	5	58	7.0	119	....
30	30	3.6	16.9	5.23	5	54	6.5	95	....
30	30	3.6	16.9	....					

III. X-rays. $D = 50$. $\delta p/p = 0.299$. Bar. 76.0 cm.; temp. 25° C.

Time.	S.	$s' = 0.12S$.	Corrected $n \times 10^{-3}$.	$b \times 10^6$ successive.	Time.	S.	$s' = 0.12S$.	Corrected $n \times 10^{-3}$.	$b \times 10^6$ successive.
0	w r 91	10.9	337	1.17	40	28	3.4	14	....
0	90	10.8	331	....	40	27	3.2	11	....
10	49	5.9	69	1.76	50	23	2.8	7.5	....
10	48	5.8	66	....	50	24	2.9	8.2	....
20	40	4.8	38	2.68	5	57	6.8	107	....
40	40	4.8	38	....	5	52	6.2	84	....
30	33	4.0	23	3.91	0	w r 86	10.3	288	....
30	30	3.6	17	....					

[1] Corrected for expansion, 231, 231, 215. [2] Mean. [3] If corrected for expansions, 414, 385, 407.

TABLE 55—Continued.

IV. X-rays. $D=15$. $\delta p/p=0.299$. Bar. 76.0 cm.; temp. 27° C.									
Time.	S.	$s'=0.12S$.	Corrected $n\times10^{-3}$.	$b\times10^{6}$ successive.	Time.	S.	$s'=0.12S$.	Corrected $n\times10^{-3}$.	$b\times10^{6}$ successive.
0	yb111	13.4	625	1.38	20	36	4.3	28	..
10	49	5.9	69	....	20	36	4.3	28	....
10	47	5.6	60	2.03	0	g′ 116	14.0	750	....

V. X-rays. $D=15$ cm. $\delta p/p=0.297$. Bar. 76.4 cm.; temp. 26° C.								
Time.	S.	$s'=0.12S$.	Corrected $n\times10^{-3}$.	Time.	S.	$s'=0.12S$.	Corrected $n\times10^{-3}$.
0	g y 124	14.9	620	50	26	3.1	10
10	54	6.5	93	50	28	3.4	14
10	49	5.9	68	30	31	3.7	18
20	41	4.9	40	30	34	4.1	24
20	35	4.2	26	10	51	6.1	78
30	29	3.5	15	5	w o 70	8.4	200
30	32	3.8	19	5	70	8.4	200
40	27	3.2	11	0	g y 133	16.0	990
40	27	3.2	11				

between c and b, and the endeavor will have to be made to select the best values from inspection.

The data of table 55, both observed and computed, in accordance with section 76, are shown in the charts (figs. 45 to 49). In fact, the data of table 52 also appear therein in a new light, the whole being summarized in table 57.

79. Remarks on tables.—In these series the constants obtained for different intervals of $t-t_0$ directly are as follows:

TABLE 56.—$1/n-1/n_0=(1/n_0+b/c)(\varepsilon^{c(t-t_0)}-1)$.

Series.	$t-t_0$.	10^3b.	c.	$10^3b/c$.	Temperature.	Pressure.
	seconds.				°	
I.	0, 15; 15, 30	0.00239	−0.0177	−0.135	27	75.3
	5, 15; 20, 30	.00286	− .0196	− .146		
II.	0, 20; 20, 40	.00082	+ .0448	− .0183	27	75.6
	10, 30; 30, 50	.00088	.0315	.0281		
III.	0, 20; 20, 40	.00061	.0411	.0149	25	76.0
	10, 30; 30, 50	.00056	.0399	.0140		
IV.	0, 10, 20	.00107	.0388	.0275	27	76.0

Mean data, series II to IV, $b=0.000,00079$, $c=0.0392$.

There is a curious consistency in the constants so determined, even when the compensating values of b and c are of different signs, as, for instance, in series I. The reason is not apparent, but the fact is noteworthy. These constants will necessarily be correct at three values of t, but the computed values of n are no better as a whole than will be the case if the first set of constants of series II, for instance, are used.

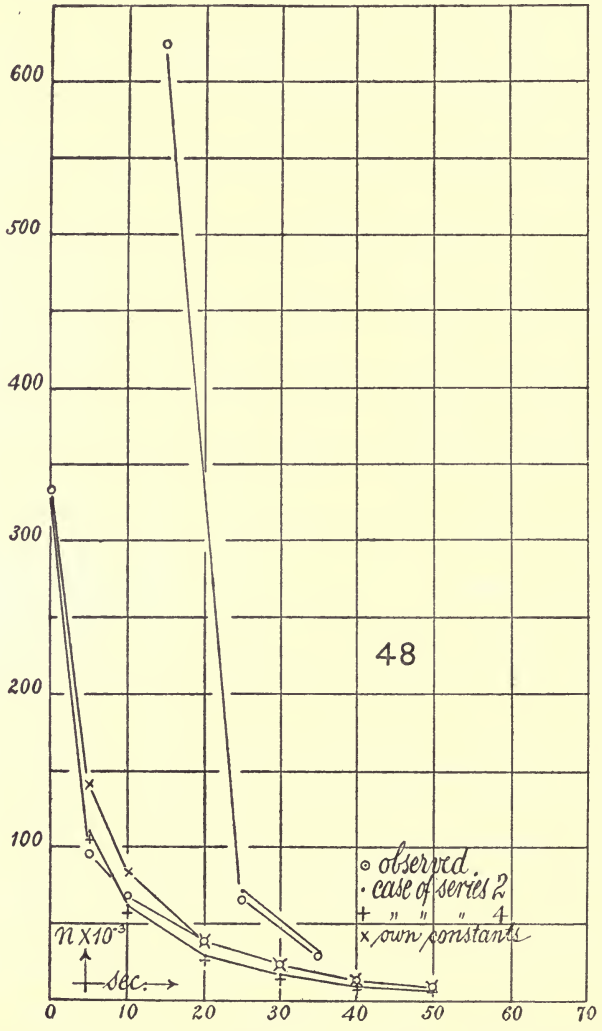

FIG. 48.—Decay of ionization in fog chamber in lapse of seconds, observed and computed.

In fact, the constant b may be arbitrarily put as a reasonable estimate* 0.000001 with $c=0.0356$ and a fair reproduction of the observations

*Townsend, McClung and Langevin find $b=1.1\times10^{-6}$ about, using electrical methods. See Rutherford's Radioactivity, pp. 41, 42, 1905.

obtained. This is shown in table 57 and the charts (figs. 45 to 49), in which the values of the earlier table 52 have been incorporated.

The charts (figs. 45 to 49) show, however, that in all cases the fall of computed curves, while not quite rapid enough at $t-t_0<10$, is somewhat too rapid for the higher time intervals. It follows that b is less than 10^{-6} and c greater than 0.035. If we take the mean of the positive values in table 56, $b=0.00079$, $c=0.039$; but the provisional constants in table 57 are in much better agreement with the observations than the direct values.

TABLE 57.—Estimated constants $b=10^{-6}$, $c=0.0356$. n given in thousands per cm³. $^1/n-{}^1/n_0=({}^1/n_0+b/c)\ (\epsilon^{c(t-t_0)}-1)$.

Series.	t.	$10^{-3}\times n$ observed.	$10^{-3}\times n$ computed.	Series.	t.	$10^{-3}\times n$ observed.	$10^{-3}\times n$ computed.
1	0	24.4	24.4	2	0	310	310
	5	17.2	18.3		5	107	107
	10	17.2	14.2		10	55	60
	15	13.7	11.1		20	29	28
	20	9.1	8.9		30	17	16
	30	5.5	5.6		40	9	10
	60	3.6	1.8		50	7	6
2	0	11.5	11.5	3	0	334	334
	5	7.2	9.1		5	95	110
	10	8.2	7.3		10	67	61
	20	5.8	4.9		20	38	28
	25	4.5	4.0		30	20	16
	30	2.6	3.3		40	12	10
	60	1.4	1.1		50	8	6
3	0	39.6	39.7	4	0	625	625
	5	28.5	28.1		10	65	70
	10	? 13.9	20.8		20	28	31
	20	? 7.7	12.4				
	30	8.0	7.9	5	0	620	620
					10	81	70
1	0	178	178		20	33	31
	5	84	82		30	17	17
	10	54	50		40	11	11
	15	28	34		50	[1]12	7
	20	25	25		30	21	17
	25	22	19		10	78	70
	30	17	14		5	200	135
	60	5	4				

[1] Continued after 1 hour's rest. Too high.

The question finally arises whether any systematic error in the standardization of coronas, and hence in the values n, could have produced an effect equivalent to the occurrence of the constant c. The equation may be written

$$n_0=\frac{c}{b}\,\frac{\left(\frac{n_0}{n}-1\right)-(\epsilon^{c\tau}-1)}{\epsilon^{c\tau}-1}$$

where $\tau = t - t_0$. If c is very small the exponential may be expanded, whence

$$n_0 = \frac{n_0/n - c\tau - 1}{b\tau}$$

and if $c = 0$, $n_0(n/n_0 - 1)/b\tau$, as above. In these equations the value of b is also given in terms of n and n/n_0 and the time τ, in a way already specified, or

$$b = \frac{1/n - 1/n_0 - (\varepsilon^{c\tau} - 1)/n_0}{(\varepsilon^{c\tau} - 1)/c}$$

Suppose now that $-dn/dt = bn^2$ for the true nucleation and that $N = A + Bn$ as the result of systematic errors of standardization. Then $-dN/dt = b'N^2 + c'N + d'$, an equation broader in form than the one ($-dn/dt = cn + bn^2$) accepted; and d' vanishes if A is very small; c' vanishes with A. Hence the possible introduction of c through the method of standardization is not excluded, however improbable, since the equation is conditioned by the occurrence of A.

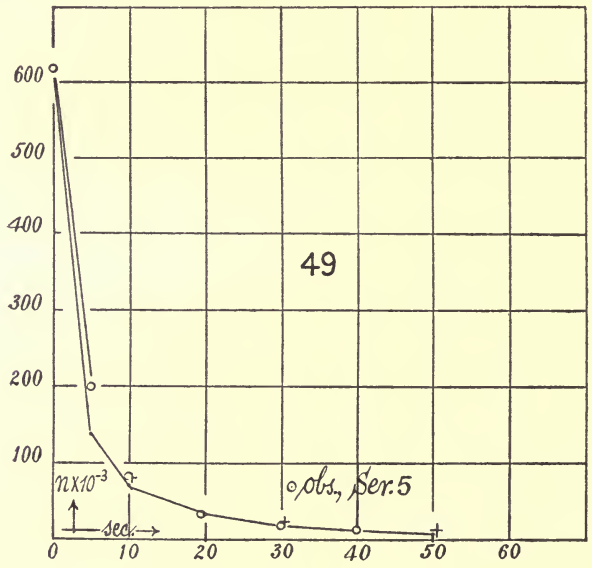

FIG. 49.—Decay of ionization in fog chamber in lapse of seconds observed and computed.

80. Conclusion.—If the rate of decay of ionized nuclei be written bn^2, the coefficient b as found by the fog chamber increases as n decreases and may reach tenfold the order of the usual electrical value $b = 10^{-6}$. The endeavor to explain this by supposing that but $1/m$ of all the ions are caught and $dn/dt = -mbn$, is not satisfactory.

It makes no difference how the small efficient nucleation is produced, whether by weak radiation, or by decay (time loss), from a larger nucleation, or by small exhaustion catching but few nuclei.

The data of the fog chamber may be explained by postulating the absorption coefficient c so that if a be the number generated per second,

$$-dn/dt = a + cn + bn^2$$

In such a case, if b is 10^{-6} the order of the corresponding decay of ions as found by condenser, and if c is of the order of 3.5×10^{-2}, the results of the fog chamber are closely reproduced for all values of nucleation.

A similar theory may possibly be extended to include the absorption of phosphorus nuclei, carried by an air current through thin tubes of different lengths and section (absorption tubes).

Finally, it is improbable, though not impossible, that the constants c may be introduced by a systematic error in the standardization of the coronas of cloudy condensation. To test this it will be necessary to devise some means by which the dust-free air in the fog chamber may be homogeneously nucleated during the experiments for standardization, so that coronas obtained may be without any distortion whatever. Such experiments, however, require considerable labor and the present work may therefore be terminated at this point of progress.